E-130, Extension
Received Aug. 12, 1980

SLAC PROPOSAL - SON OF E130

Precise Measurements of Asymmetries in Polarized Deep Inelastic Scattering.

Part I. Scattering of Longitudinally Polarized Electrons from Longitudinally Polarized Protons and Deuterons.

Part II. Scattering of Longitudinally Polarized Electrons from Transversely Polarized Protons.

Yale-SLAC-Argonne-Berne-Bielefeld-
CCNY-Saclay-Tsukuba Collaboration
V.W. Hughes, Spokesman

August, 1980

Title: Precise measurements of asymmetries in polarized deep inelastic scattering.

Part I. Scattering of longitudinally polarized electrons from longitudinally polarized protons and deuterons.

Part II. Scattering of longitudinally polarized electrons from transversely polarized protons.

Experimenters: V.W. Hughes (spokesman), Yale University.

Yale, SLAC, Argonne, Berne, Bielefeld, CCNY, Saclay, Tsukuba group.

Beam: Polarized electron (PEGGY I). energy, 22.7 GeV; current, 5×10^8 e^-/pulse; pulse length, 1.5 μsec; pulse repetition rate, 120 pps.

Target: Hydrocarbon polarized proton or polarized deuteron target, with volume of 2.5 cm x 2.5 cm x 3.8 cm. Set up in End Station A (ESA).

Experimental equipment and materials requested of SLAC:

Identical to E130.

Date when equipment ready:

Polarized electron source - Available now; needs to be set up again.

Polarized target - Available now.

Spectrometer - Available now.

End Station A Counting House - VAX Computer needed. Otherwise available now.

Running time required:

Checkout: Six weeks, at 10 to 60 pps

Data-taking: 500 hrs at 180 pps.

Computers and data analysis:

VAX/780 in ESA counting house for on-line data-taking.

Triplex for off-line data analysis - 100 hrs.

Period required for data analysis - about 6 months.

Table of Contents

Abstract

Relatively precise measurements of asymmetries in deep inelastic scattering of longitudinally polarized electrons by longitudinally polarized protons and deuterons are proposed as a continuation of our E130 experiment. With the 5^{o} setting of our spectrometer the kinematic range will be studied from about $x = 0.08$ to $x = 0.5$ with $Q^2 \simeq 2$ to 3 $(GeV/c)^2$. These measurements with the longitudinal target polarization should yield precise values for the virtual photon-proton asymmetry A_1 for the proton and should also determine A_1 for the neutron. With the transverse target polarization, measurements should determine the second proton structure function A_2.

These results will provide the first experimental information on A_1 for the neutron and on A_2 for the proton. The data are valuable to test the Bjorken sum rule, scaling for spin dependent structure functions, and modern models of nucleon structure.

I. STATUS OF SLAC E130 RESULTS

OUTLINE

Introduction

Paper submitted to XX International Conference on High Energy Physics, Wisconsin, July 1980.

Figure I, indicating kinematic points now measured for the proton (E80 and E130 results).

Figure II, relating to Bjorken sum rule.

Figure III, values of A_1 for the proton and comparison with some theories.

Figure IV, showing elastic and resonance region electron-proton raw asymmetry data for A.

INTRODUCTION

SLAC E130 is entitled "Precise Measurements of Asymmetries in Deep Inelastic Scattering of Polarized Electrons by Polarized Protons and by Polarized Deuterons" (see Appendix I). This experiment was set up in End Station A in Spring 1979. Check out was done in part of June and July of 1979 as well as part of the Fall of 1979. Data-taking with the 10^{o} spectrometer setting (Part I of E130) was completed by early April, 1980 and used about 400 factored hours of beam time.

Part I of E130 was devoted to measuring the asymmetry A_1 for the proton at higher Q^2 and x values than obtained in our original polarized electroproduction experiment SLAC E80. The data were taken with a 10^{o} setting of our new large acceptance spectrometer. Preliminary results are given in our paper submitted to the XX International Conference on High Energy Physics (Wisconsin, July 1980) (see following pp. 5).

These new data will provide an improved test of the Bjorken sum rule using the same method as described for SLAC E80 (Phys. Rev. Lett. 41, 70 (1978), Appendix IV). The figure and results are given in Fig. II, p. 7.

Comparison of our measured values of $A/D \simeq A_1$ with theoretical predictions for several models of proton structure are shown in Fig. III. Although only preliminary data are available, it is clear that we easily distinguish among different models. Our results are consistent only with models 4 and 6, which are, respectively, an unsymmetrical model in which the entire spin of the nucleon is carried by a single quark in the limit of x=1, (Kaur, 1977) and a model based on source theory. (Schwinger, 1977)

Resonance region data were also obtained during our run. Measured values of the electron-proton asymmetry A versus missing mass W are shown in Fig. IV.

R. Carlitz and J. Kaur, Phys. Rev. Lett 38, 673, 1102(E) (1977); J. Kaur, Nucl. Phys. B128, 219 (1977).

J. Schwinger, Nucl. Phys. B123, 223 (1977).

The kinematics correspond to $Q^2 \simeq 1$ $(GeV/c)^2$, and the data are of comparable quality to those obtained in E80 where Q^2 was 0.5 and 1.5 $(GeV/c)^2$. (Appendix V). These E130 data are raw, on-line results and are not radiatively corrected.

Submitted to the XX International Conference on High Energy Physics,
University of Wisconsin, July 17-23, 1980.

FURTHER MEASUREMENTS OF SPIN DEPENDENT STRUCTURE FUNCTIONS OF THE PROTON IN DEEP INELASTIC AND RESONANCE REGION e-p SCATTERING*

G. Baum, M.R. Bergstrom, P.R. Bolton, J.E. Clendenin, N.R. DeBotton, S.K. Dhawan, R.A. Fong-Tom, Y.-N. Guo, V.-R. Harsh, V.W. Hughes, K. Kondo, M.S. Lubell, R.H. Miller, S. Miyashita, K. Morimoto, U.F. Moser, I. Nakano, R.F. Oppenheim, D.A. Palmer, L. Panda, W. Raith, N. Sasao, K.P. Schüler, M.L. Seely, J. Sodja, P.A. Souder, S.J. St. Lorant, K. Takikawa, and M. Werlen

University of Berne, University of Bielefeld, KEK, Kyoto University, Peking, SACLAY, SLAC, University of Tsukuba, and Yale University

ABSTRACT

Further measurements at SLAC of the asymmetry in deep inelastic and resonance region scattering of longitudinally polarized electrons by longitudinally polarized protons have been made using a new large acceptance spectrometer. Preliminary results are reported for the DIES data for the kinematic range $0.2<x<0.65$ and $3.5<Q^2<10.0$ $(GeV/c)^2$.

New measurements have just been completed at SLAC of asymmetries in the scattering of longitudinally polarized electrons by longitudinally polarized protons.

The basic quantity determined is the asymmetry $A=[d\sigma(\uparrow\downarrow)-d\sigma(\uparrow\uparrow)]/[d\sigma(\uparrow\downarrow)+d\sigma(\uparrow\uparrow)]$, in which $d\sigma$ denotes the differential cross section $d^2\sigma(E, E', 0)/d\Omega dE'$ for electrons of incident (scattered) energy E (E') and laboratory scattering angle 0, and the arrows denote the antiparallel and parallel longitudinal spin configurations. The momentum and scattering angle of the scattered electrons are observed, and the experimental asymmetry $A = P_e P_p F A$ is measured, in which P_e is the electron-beam polarization, P_p is the proton-target polarization, and F is the fraction of detected electrons scattered from the free (polarizable) protons in the complex target.

The polarized electron source (PEGGY I) is based on the photoionization of a polarized Li atomic beam and provided an intensity on the target of 5×10^8 e^-/pulse with a 1.5μs pulse width and a 120 H_z repetition rate. (Alguard et al., 1976a; Alguard et al., 1979) The electron polarization was measured by Möller scattering (Cooper et al., 1975) using a double arm coincidence detector with shower counters and a scintillation hodoscope, and was determined to be 0.80 ± 0.04. The polarized proton target was the butanol (doped with porphyrexide) target used in our earlier measurements. (Alguard et al., 1976a; Ash, 1976) Reduction of the cryostat operating temperature to 0.99°K through increased pumping speed and improved cryostat design and increase in the microwave power to the target led to values of initial proton polarization before irradiation of 0.75 to 0.80 and of average polarization of about 0.6. The steering and energy control of our rastered beam was based on the use of microwave beam position monitors as described in earlier publications (Alguard et al., 1976a; Prescott et al., 1978; Cottrell et al., 1979), and the mean energies and positions and angles of the two helicity beams were maintained close enough to each other to avoid false asymmetries.

The principal new feature of the present experiment on polarized electroproduction is the use of a new large acceptance spectrometer (Fig. 1). The spectrometer has two large dipole magnets and a detector system which consists of a 1m diameter x 4m long N_2 gas Cerenkov counter, a 4000 wire PWC system, a hodoscope, and a segmented lead glass shower counter. The spectrometer may cover momenta up to 18 GeV/c and its acceptance $\int d\Omega \frac{dp}{p}$ is 0.3 msr with the total momentum acceptance $\Delta p/p$ being about 50%. The momentum resolution of the spectrometer $\delta p/p$ is better than ± 1%.

The gain in effective data-taking rate for our present experiment as compared with our earlier and similar experiment (Alguard et al., 1976b; Alguard et al., 1978) is a factor of 14, which is due principally to the larger momentum acceptance of our spectrometer.

Data were obtained with our spectrometer set at a 10^{o} scattering angle for three different kinematic conditions, as follows:

(1) E_o = 22.6 GeV; E' = 11.5 GeV (Deep inelastic region, high Q^2)
$5.7 < Q^2 < 10.0$ $(GeV/c)^2$; $0.2 < x < 0.65$
0.43×10^6 events

(2) E_o = 16.2 GeV; E' = 10.0 GeV (Deep inelastic region, intermediate Q^2)
$3.5 < Q^2 < 5.7$ $(GeV/c)^2$; $0.2 < x < 0.65$
0.53×10^6 events

(3) E_o = 6.4 GeV; E' = 5.2 GeV (Elastic and resonance region),
$0.75 < Q^2 < 1.2$ $(GeV/c)^2$; $0.9 < W < 2.4$ GeV,
2.3×10^6 events.

No false asymmetries were observed. True asymmetries ranged from about -0.01 to +0.035. For the deep inelastic regions the event rates were about 0.01 to 0.02 events/pulse, and for the elastic and resonance region about 1 event/pulse. Values of F were measured

using an unpolarized electron beam on C and CH_2 targets, and were also obtained from other available experimental data. A counting rate asymmetry A of about +0.04 was observed for elastic scattering. This result agrees within our error with the asymmetry predicted for elastic scattering, and provides an overall check of our experimental method.

Preliminary results of our new deep inelastic asymmetry measurements are shown in Figures 2 and 3. We wish to emphasize that these are "on-line" results, which must be checked and refined by off-line analysis. Furthermore, these results are not yet radiatively corrected. The variables used are the same as in our earlier publications (Alguard et al., 1976a, 1976b). The quantity $A/D=A_1+\eta A_2$ is the virtual photon-proton asymmetry in which D is a depolarizing factor (calculated with $R=\sigma_L/\sigma_T=0.25$); the quantity A_1 equals $(\sigma_{1/2}-\sigma_{3/2})/(\sigma_{1/2}+\sigma_{3/2})$, in which $\sigma_{1/2}(\sigma_{3/2})$ is the total absorption cross section when the z component (z is the direction of the virtual photon momentum) of angular momentum of the virtual photon plus proton is 1/2(3/2); the quantity ηA_2 is a relatively small interference term so that $A/D \simeq A_1$.

Figure 2 displays all the available deep inelastic asymmetry data with the earlier results (Alguard et al., 1978) as open circles and the present preliminary results as solid circles. All errors are one standard deviation total errors, which include the statistical counting error and systematic errors associated with P_e, P_p and F, added in quadrature. For the present results each of these systematic errors is taken to be ±5%. The new data extend considerably our knowledge of the virtual photon-proton asymmetry A/D to higher Q^2 and higher x. A significant verification of the predicted scaling property of A_1 is indicated in Fig. 2.

Figure 3 shows the values of A/D vs x as open diamonds for the earlier results

(Alguard et al., 1978) and as solid squares for the present results. For a given x value data for different Q^2 have been combined assuming that the A/D values are independent of Q^2. A careful comparison with theoretical predictions based on models of proton structure has not yet been done, but it is clear that the quality and quantity of data shown in Fig. 3 will allow us to test significantly various theoretical predictions such as those given in Fig. 3 of the earlier publication of Alguard et al., 1978.

*Research support in part by the U.S. Department of Energy under Contracts No. EY-76-C-3075 and No. EY-76-C-03-0515, the German Federal Ministry of Research and Technology, the Japan Society for the Promotion of Science, and the University of Tsukuba.

References

M.J. Alguard et al., Phys. Rev. Lett. 37, 1258 (1976a).

M.J. Alguard et al., Phys. Rev. Lett. 37, 1261 (1976b).

M.J. Alguard et al., Phys. Rev. Lett. 41, 70 (1978).

M.J. Alguard et al., Nucl. Inst. and Meth. 163, 29 (1979).

W.W. Ash, High Energy Physics with Polarized Beams and Targets, ed. M.L. Marshak (American Institute of Physics, New York, 1976), 485.

P.S. Cooper et al., Phys. Rev. Lett. 34, 1589 (1975).

R.L.A. Cottrell, et al., Nucl. Inst. Meth. 164, 405 (1979).

C.Y. Prescott et al., Phys. Lett. 77B, 347 (1978).

Figure Captions

1. Schematic diagram of experimental apparatus showing the new spectrometer.
2. Plot of A/D values vs Q^2 for three different ranges of $x(x=Q^2/2M\nu,\ \nu=E-E')$. Older data are indicated by open circles and new data by solid circles.
3. Plot of A/D values vs x. Older data are indicated by open diamonds and new data by solid squares.

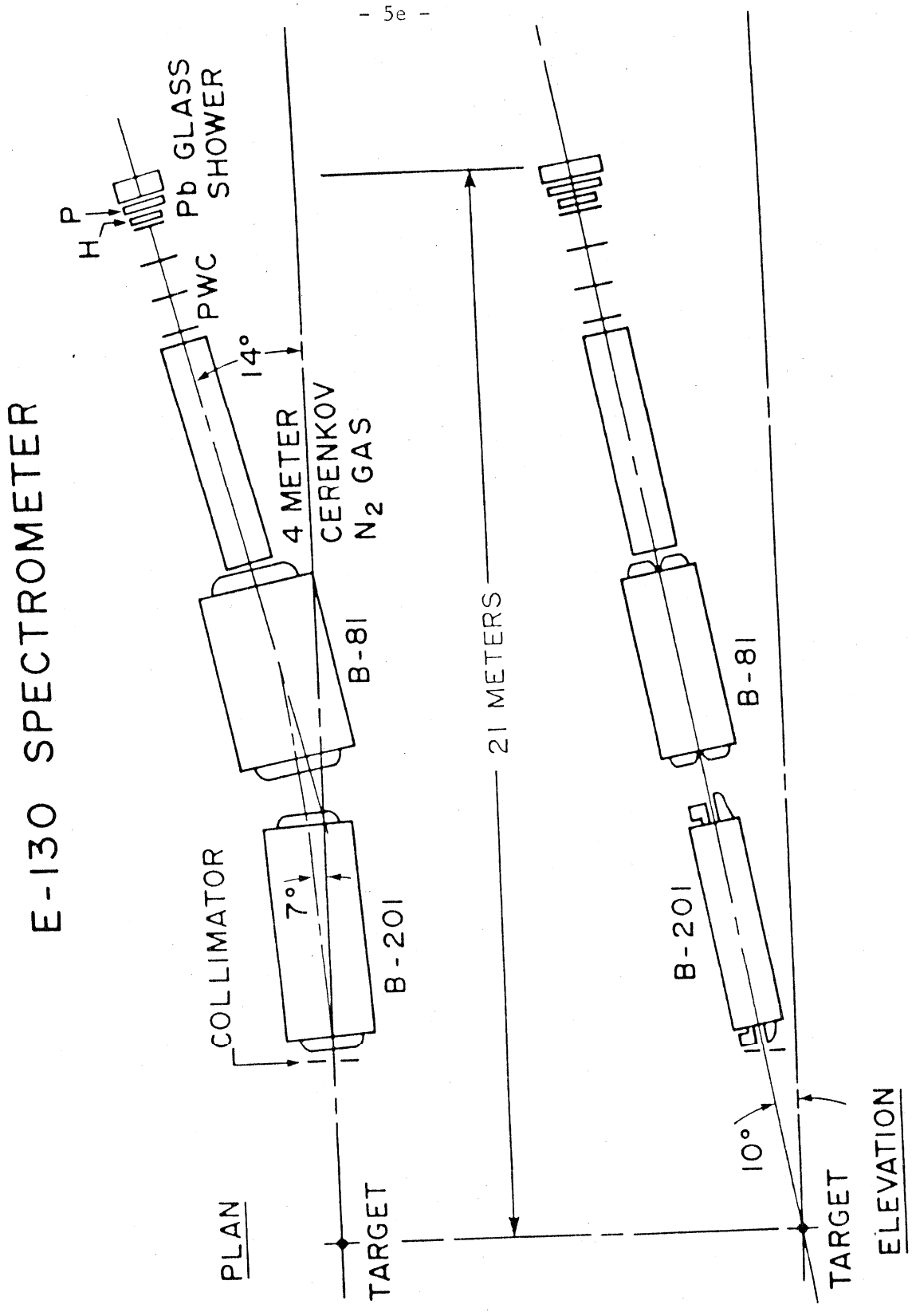
E-130 SPECTROMETER
P
H
Pb GLASS SHOWER
PWC
14°
4 METER CERENKOV N_2 GAS
B-81
21 METERS
COLLIMATOR
7°
B-201
PLAN
TARGET
B-81
B-201
10°
TARGET
ELEVATION

Fig. 1

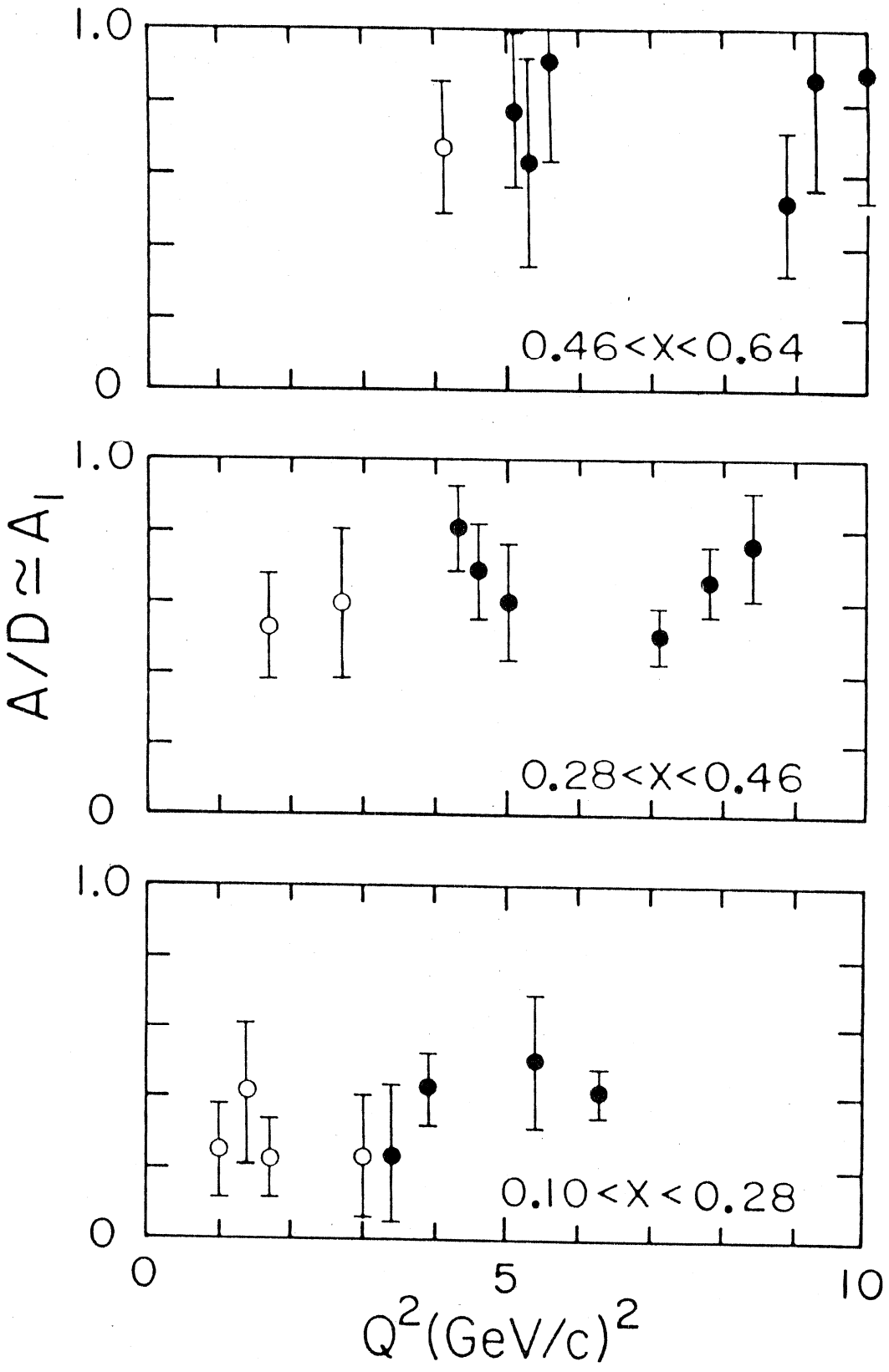

Fig. 2

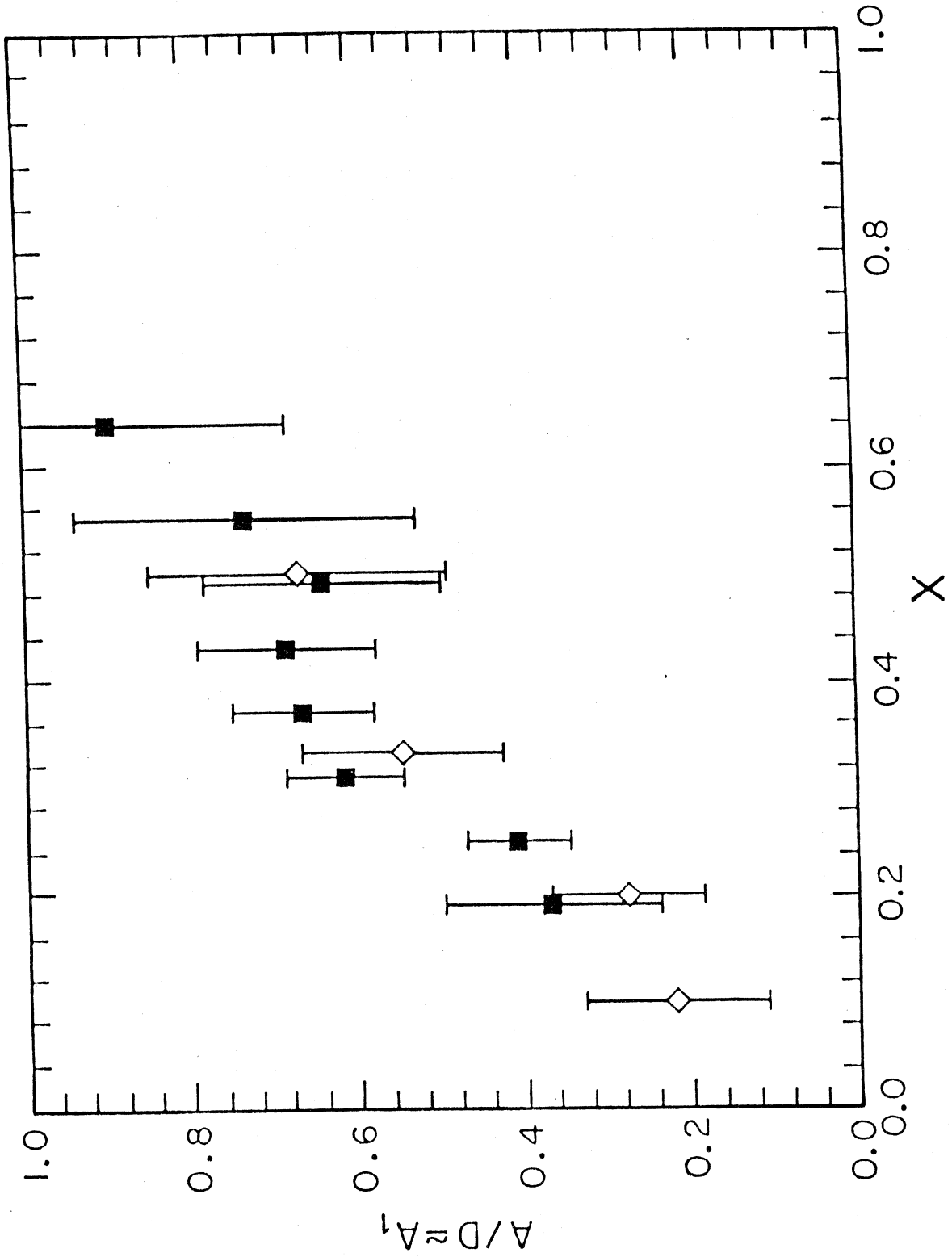

Fig. 3

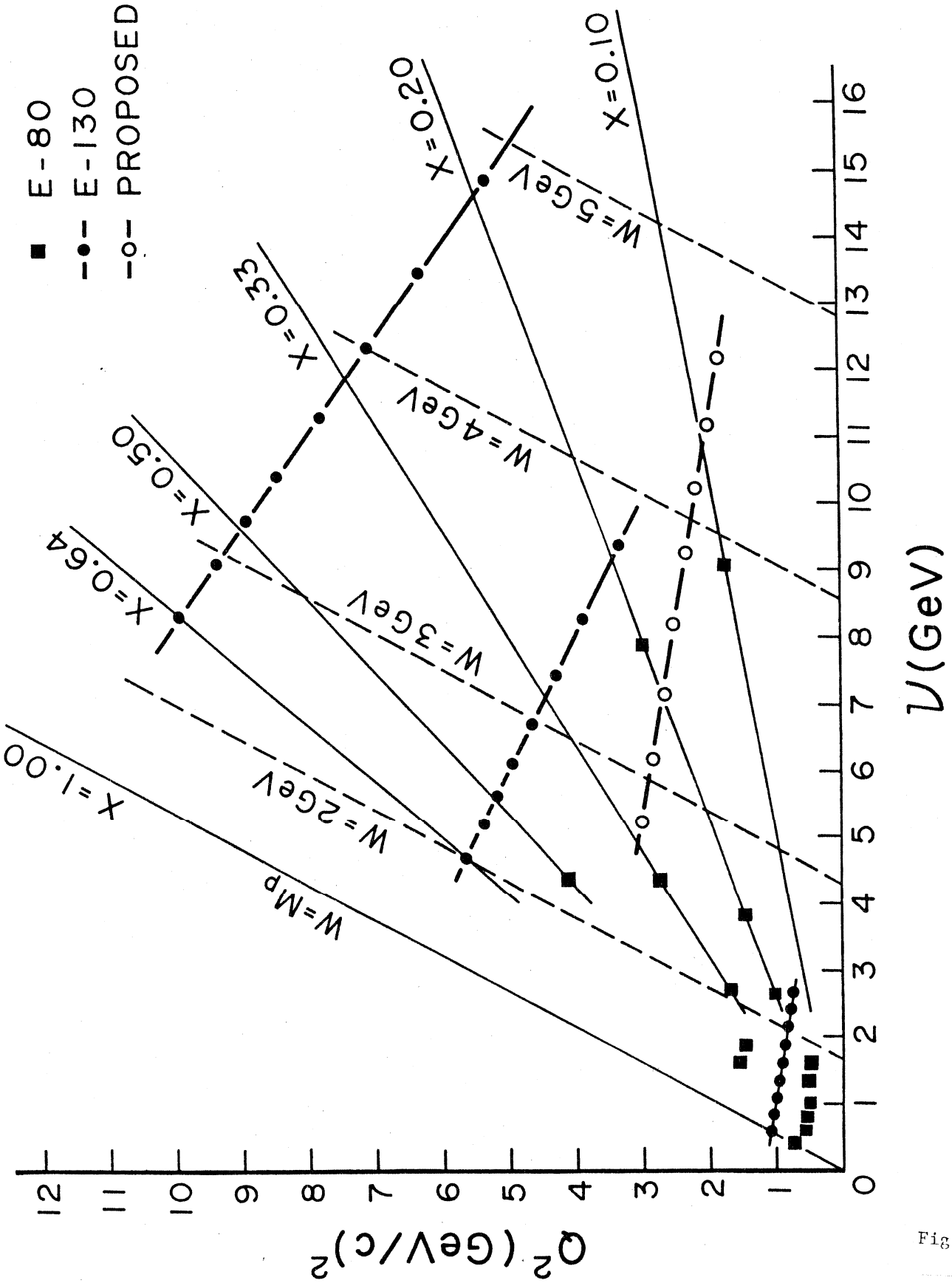
E-80
E-130
PROPOSED
X=0.10
X=0.20
X=0.33
X=0.50
X=0.64
X=1.00
W=5GeV
W=4GeV
W=3GeV
W=2GeV
W=Mp
ν(GeV)
Q² (GeV/c)²

Fig. I

Bjorken Sum Rule:

$$S_{Bj} = \int_0^1 \frac{dx}{x} \left(A_1^p F_2^p - A_1^n F_2^n\right) = \frac{1}{3}\left|\frac{g_A}{g_V}\right| = 0.417 \pm 0.003$$

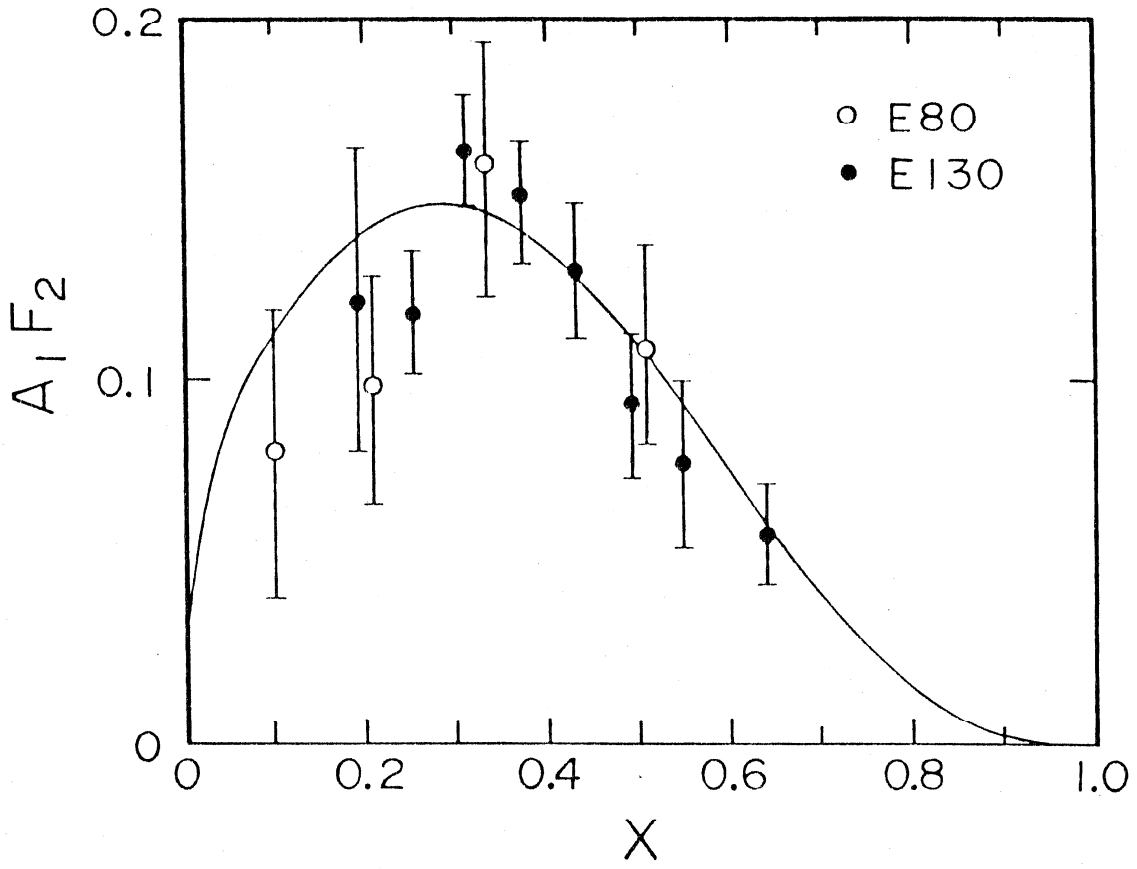

Experiment:

(a) Fit to data (E80 + E130 prelim.): $A_1^p = (0.90 \pm 0.05)\, x^{1/2}$

(b) F_2^p from Buras and Gaermers (1978) (Nucl. Phys. B132, 249 (1978).

(c) Assume $A_1^n = 0$

$$S_{Bj}(\text{exp}) = 0.47 \pm 0.03$$

Comparison with Bjorken sum rule.

Fig. II

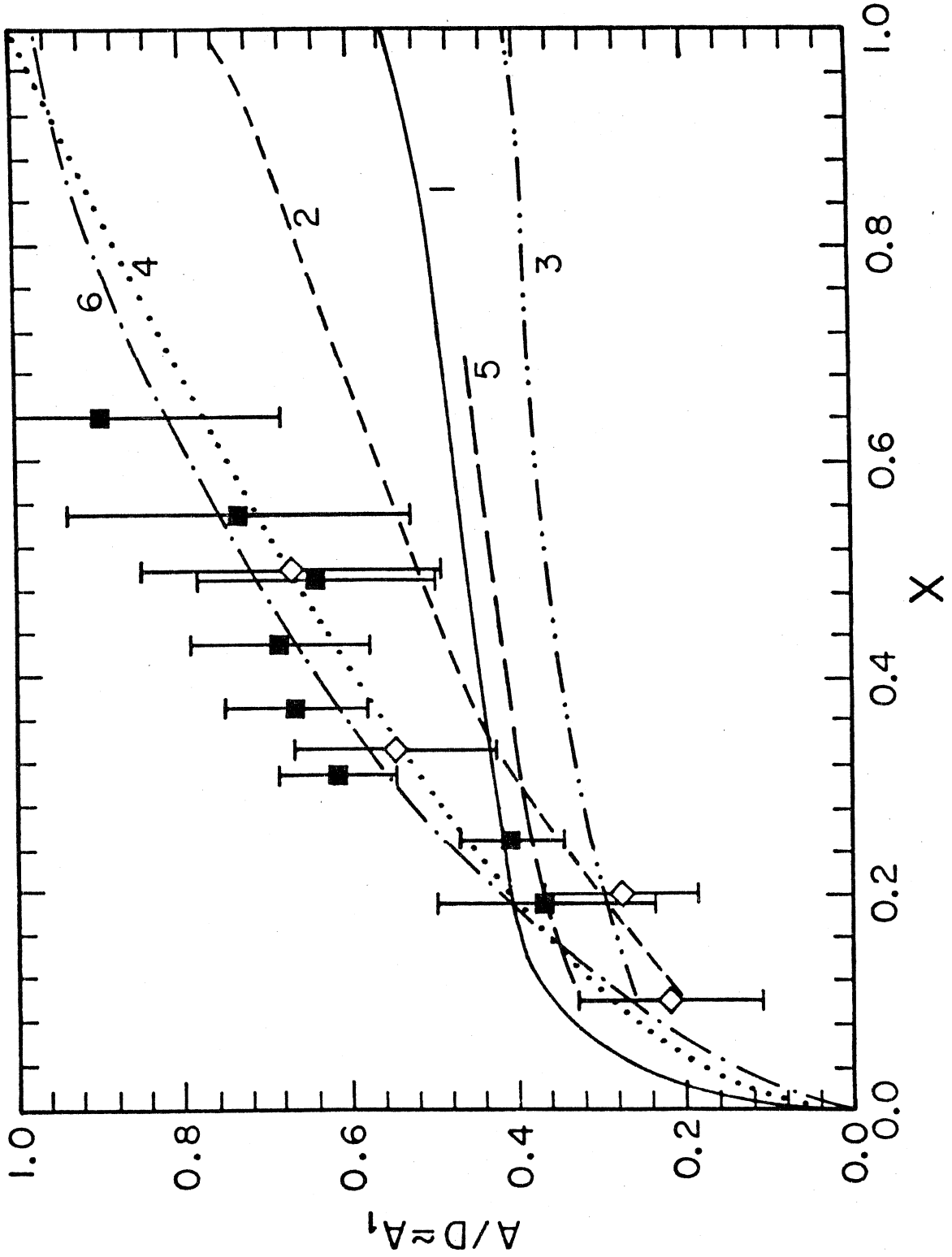

Values of A_1 for the proton and comparison with some theories.
(References to the theoretical papers are given in Appendix IV.)

Fig. III

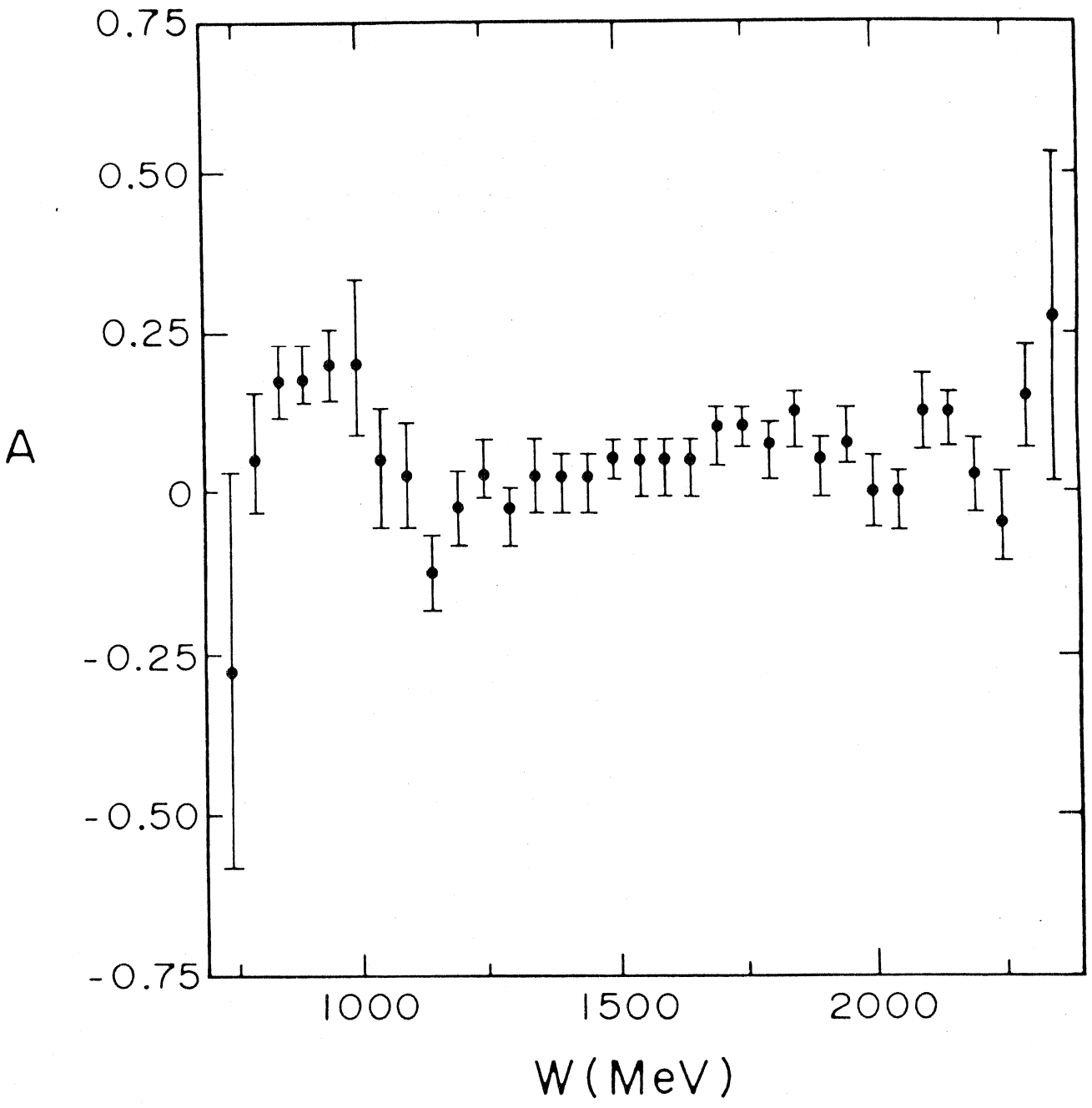

Elastic and resonance region electron-proton raw asymmetry data for A. (E130)

Fig. IV

II. MOTIVATION FOR SON OF E130

Part I of our present proposal is identical to Part II of E130. This part involves the measurement of asymmetry for the scattering of longitudinally polarized electrons by longitudinally polarized protons and by longitudinally polarized deuterons. By appropriate subtraction we can determine the asymmetry A_1 for the neutron. Relatively high precision data will be obtained for both the proton and the deuteron in the kinematic range, $2<Q^2<3$ $(GeV/c)^2$ and $0.08<x<0.5$.

The motivation for this Part I was discussed in our E130 proposal (see Appendix I) and has not changed substantially. Our measurements would provide the first data on electron-neutron asymmetry and hence the first direct information on the internal spin structure of the neutron. Models (see Fig. V) predict that the virtual photon-neutron asymmetry A_1^n should be relatively small for the neutron and hence very different from A_1^p. Our predicted measurement accuracy (see Tables V and VI) should easily reveal this qualitative behaviour. Since the Bjorken sum rule involves both A_1^n and A_1^p, a measurement of A_1^n is necessary as part of the test of the Bjorken sum rule.

Accurate values of A_1^p will aid in the discrimination of nucleon models (Fig. III). The data, particularly for small x, will also improve our test of the Bjorken sum rule. (Appendix IV) QCD corrections to the Bjorken sum rule have been discussed in several recent papers [Kodaira et al, 1979; Matsuda and Uematsu, 1980], and our more precise and extensive data will be useful for comparison with these theoretical predictions as well.

Our E80 and E130 data obtained thus far (see 1980 Wisconsin paper, p. 5) provide a test of scaling for the spin dependent structure function A_1^p in the SLAC kinematic range up to $Q^2 \simeq 10$ $(GeV/c)^2$. The more precise data we propose here will improve this test. Also the new data, particularly for small x,

will be useful for a more sensitive test of scaling violation when combined with the anticipated data on A_1^p up to $Q^2 \simeq 100$ $(GeV/c)^2$ from the European Muon Collaboration at CERN. Scaling violation for the spin dependent structure function is a topic of current interest to QCD and has been discussed in several recent theoretical papers. [Matsuda and Uematsu, 1980; Kodaira, 1980; Darrigol and Hayot, 1978; Joshipura and Roy, 1980].

The extensive and relatively precise data we will have on A_1^p after completion of Part I of Son of E130, together with our E80 and E130 data (see Fig. I), will enable us to evaluate moments of the structure function A_1^p, which are particularly useful for comparison with theoretical discussions. [Kodaira et al, 1979; Lam and Li, 1980]

The basic data we obtain on the spin structure of the proton and neutron serve as fundamental input to the understanding of polarization phenomena in hadron-hadron scattering. [Babcock et al, 1979; Hidaka et al, 1979; Hidaka, 1980; Sivers, 1978]

Part II is designed to measure the second independent virtual photon-proton structure function A_2, which arises from the interference between transverse and longitudinal photon-nucleon amplitudes. The quantity A_2 can be expressed

$$A_2 = \frac{2\sigma_{TL}}{\sigma_{1/2} + \sigma_{3/2}}$$

where $\sigma_{1/2}(\sigma_{3/2})$ is the total absorption cross section when the z component (z is the direction of the virtual photon momentum) of angular momentum of the virtual photon plus proton is 1/2(3/2), and σ_{TL} is the interference term, which may be negative. A positivity limit requires

$$|A_2| < \sqrt{R}$$

where $R = \sigma_L/\sigma_T$ is the ratio of the cross sections for absorption of longitudinal and transverse virtual photons.

In the past models of nucleon structure used to either ignore A_2 or assume $A_2 = 0$. Indeed, simple parton models predict that A_2 will be considerably smaller than its positivity limit. However, some more recent theories [Hughes, 1977; Wandzura and Wilczek, 1977; Hidaka et al, 1979] point out that A_2 is related to finite transverse momenta of the quarks and to confinement, and they predict rather large values for A_2 (Fig. VI). The quantity A_2 is somewhat analogous to the quantity R. However, our measurements of A_2 should be more accurate than current experimental measurements of R. Furthermore, our measurement of A_2 would provide a lower limit for R.

In addition to the intrinsic interest in A_2 and its importance to specific theories of nucleon structure, it is essential for us to measure A_2 in order to confirm that our measurements of the asymmetry A in the scattering of longitudinally polarized electrons by longitudinally polarized protons determine A_1 to a good approximation through the relation $A/D = (A_1+\eta A_2)/D \simeq A_1$. Or, alternatively expressed, there are two independent structure functions A_1 and A_2, and two independent measurements are needed to determine them.

Finally, measurements of the spin dependent structure functions for the proton are relevant to the old, interesting and important problem of the hyperfine structure interval $\Delta\nu$ in the ground state of hydrogen. [Brodsky and Drell, 1970] The value of $\Delta\nu(H)$ has been measured with an accuracy of about 1 part in 10^{12}. However, the theoretical value of $\Delta\nu$ is known only to about 4 parts in 10^6. The dominant uncertainty in the theory arises from the polarizability of the proton. Values of the spin dependent structure functions A_1^p and A_2^p, which we determine, will permit an evaluation of this proton polarizability contribution to $\Delta\nu(H)$ [Heimann, 1973; Souder and Hughes, 1979].

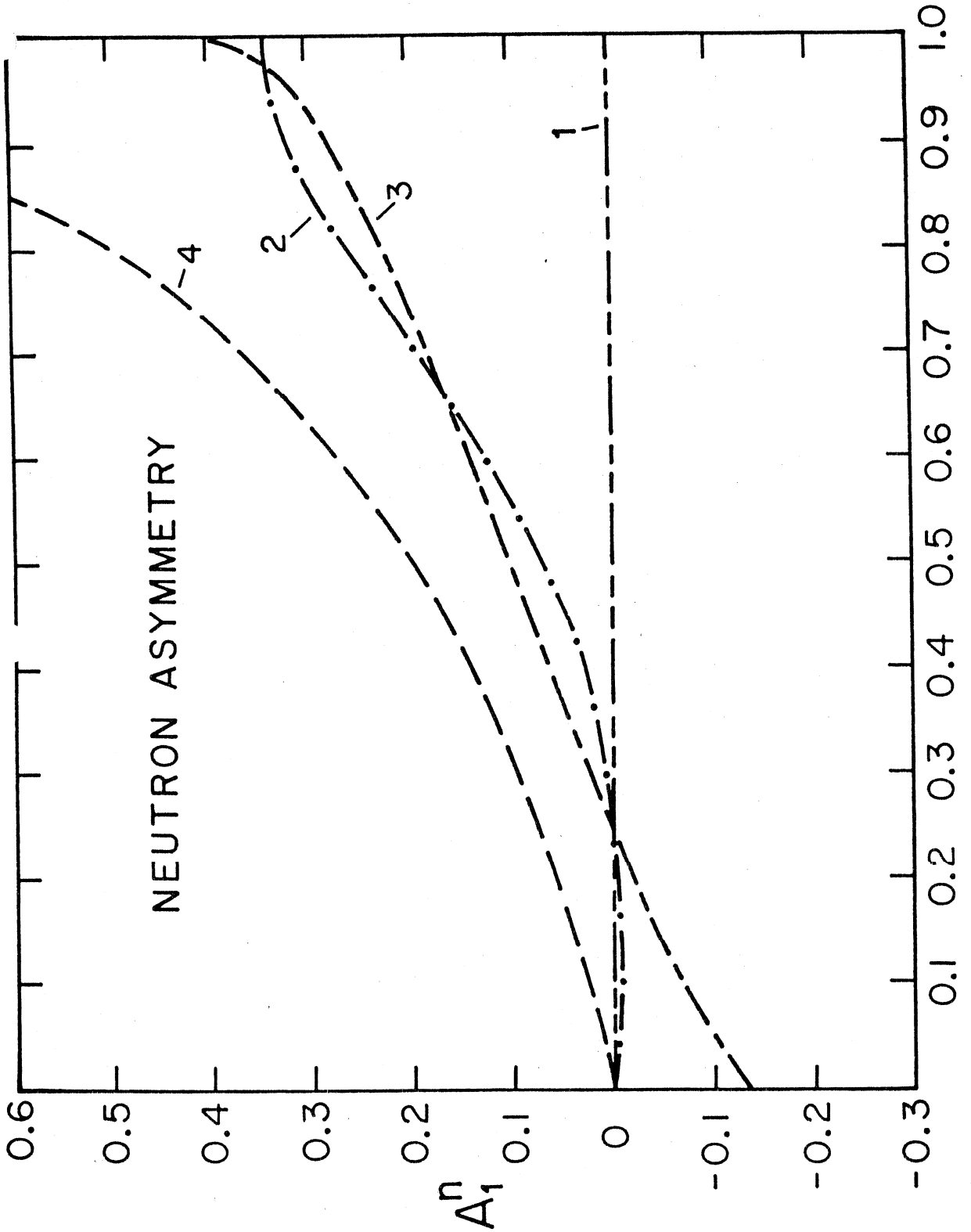

1. SYMMETRICAL VALENCE QUARK, 2. REFINED SYMMETRICAL VALENCE QUARK
3. CURRENT QUARKS, 4. UNSYMMETRICAL MODEL
(See Appendix IV for references)

Fig. V

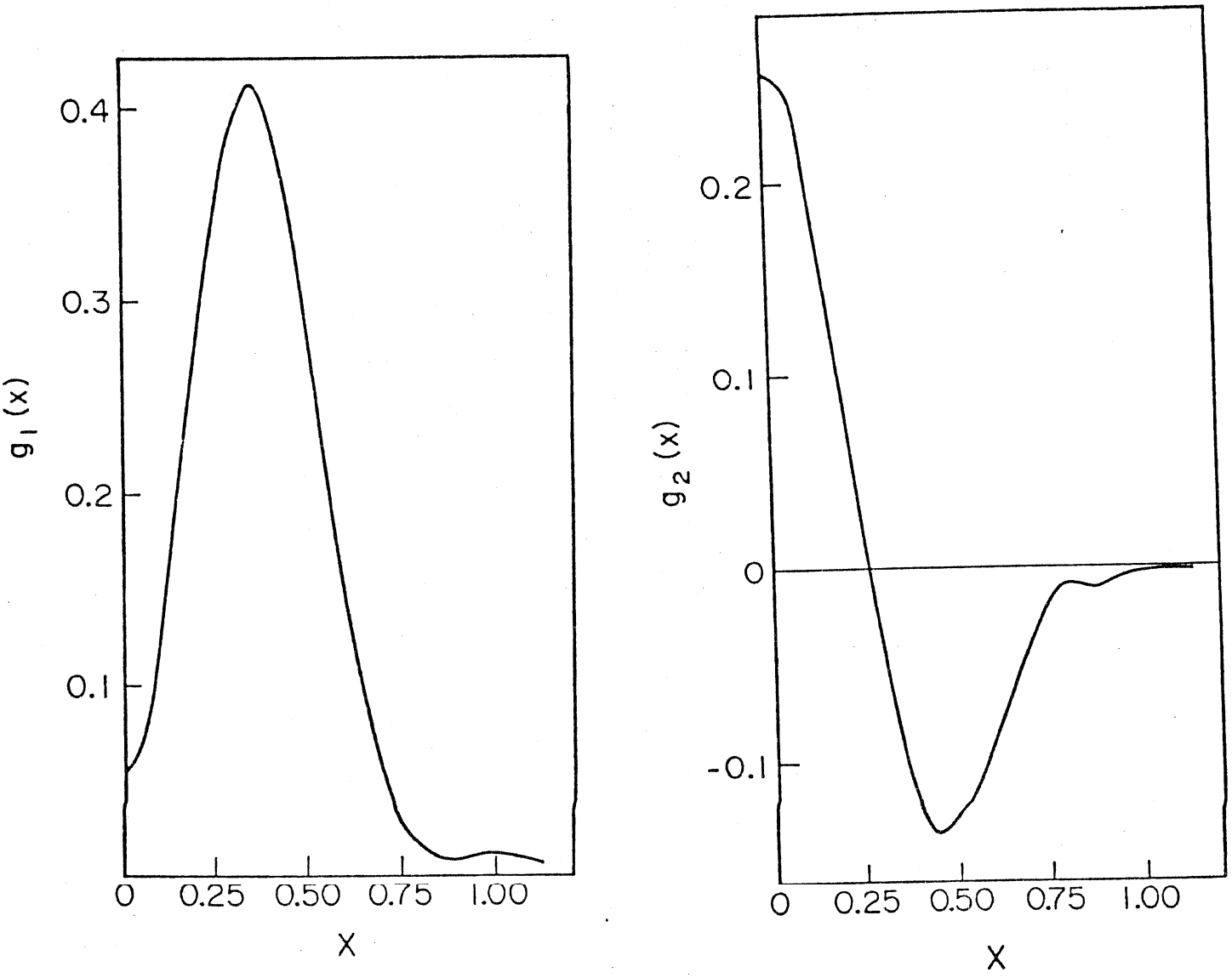

Theoretical predictions for the spin dependent structure functions $g_1(x)$ and $g_2(x)$, which determine $A_2(x)$, based on the MIT bag model [R.J. Hughes, Phys. Rev. D 16, 622 (1977)].

Fig. VI.

References for II

(1) J. Babcock et al., Phys. Rev. D 19, 1483 (1979).

(2) S. J. Brodsky and S.D. Drell, Ann. Rev. Nucl. Sci. 20, 147 (1970).

(3) R. Carlitz and J. Kaur, Phys. Rev. Lett. 38, 673, 1102(E) (1977); J. Kaur, Nucl. Phys. B 128, 219 (1977).

(4) F. Close, Phys. Lett. 43B, 422 (1973).

(5) O. Darrigol and F. Hayot, Nucl. Phys. B 141, 391 (1978).

(6) R.L. Heimann, Nucl. Phys. B 64, 429 (1973).

(7) K. Hidaka, Phys. Rev. D 21, 1316 (1980).

(8) K. Hidaka et al., Phys. Rev. D 19, 1503 (1979).

(9) R.J. Hughes, Phys. Rev. D 16, 622 (1977); R.L. Jaffe, Phys. Rev. D 11, 1953 (1975).

(10) A.S. Joshipura and P. Roy, Phys. Lett. B 92, 348 (1980).

(11) J. Kaur, Nucl. Phys. B 128, 219 (1977).

(12) J. Kodaira, Nucl. Phys. B 165, 129 (1980).

(13) J. Kodaira et al., Phys. Rev. D 20, 627 (1979).

(14) J. Kuti and V.W. Weisskopf, Phys. Rev. D 4, 3418 (1971).

(15) C.S. Lam and B.A. Li, SLAC PUB 2505 (1980).

(16) C.S. Lam and B.A. Li, SLAC PUB 2506 (1980).

(17) S. Matsuda and T. Uematsu, Nucl. Phys. B 168, 181 (1980).

(18) J. Schwinger, Nucl. Phys. B 123, 223 (1977).

(19) D. Sivers in High Energy Physics with Polarized Beams and Polarized Targets, Ed. G.H. Thomas (AIP Conf. Proc. No. 51, 1978) p. 505.

(20) P.A. Souder and V.W. Hughes, High-Energy Physics in the Einstein Centennial Year (1979), ed. B. Kursunoglu et al., (Plenum Publishing Corp., New York, 1979) p. 395-439.

(21) S. Wandzura and F. Wilczek, Phys. Lett. B 72, 195 (1977).

III. DESCRIPTION OF EXPERIMENT

Part I. With Longitudinal Target Polarization

Part I is identical to the 5^{o}-measurements of the E130 proposal which have not yet been done (appendix I). As originally proposed,we plan to use a polarized deuteron target as well as a polarized proton target. The small angular setting of the spectrometer will provide the high counting statistics which are required for precise asymmetry measurements for the proton and deuteron and hence for a determination of the asymmetry of the neutron. The operation of our experiment is detailed in our paper to the 1980 Wisconsin Conference (p. 5 of this proposal). We include some further information below. Figure VII shows the actual experimental setup that exists in End Station A with the Møller scattering electron polarimeter upstream of the polarized proton target and our new spectrometer. A schematic diagram of the spectrometer is shown in Fig. X.

The operating characteristics of the polarized electron source (PEGGY I) are given in Table I. We should point out that in E130 the average intensity available in End Station A was 5×10^{8} e^{-}/pulse, somewhat lower than the value of 7×10^{8} e^{-}/pulse in E80, and a factor of 3 less than the intensity projected in our E130 proposal. Our present proposal assumes the same intensity of 5×10^{8} e^{-}/pulse. It is worthwhile, however, to continue efforts to improve the beam intensity available at the target. We plan to upgrade the UV-optics and also to try to increase the flashlamp output in PEGGY. In order to improve the overall transmission, which was 20 to 40% in E130, more reliable current monitors in the PEGGY beam transport and along the accelerator should be considered. The measurement of the electron polarization by Møller scattering was done using a double arm coincidence technique for the first time, which gave very satisfactory results. With the single arm techniques employed in earlier experiments, background subtraction used to be an important source of error in the measurement of the electron polarization. A spectrum of the coincidence signal is shown in Fig. VIII and indicates only a very small background.

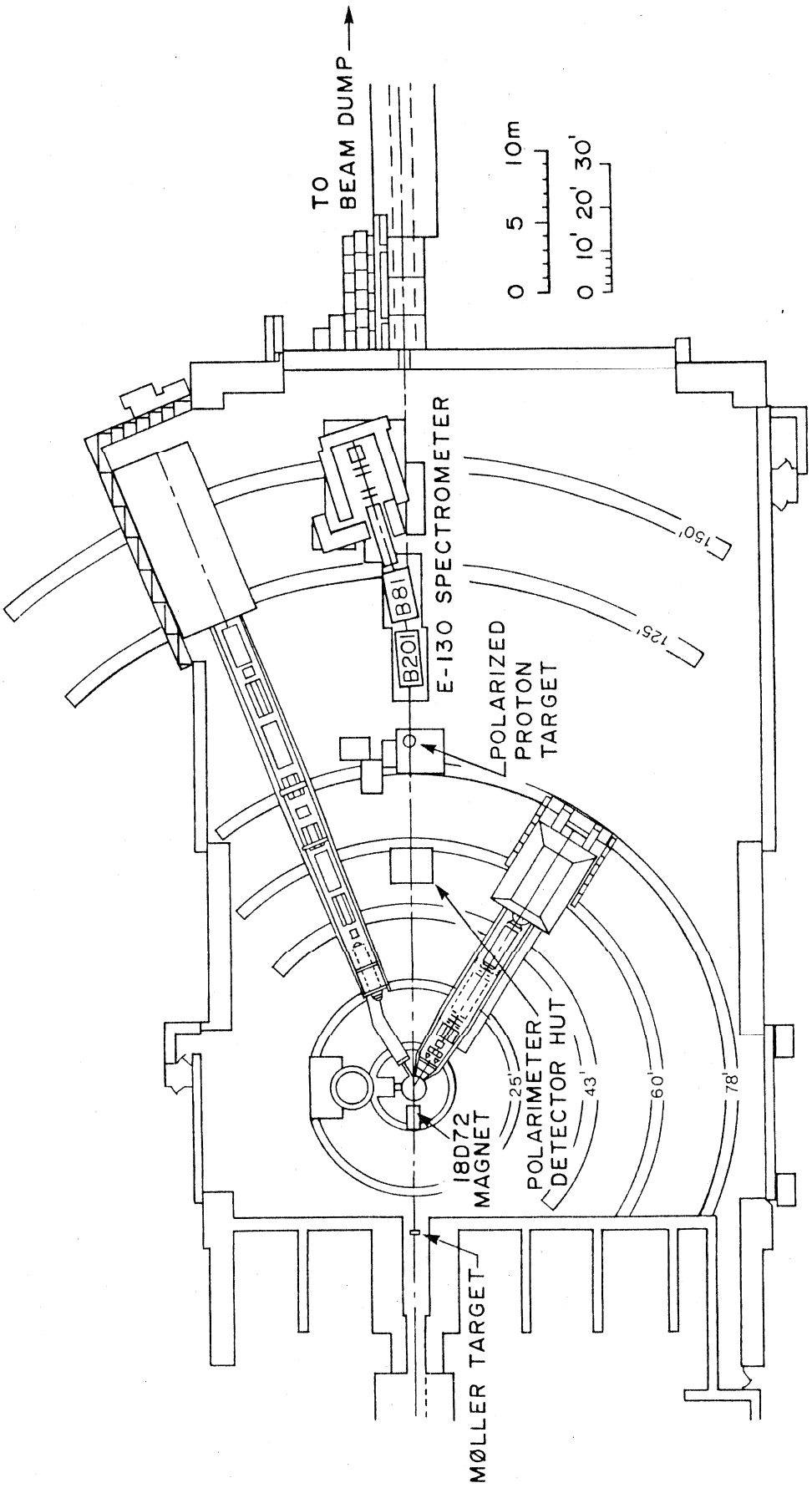

E-130 SET-UP IN END STATION A

Fig. VII.

Table I. Operating Characteristics of Polarized Electron Beam

Characteristic	Value
Pulse length	1.5 μs
Repetition rate	180 pps
Average intensity at GeV Energies (E130)	5×10^8 e^-/pulse
Pulse to pulse intensity variation	<5%
Polarization	0.80 ± 0.03
Polarization reversal time	3s
Intensity difference upon reversal	<5%
Lifetime of Li oven load	175 h
Time to reload lithium	40 h
Overall availability	75%

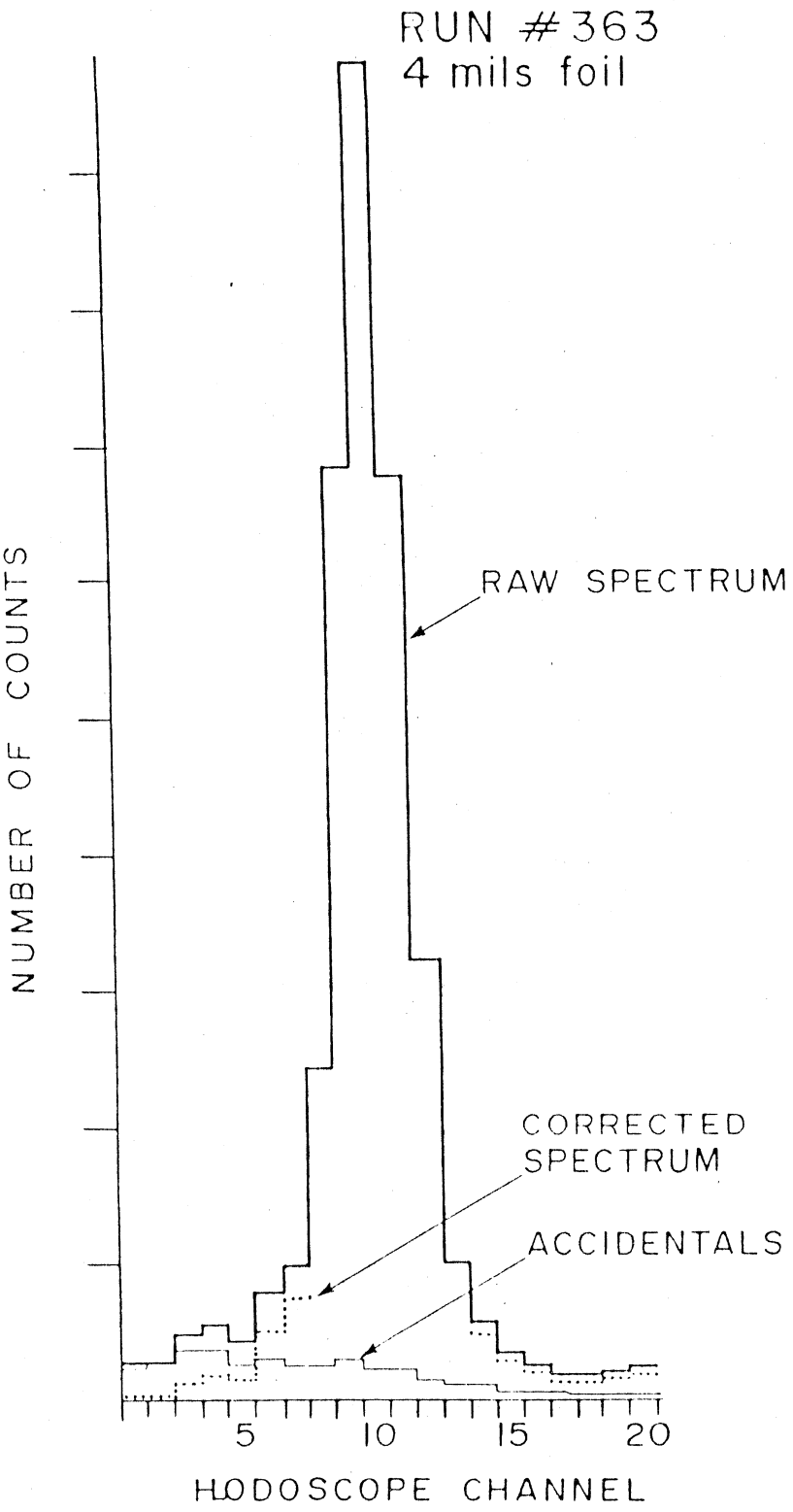

MØLLER SIGNAL (Coincidence Technique)

Fig. VIII

The operating conditions of the polarized proton target are shown in Table II. A higher polarization was obtained then in E80 due to reduction in the cryostat operating temperature and to increased microwave power. Last month we studied the deuteron polarization again and obtained a value of $P_D = 0.28$, somewhat higher than assumed in our E130 proposal. Also it has been found at the University of Bonn that a deuterated butanol target is about a factor of 2 more resistant to radiation damage than a normal butanol - porphyrexide target. Hence the average deuteron polarization for our present proposal is taken as indicated in Table II and is almost a factor of 2 larger than the value projected in our E130 proposal.

Recent measurements we have made at SLAC on dynamic nuclear polarization of irradiated targets (Seely et al., 1980) indicate that it may be possible to use NH_3 as the material in a polarized target. (Niinikoski, 1979 and Althoff, 1980) If this is possible, a gain in polarization by a factor of about 1.3 (ratio of number of polarizable protons in NH_3 to that in butanol) and in effective counting rate by about 50% would be obtained. Furthermore, there are indications that radiation damage of a pure NH_3 target may be significantly less than that of our usual butanol-porphyrexide target. Further tests by our group at SLAC are required to pursue this possibility.

We are presently testing and will soon install a different and higher power 130 GHz microwave system, which should improve the polarization and other operating conditions of our target.

M.L. Seely, et al., Paper submitted to the Fifth International Symposium on Polarization Phenomena in Nuclear Physics, Santa Fe, August 1980.

T.O. Niinikoski et al., Phys. Lett. 72A, 141 (1979).

K. Althoff, Private Communication, 1980.

Table II. Operating Characteristics of Polarized Target

Characteristic	Value
Magnetic field	50 kG
Temperature	$0.99^{o}K$
Target material	Butanol-porphyrexide
Microwave power to cavity	~425 mW
LHe consumption	10 LL/hr.
Initial proton polarization	0.75 to 0.80
Polarizing time	~4.4 min.
Depolarizing dose (1/e)	3×10^{14} e^{-}/cm^{2}
Average proton polarization (E130)	0.6
Initial deuteron polarization	0.28
Average deuteron polarization (projected)	0.23

Part II. With New Transversely Polarized Target.

Measurement of the second spin dependent structure function A_2 for the proton requires that the proton polarization be transverse to the longitudinally polarized electron beam and lie in the plane of the electron scattering. The asymmetry to be measured will be:

$$A_T = \frac{d\sigma_{\rightarrow\uparrow} - d\sigma_{\leftarrow\uparrow}}{d\sigma_{\rightarrow\uparrow} + d\sigma_{\leftarrow\uparrow}} = d[\zeta A_1 - A_2]$$

where the symbols are defined in Table VII and in (Gilman, 1973). The kinematic values are such that the measurement of A_T determines principally A_2. The experimental technique for measuring A_T is the same as that for measuring A with a longitudinally polarized target.

The incident and scattered electron beam will be deflected slightly by the transverse B field of the magnet in the polarized target. The deflection of the scattered electron beam can be readily accounted for in the measurement of the scattering angle. The incident beam will require either a beam dump inside the End Station or a compensation field downstream of the target in order to reach the ESA East Dump.

Polarized Target

The only change in the experiment for Part II as compared to Part I is the change in the polarized target to provide a transverse proton polarization. The E130 polarized target system will be used with several important but relatively inexpensive modifications.

We propose to build a new magnet which will provide a transverse magnetic field of 5 T over a 50 cm^3 target volume with a precision of approximately 5×10^{-5}. The gap between the magnet pole faces will be reduced to about 10 cm which requires that the cryostat vacuum jacket and cooling system be reduced correspondingly. This is a minor change which was anticipated in the design of the existing cryostat. The target cup, support insert tube, and extractor box will remain unchanged.

F. Gilman in SLAC PUB-SLAC 167, Vol. I, (1973) p. 71.

Table III. Superconducting Magnet with Transverse Field (Specifications)

- 5.05 T transverse central field, $\pm 5 \times 10^{-5}$ precision over 50 cm^3

- 2 opposed coils, with conical pole faces in a modified Helmholtz configuration

- Hollow pole pieces for insertion of ferromagnetic shims if required.

- General overall dimensions:

inner radius	2 cm
outer radius	24 cm
taper	15
separation(coils)	12 cm
separation(forms)	10 cm
height (overall)	40 cm
winding density	3600 turns/coil
construction	layer wound on 316 stainless steel formers, G 10 spacers between layers.
cooling	percolation, liquid helium at 4.45° K
stability	intrinsic
insulation	formvar
supply current	900 A @ 5.1 T

conductor: NbTi multifilament, copper clad, copper to superconductor ratio 1.25

Twist pitch: 1 turn per 2.5 cm

conductor size .350 x .175 cm^2, rectangular, wound in easy direction

filament size not to exceed 75 μm

inductance ~2 H

Stored energy: 810 Kj

charging voltage ~ 5V

Superconducting Magnet

The new magnet will be a 5 T modified set of Helmoholtz coils with their axis vertical and with conical pole faces, separated by about 10 cm. The pole faces will be at ~15° with respect to the horizontal axis, which will comfortably accomodate a 10·5° scattered beam. The coils will be wound on separate coil forms and the final field homogeneity will be achieved by a combination of mechanical shims and 2 sets of compensating windings. The design is such that the new magnet can be used with the existing power supply, leads and instrumentation. To install it, it will not be necessary to remove the present magnet and vacuum system assembly; the existing helium vessel can be removed in situ and the magnet removed by opening only 2 welds. The helium vessel itself with all the associated support, insulation etc. will remain unaffected. The support system of the new magnet, its base tube and electrical connections will be unchanged. All the materials used in its construction are readily available items of commerce.

Cryostat

The outside diameter of the cryostat vacuum vessel will be reduced to 7.5 cm. The change in diameter will be made at the existing cone-to-cylinder transition, in a region which will accomodate the existing heatexchanger. The latter will be moved 15 cm up-beam from its present position. During the development of this cryostat we experimented with such a displacement in order to measure the degree to which the position of the test exchange affects the performance of the cryostat: we found no significant changes. Some minor modifications to the cold end of the microwave system will also be made.

We hope that the smaller diameter of the cryostat vacuum jacket will permit us to install a somewhat thinner aluminum exit window, and a more efficiently cooled liquid nitrogen shield. However these changes are quite small, both from the cost and from the manpower point of view.

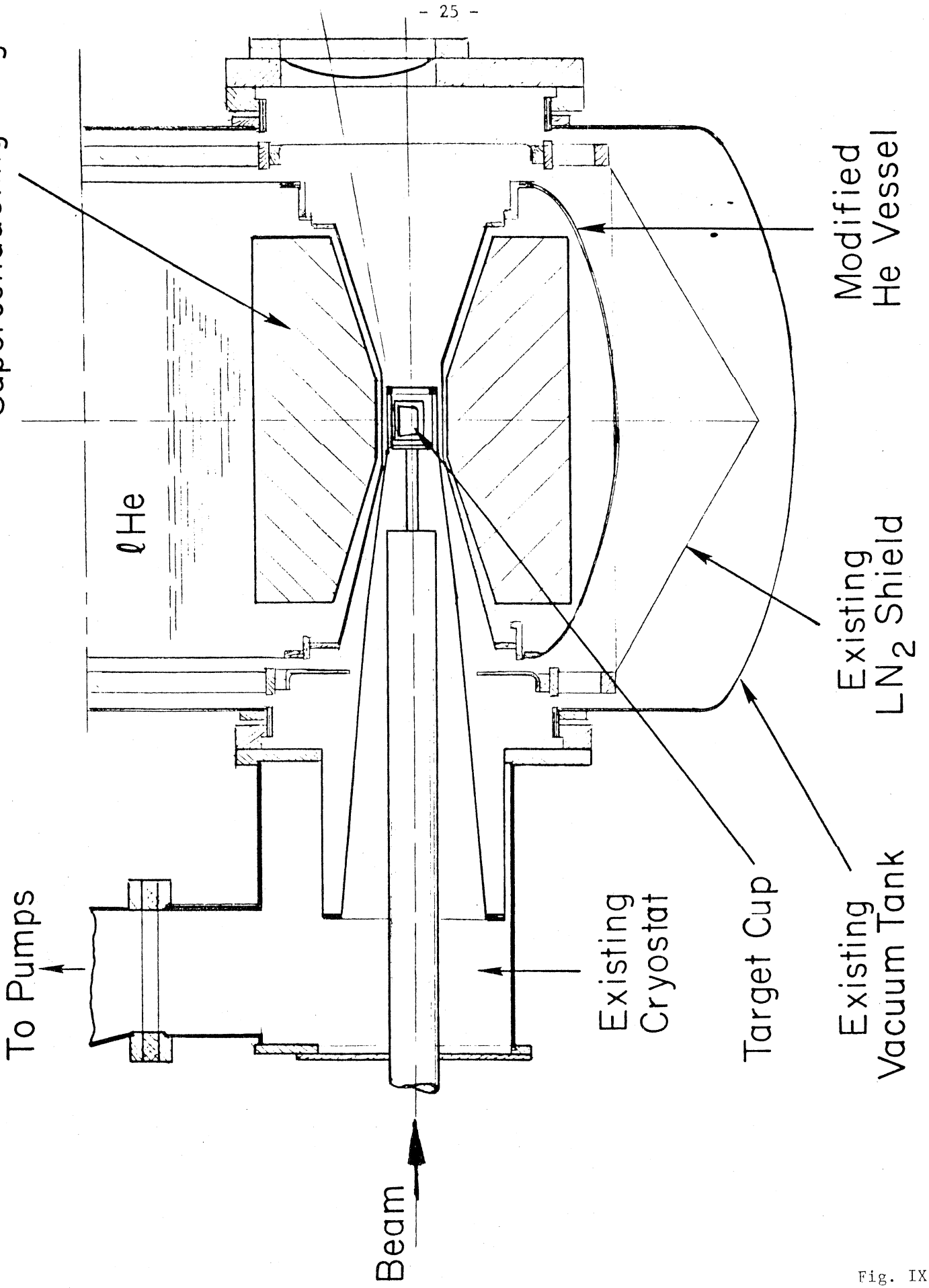
Superconducting Magne
Modified
He Vessel
ℓ He
Existing
LN_2 Shield
To Pumps
Existing
Cryostat
Target Cup
Existing
Vacuum Tank
Beam

Fig. IX

Spectrometer

The existing E130 spectrometer will be used and will have to be changed over from its present 10^{o}-setup to a scattering angle of 5^{o}. Detailed plans and hardware required for the change over have been prepared by the spectrometer facilities group and it is anticipated that the physical setup will take 4-8 weeks. Installation of detector cables and electronics will take an extra 2 weeks.

A schematic layout of the E130 spectrometer is shown in Fig. X. In contrast to the standard 8-GeV/c and 20 GeV/c spectrometers at SLAC, the E130 spectrometer is of the non-focussing type and uses bending magnets only. The particle momenta are determined by ray tracing in a PWC-system. The spectrometer takes a very large momentum bite ($\Delta p/p \approx \pm 25\%$) and its acceptance $\int d\Omega\, dp/p$ is approximately one (two) order(s) of magnitude(s) larger than that of the 8 GeV/c (20 GeV/c) spectrometer. The momentum resolution $\Delta p/p$ of $\pm 1\%$ is actually better than we need in the deep inelastic region.

Electron identification is accomplished with a segmented total absorption lead glass shower counter and a 4m long nitrogen gas Cerenkov counter which may be operated at subatmospheric pressure. In addition to the PWC system ($\approx$4000 wires) there is a scintillator hodoscope with 12 x 16 segments and scintillator trigger counters. The useful detector area is 32 cm x 90 cm.

The detectors have been tested extensively under test beam conditions and performed quite well in the E130 experiment at the spectrometer setting of 10^{o}. Under these conditions we had very clean PWC tracks (1.01 track/trigger). Only the redundant, aperture defining scintillation counters proved rather useless due to sensitivity to soft background. The combined pion rejection capability of the lead glass and gas Cerenkov counters will also be sufficient at the 5^{o} setting where the π/e ratio is expected to be <6.

Data Tables, Statistical and Systematic Errors

The following tables IV-VII give kinematic information, cross sections, expected counting rates and statistical errors for the three proposed data types (Proton A_1, Deuteron A_1, and Proton A_2) computed for the running times listed in table VIII.

Most of the variables used in table IV are explained in Alguard et al., Phys. Rev. Lett. 37, 1261 (1976) (see appendix III). There are also some new kinematic quantities relating to the tranverse electron-proton asymmetry $A_T = d(\zeta A_1 - A_2)$. The factor d may be interpreted as a depolarization factor which degrades the electron polarization to a smaller virtual photon polarization and it is analogous to the factor D in the usual formula for the longitudinal asymmetry. A similar correspondence exists between the factors ζ and η .

The counting rates for regular and deuterated butanol targets are based on the nucleon cross sections listed in table IV. No radiative corrections have been made to the cross sections and counting rates. The solid angle $\Delta\Omega$ refers to the spectrometer solid angle which varies with E' and is largest near the central momentum. For the A_1-data we choose a central momentum setting of the spectrometer of 14 GeV/c. For the A_2-data we choose 15 GeV/c in order to emphasize the high x-region.

In addition to the statistical errors there are the usual systematic errors of 3-5% associated with the measurements of P_e, P_p, P_d, and F. In principle, due to radiative effects the actual counting statistics will be modified, and also there will be errors associated with the radiative corrections to be applied to the measured asymmetries. We have estimated the radiative effects on A_1 for the proton and find that the error will be increased only by $\Delta A_1/A_1 \approx 0.5 - 1.5\%$.

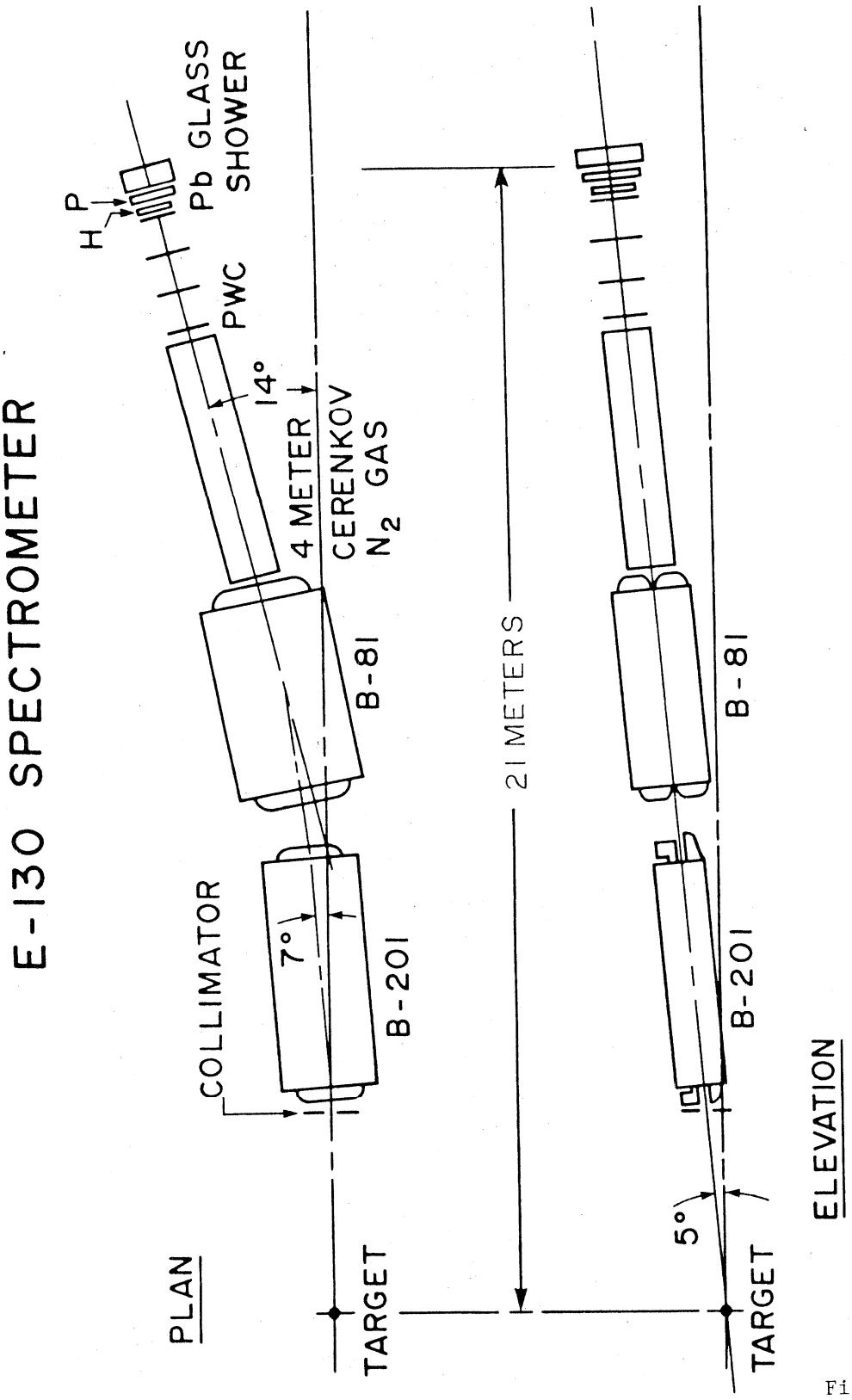
E-130 SPECTROMETER
H
P
Pb GLASS SHOWER
PWC
14°
4 METER CERENKOV N_2 GAS
B-81
21 METERS
COLLIMATOR
7°
B-201
PLAN
TARGET
B-81
B-201
5°
TARGET
ELEVATION

Fig. X

Table IV: Kinematics and Cross Sections (E = 22.66 GeV, $\theta = 5^{o}$)

E'	ν	Q^2	W	ω	x	ϵ	$D^{(a)}$	η	$d^{(a)}$	ζ	F_2^p	$d^2\sigma/(d\Omega dE'/E')$ P	$\frac{1}{2}(p+n)$
(GeV)	(GeV)	$(GeV/c)^2$	(GeV)									$(x10^{-30}$	$cm^2/sr)$
19.5	3.16	3.36	1.86	1.76	.568	.985	.122	.523	.122	.527	.131	2.28	1.72
19.0	3.66	3.28	2.11	2.10	.476	.981	.142	.442	.141	.446	.188	2.76	2.18
18.5	4.16	3.19	2.34	2.45	.408	.976	.163	.379	.162	.384	.236	2.98	2.43
18.0	4.66	3.10	2.55	2.82	.355	.970	.184	.328	.183	.333	.273	3.01	2.52
17.5	5.16	3.02	2.75	3.21	.312	.964	.206	.289	.204	.294	.301	2.93	2.51
17.0	5.66	2.93	2.93	3.62	.276	.957	.228	.256	.225	.262	.321	2.78	2.43
16.5	6.16	2.85	3.10	4.06	.246	.948	.250	.228	.247	.234	.336	2.61	2.31
16.0	6.66	2.76	3.26	4.53	.221	.939	.273	.204	.269	.211	.345	2.43	2.18
15.5	7.16	2.67	3.41	5.03	.199	.929	.296	.184	.291	.191	.352	2.25	2.04
15.0	7.66	2.59	3.56	5.56	.180	.917	.320	.166	.313	.174	.356	2.08	1.90
14.5	8.16	2.50	3.70	6.12	.163	.905	.343	.150	.334	.158	.357	1.92	1.77
14.0	8.66	2.41	3.84	6.73	.149	.891	.368	.136	.357	.144	.358	1.77	1.74
13.5	9.16	2.33	3.97	7.38	.136	.876	.392	.123	.379	.132	.358	1.63	1.53
13.0	9.66	2.24	4.09	8.09	.124	.860	.417	.112	.401	.121	.357	1.51	1.42
12.5	10.16	2.16	4.22	8.85	.113	.843	.442	.102	.423	.111	.355	1.40	1.32
12.0	10.66	2.07	4.34	9.67	.103	.824	.467	.093	.444	.103	.353	1.29	1.23
11.5	11.16	1.98	4.45	10.56	.095	.804	.493	.084	.465	.094	.351	1.20	1.15
11.0	11.66	1.90	4.57	11.54	.087	.783	.518	.073	.485	.083	.349	1.12	1.07
10.5	12.16	1.81	4.68	12.60	.079	.760	.544	.070	.506	.081	.346	1.04	1.00
10.0	12.66	1.72	4.79	13.78	.073	.736	.570	.063	.525	.074	.344	.97	.94

$$A = D(A_1 + \eta A_2), \quad D = \frac{E - E'\epsilon}{E(1 + \epsilon R)}, \quad \eta = \frac{\epsilon(Q^2)^{\frac{1}{2}}}{E - E'\epsilon}$$

$$\epsilon = \frac{1}{1+2(1+\nu^2/Q^2)\tan^2\frac{1}{2}\theta}$$

$$A_T = d(\zeta A_1 - A_2), \quad d = \left(\frac{2\epsilon}{1+\epsilon}\right)^{\frac{1}{2}} D \qquad \zeta = \frac{1+\epsilon}{2\epsilon}\eta$$

(a) We assume $R = \sigma_L/\sigma_T = 0.25$

Table V: Kinematics and Counting Rates for Proton A_1 - Data (E = 22.66 GeV, $\theta = 5^o$)

E' (GeV)	ν (GeV)	Q^2 $(GeV/c)^2$	W (GeV)	ω	x	$\Delta\Omega$[a] (msr)	events/pulse[b]	events/100 hrs[c] $(x10^6)$	stat. error in Δ[d] $(x10^{-4})$	stat. error in A_1^p[e]
19	3.66	3.28	2.11	2.10	.476	.39	.029	1.9	7.2	.071
18	4.66	3.10	2.55	2.82	.355	.46	.037	2.4	6.5	.051
17	5.66	2.93	2.93	3.62	.276	.53	.041	2.7	6.1	.039
16	6.66	2.76	3.26	4.53	.221	.60	.044	2.9	5.9	.032
15	7.66	2.59	3.56	5.56	.180	.66	.045	2.9	5.9	.028
14	8.66	2.41	3.84	6.73	.149	.63	.040	2.6	6.2	.025
13	9.66	2.24	4.09	8.09	.124	.50	.029	1.9	7.2	.026
12	10.66	2.07	4.34	9.67	.103	.35	.019	1.2	9.1	.033
11	11.66	1.90	4.57	11.54	.087	.21	.011	0.7	11.8	.035
10	12.66	1.72	4.79	13.78	.073					

(a) Central momentum of spectrometer set to 14 GeV/c.

(b) Assumes 0.5 x 10^9 e^-/pulse, a 3.8 cm long Butanol target of density 0.6 g/cm^3, and a 20% loss due to beam rastering.

(c) Assumes 180 pulses/second

(d) $\Delta = P_e P_p F A$ is the raw counting rate asymmetry.

(e) $A_1^p \approx A^p/D = \Delta/(P_e P_p F D)$, we assume $P_e = 0.80$, $\langle P_p \rangle = 0.60$, F = 0.13, and $nA_2 = 0$.

Table VI: Kinematics and Counting Rates for Deuteron A_1 - Data (E = 22.66 GeV, $\theta = 5^o$)

E' (GeV)	ν (GeV)	Q^2 $(GeV/c)^2$	W (GeV)	ω	x	events/pulse[a]	events/200 hrs ($\times 10^6$)	stat. error in Δ ($\times 10^{-4}$)	stat. error in A_1^d[b]	stat. error in A_1^n[c]
18	4.66	3.10	2.55	2.82	.355	.087	11.3	3.0	.031	.082
16	6.66	2.76	3.26	4.53	.221	.098	12.7	2.8	.021	.055
14	8.66	2.41	3.84	6.73	.149	.076	9.8	3.2	.018	.048
12	10.66	2.07	4.34	9.67	.103	.034	4.4	4.8	.022	.059
10	12.66	1.72	4.79	13.78	.073					

(a) Assumes a deuterated Butanol target, all other conditions as for Table IV.

(b) $A_1^d = \Delta/(P_e P_d F_d D)$, we assume $P_e P_d F_d = 0.042$

($P_e = 0.80$, $\langle P_d \rangle = \langle P_p \rangle = \langle P_n \rangle = 0.23$, $F_d = F_p + F_n = 0.13 + 0.10 = 0.23$).

(c) $A_1^n \approx A^n/D = (F_d/F_n) A_1^d - (F_p/F_n) A_1^p$

Table VII: Kinematics and Counting Rates for Proton A_2 - Data (E = 22.66 GeV, $\theta = 5^o$)

E' (GeV)	ν (GeV)	Q^2 $(GeV/c)^2$	W (GeV)	w	x	$\Delta\Omega$[a] (msr)	events/pulse	events/200 hrs ($\times 10^6$)	stat. error in Δ_T[b] ($\times 10^{-4}$)	stat. error in A_T/d[c]
19.5	3.16	3.36	1.86	1.76	.568	.45	.029	3.8	5.2	.059
18.5	4.16	3.19	2.34	2.45	.408	.51	.040	5.2	4.4	.039
17.5	5.16	3.02	2.75	3.21	.312	.57	.046	6.0	4.1	.029
16.5	6.16	2.85	3.10	4.06	.246	.64	.049	6.4	4.0	.024
15.5	7.16	2.67	3.41	5.03	.199	.67	.047	6.1	4.0	.020
14.5	8.16	2.50	3.70	6.12	.163	.59	.040	5.2	4.4	.020
13.5	9.16	2.33	3.97	7.38	.136	.43	.026	3.4	5.4	.022
12.5	10.16	2.16	4.22	8.85	.113	.31	.018	2.3	6.5	.023
11.5	11.16	1.98	4.45	10.56	.095	.19	.010	1.3	8.8	.029
10.5	12.16	1.81	4.68	12.60	.079					

(a) Central momentum of spectrometer set to 15 GeV/c, transverse target polarization, otherwise as for Table IV.

(b) $\Delta_T = P_e P_p F A_T$

(c) $A_T/d = \zeta A_1 - A_2$

Table VIII: Running Time

Data Collection*	Factored Hours
Proton (Longitudinal target polarization)	100
Deuteron (Longitudinal target polarization)	200
Proton (Transverse target polarization)	200
Checkout, including background studies and Møller measurement 6 weeks at 10 to 60 pps	

Our plan for data-taking is first to obtain data on proton and deuteron asymmetries with longitudinal target polarization. This requires moving our spectrometer to its 5^{o} setting from its present 10^{o} setting (estimated to take about 8 weeks of work in End Station A), reestablishing PEGGY I in the injector tunnel (estimated to take about 4 months), and reestablishing a VAX computer in the ESA counting house(estimated to take about 3 months after the computer is available.)

Secondly,we will obtain data with the transverse target polarization. This will require replacing our present superconducting magnet which provides a longitudinal magnetic field with a new superconducting magnet which provides a transverse magnetic field. If the new magnet is available, this change will require about 6 months to do. Then the data-taking on the proton with the transverse target polarization could be completed.

* All data will be taken with the single 5^{o} setting of our spectrometer.

Group Proposing Son of E130 Experiment

YALE

M.R. Bergstrom
P.R. Bolton
S.K. Dhawan
R.A. Fong-Tom
V.R. Harsh
V.W. Hughes (spokesman)
R.F. Oppenheim
K.P. Schuler
M.L. Seely
P.A. Souder
M.E. Zeller
Students

SLAC

S. St Lorant
R. Miller

ANL

A. Yokosawa

UNIVERSITY OF BERNE

U. Moser

UNIVERSITY OF BIELEFELD

G. Baum
W. Raith

CCNY

M.S. Lubell

SACLAY

N. de Botton

UNIVERSITY OF TSUKUBA; KEK

K. Kondo
S. Miyashita
K. Morimoto
I. Nakano
K. Takikawa
Students

Table IX: Required Equipment and Facilities

Item	Status	Responsibility
Polarized electron source (Peggy I)	Need to reinstall in injector tunnel	SLAC-Yale
	UV Optics to have recoating of mirrors	Yale
	Gas compressor older Corken	Yale-owned
	New one needed	SLAC ($6000)
Polarized target	Available and set up for longitudinally polarized target.	
	New superconducting magnet for transverse polarization to be built	Tsukuba-Yale
	Cryostat modifications and new magnet installation	SLAC-Yale
Spectrometer	Available. Must be moved to 5^{o} Scattering angle	SLAC
	Electronics. HEEP equipment (see following list)	SLAC
End Station A	VAX/780 Computer	Yale (or SLAC) (DOE has indicated to our Yale group that they will plan to provide this computer to our group, probably on lease-purchase agreement. (See page 37)

August 1, 1980

SLAC Electronic Equipment used in E130 and needed for Son of E130

HEEP EQUIPMENT

Item	Model No.	Quanity
ADC, 12 channel	LRS 2249A	3
Analog MPX	LRS 2232A	3
Bipolar fan in	127B	1
Bipolar fan in	LRS 127D	3
CAMAC crate		8
Coinc.	EGG C 144/N	2
Coinc.	J 103	11
Coinc. latch	C 124	5
Crate controller	CCA-2	5
Dataway display	Joerger DD	2
Droege boxes	VK 5900	6
Dual amp (adjustable gain)	LRS 333	1
Dual disc.	161	1
Dual scalers	Jorway 80	26
Fan in/out	J 102	11
Gate & delay gen.	Ortec	2
Gate generator	GG 200/N	3
Gate generator	Joerger GG	4
Gate generator	108-177-29-RO	1
Level Translator	RS 688 AL	1
Linear fan in/out	428	1
Linear fan out	128	1
Logic	LRS 364A	1
Multilevel output	446-601	1
Nim bins with 6v		5
Nim bins w/o 6v		13
Octal disc.	LRS 620	1
Octal disc.	620 AL	1
Octal disc.	LRS 623	7
Quad coinc.	622	3
Quad disc.	321 B	1
Quad scalers	Joerger S1	13
QVT-old model modified	QVT	2
QVT	30001/3157/DPPQ7	1
16 channel DCR	LRS 2340B	4
Strobed coinc.	C 126/N	5
Switch input register	BiRa 2501	2
TSI-dual scalers		6
12 channel ADC	2249A	1
12 channel Amplifier	612	3
12 channel scaler	LRS 2551	1
Updating disc.	TR204AN	13
Verification Module	135-102	2
Bipolar fan in	128	1

LEEP EQUIPMENT

Data Pulsers	2
485 scopes	2
475 scopes	1
H.P. scope	1
Ligna Sweep	1
Misc. D.C. Power Supplies	4

COMPUTER

5 YEAR LEASING ARRANGEMENT

Monthly payment = .023 x $215K = $4.9K.

Buy out at the end of 60 months pay 10% of original cost to buy the system.

Total cost under lease to buy system:

= 60 x $4.9K + $215K x .1

= 294 + 21.5K

= $315.5K

Delivery: 12 months after receipt of order.

POLARIZED TARGET

Cost Estimate

It is very difficult at this time to estimate the costs for the various changes; this cost estimate must therefore be regarded as being very preliminary.

Magnet, complete, 2 coils, not shimmed for maximum field homogeneity but tested to verify performance $65 K, magnet optimization, 3 cycles $3.6 K

magnet installation	3 man weeks	
magnet tests(helium)	$1.5 K	
modifications to helium vessel	$ 0.75K	
modifications to nitrogen shield	$ 3.5K	
modifications to cryostat	4 man weeks	$0.5K M&S
tests of magnet and cryostat (helium, 3 cycles)		$4.5 K
miscellaneous mechanical , electrical		$1.5 K

APPENDIX I

SLAC Proposal E-130

Supplement No. 1

May 5, 1977

SLAC PROPOSAL - E130

Precise Measurements of Asymmetries in Deep Inelastic Scattering of Polarized Electrons by Polarized Protons and by Polarized Deuterons

Yale-SLAC-Bielefeld-Tsukuba Group
(V.W. Hughes, correspondent)
First submitted, December 23, 1976
Revised, May 2, 1977

Title: Precise measurements of asymmetries in deep inelastic scattering of polarized electrons by polarized protons and by polarized deuterons.

Experimenters: V.W. Hughes (correspondent), Yale University
M.J. Alguard, M.R. Bergstrom, J.E. Clendenin, S. Dhawan, R. Fong-Tom V.W. Hughes, M.S. Lubell, R.F. Oppenheim, D.A. Palmer, N. Sasao, K.P Schüler, P.A. Souder, and M.E. Zeller - Yale University.

R.H. Miller and S.J. St Lorant - SLAC.

G. Baum and W. Raith - University of Bielefeld, West Germany.

K. Kondo and S. Miyashita - University of Tsukuba, Japan.
K. Morimoto, KEK, Japan

Beam: Polarized electron (PEGGY I). Energy, 22 GeV; current, 1.5×10^9 e^-/pulse; pulse length, 1.5 μsec; pulse repetition rate, 180 pps.

Target: Hydrocarbon polarized proton or polarized deuteron target, 2.5 cm x 2.5 cm x 3.8 cm. Set up in End Station A (ESA).

Experimental equipment and materials requested of SLAC
- One deflector magnet, 5D36
- Beam monitors: Two toroid charge monitors (#0 and #1);
- Beam dump, SEQ, and associated shielding
- One spectrometer using two existing ESA magnets
  - Supporting frame for magnets and detector house
  - Substantial shielding for detector house
- Lead glass shower counter (available from SFG)
- Counting room electronics (ESA)
- Existing SLAC-Yale polarized target
  - Liquid He for polarized target (220 ℓ/day); also LN_2 (100 ℓ/day
- Möller spectrometer being developed for E122

Date when equipment ready:
- Polarized electron source (Fall, 1977).
- Polarized target (Spring, 1978).
- Spectrometer (Summer, 1978).

Running time required:
- Check out: 250 hrs at 10 to 30 pps.
- Data-taking: 600 hrs at 180 pps.

Computers and data analysis:
- One SDS 9300 in ESA counting house for program debugging-
- One SDS 9300 in ESA counting house for on-line data taking.
- SLAC 360-91 for off-line analysis - 100 hrs.
- Period required for data analysis - about 6 months.

Table of Contents

Abstract

Relatively precise measurements of asymmetries in deep inelastic scattering of polarized electrons by polarized protons and by polarized deuterons are proposed. More than an order of magnitude increase in data rate as compared to SLAC experiment E-80 will be achieved, principally by the use of a larger acceptance spectrometer. A wider kinematic range will be studied extending from about $\omega = 1.5$ to $\omega = 13$, with Q^2 values up to 9 $(GeV/c)^2$. These measurements should yield overall precisions in the determination of the virtual photon-proton asymmetry A_1^p of about 0.03 to 0.08, as compared to our present E80 errors of 0.1 to 0.25. From the deuteron and proton measurements the virtual photon-neutron asymmetry A_1^n should be determined with an error of about 0.05 to 0.10.

The much more precise data on A_1^p over a wider kinematic range, and in particular for lower ω and higher Q^2 values, will improve significantly the test of scaling for A_1^p and will provide unique information about the spin structure of the nucleon to distinguish and test models of proton structure. Data on the neutron asymmetry A_1^n (which will be more accurate than our E80 data on the proton) will be the first such information and hence is exploratory. It will provide a new test of the quark-parton viewpoint for the neutron, including the predictions of the models for the spin structure of the neutron and an improved test of the Bjorken sum rule which requires values of A_1^n.

I. Status of SLAC E-80 Results, Including 1976 On-Line Results.

Introduction.

Physical Review Letters (M.J. Alguard et al., Phys. Rev. Lett. 37, 1258 (1976); 37, 1261 (1976).

Graph indicating kinematic points measured in 1975 and 1976 (Figure 1)

Deep inelastic scattering.

Table 1 of asymmetry values.

Graph of A_1 values and comparison with some theories (Figure 2).

Bjorken sum rule (Figure 3).

Resonance region.

Table 2 of asymmetry values.

Graph of asymmetry values (Figure 4).

Introduction

During the three cycles of our data-taking period for SLAC E-80 we made asymmetry measurements for one elastic, seven (7) deep inelastic, and seven (7) resonance region points. Fig. 1 shows our data points as a function of ν and Q^2, where ν is the laboratory virtual photon energy and Q^2 is its four momentum squared. Our deep inelastic points covered the range of ω from 2 to 10 with Q^2 of 1.0 to 4.0 $(GeV/c)^2$.

Off-line analysis is completed for the data taken in 1975, and the results are published in Phys. Rev. Lett. 37, 1258 (1976); 37, 1261 (1976). (Our notation is defined in these publications.)

Table 1 and Table 2 show the published and the preliminary (on-line) results of the asymmetry measurements in the deep inelastic and resonance regions, respectively. Measured values for $A/D \approx A_1$ are plotted in Fig. 2, together with several theoretical predictions for A_1 in deep inelastic scattering. Fig. 3 shows the on-line resonance region data.

Off-line analysis of our 1976 elastic and deep inelastic data is well under way and we expect to have final asymmetry values within 1 or 2 months. The effect of radiative corrections is also being studied, and we expect to have useful answers this summer. For the lower ω deep inelastic points radiative corrections to the asymmetry values are expected to be small, but for the ω=10 point the correction is estimated to be significant.

We have evaluated the integral appearing in the Bjorken sum rule using our data together with the assumptions $A_2^p = 0$ and $A_1^n = 0$ (Fig. 3: p. 10).

Generally, our deep inelastic results, which give large positive values for the lepton-proton asymmetry A and hence also for the virtual photon-proton asymmetry A_1, confirm the predictions of the quark-parton viewpoint. The Bjorken sum rule, scaling for A_1, and the proton model predictions for A_1 are consistent with our results.

The studies in the resonance region were exploratory. Beyond the off-line determination of asymmetry values, considerable analysis will be required to account for radiative and background corrections. Then the implications of the results for duality predictions on the spin dependence of resonance electroproduction and their relation to results from multipole analysis of other photoproduction and electroproduction data must be considered.

VOLUME 37, NUMBER 19 PHYSICAL REVIEW LETTERS 8 NOVEMBER 1976

Elastic Scattering of Polarized Electrons by Polarized Protons*

M. J. Alguard, W. W. Ash, G. Baum, J. E. Clendenin, P. S. Cooper, D. H. Coward, R. D. Ehrlich, A. Etkin, V. W. Hughes, H. Kobayakawa, K. Kondo, M. S. Lubell, R. H. Miller, D. A. Palmer, W. Raith, N. Sasao, K. P. Schüler, D. J. Sherden, C. K. Sinclair, and P. A. Souder

University of Bielefeld, Bielefeld, West Germany, and City University of New York, New York, New York 10031, and Nagoya University, Nagoya, Japan, and Stanford Linear Accelerator Center, Stanford, California 94305, and University of Tsukuba, Ibaraki, Japan, and Yale University, New Haven, Connecticut 06520

(Received 5 August 1976)

We report on a new type of high-energy electron-proton scattering experiment in which longitudinally polarized electrons are scattered from longitudinally polarized protons. The asymmetry in elastic scattering at $Q^2 = 0.765$ (GeV/c)^2 was measured; our result agrees with the theoretical asymmetry and determines the sign of G_E/G_M to be positive.

In this Letter we describe a high-energy electron-proton scattering experiment in which polarized electrons are scattered from polarized protons, and present the first results for elastic scattering. Our first results for deep inelastic scattering are reported in the following Letter.[1]

The momentum and scattering angle of the scattered electrons were measured when longitudinally polarized electrons were scattered from longitudinally polarized protons. The basic quantity measured was the antiparallel-parallel asymmetry A in the differential cross sections given by

$$A = \frac{d\sigma(\uparrow\downarrow) - d\sigma(\uparrow\uparrow)}{d\sigma(\uparrow\downarrow) + d\sigma(\uparrow\uparrow)}, \tag{1}$$

in which $d\sigma$ denotes the differential cross section $d\sigma(E, \theta)/d\Omega$ for incident electron energy E and laboratory scattering angle θ, and the arrows denote the antiparallel and parallel spin configurations.

If elastic scattering is described by the one-photon-exchange approximation, then the asymmetry can be expressed as[2]

$$A = \frac{\tau G_M}{G_E}\left\{\frac{2M}{E} + \frac{G_M}{G_E}\left[\frac{2\tau M}{E} + 2(1+\tau)\tan^2\frac{\theta}{2}\right]\right\} \times \left\{1 + \tau\left(\frac{G_M}{G_E}\right)^2\left[1 + 2(1+\tau)\tan^2\frac{\theta}{2}\right]\right\}^{-1}, \tag{2}$$

in which $\tau = Q^2/4M^2$, $q^2 = -Q^2 = -4EE'\sin^2(\theta/2)$ is the square of the four-momentum of the virtual photon, M is the proton mass, E' is the scattered electron energy, and G_E and G_M are the electric and magnetic elastic form factors of the proton. The electron mass has been neglected. We chose to measure A for elastic scattering primarily to test the validity of our experimental method. Alternatively, we can regard our measurement as a test of Eq. (2) and as a determination of the sign of G_E/G_M.

The polarized electron source (PEGGY), which serves as an injector to the 20-GeV Stanford linear accelerator, is based on photoionization of a polarized Li^6 atomic beam by a pulsed uv light source.[3] Typical characteristics of the polarized electron beam are given in Table I. The electron polarization, P_e, was measured by Mott scattering at the output of PEGGY and by Møller scattering at high energy. The value given for P_e is based on the Møller scattering measurements.[4,5] The uncertainty, $\delta P_e/P_e = 12\%$, includes counting statistics (10%) and the uncertainty in the uv light intensity for photoionization. (The polarization depends upon light intensity through a depolarizing resonant two-photon ionization process.[6])

Protons were polarized by the method of dynamic nuclear orientation in a butanol target doped with 1.4% porphyrexide.[7] Typical operating conditions are given in Table II. The techniques of beam rastering and target annealing[8] were used to reduce the effects of radiation damage to an acceptable level. Targets were annealed about every two hours and replaced after about five exposures to the beam. The continuously

TABLE I. Characteristics of polarized electron beam.

Characteristic	Value
Pulse length	1.5 μsec
Repetition rate	120 pulses/sec
Electron intensity (at high energy)	$\sim 10^9 e^-$/pulse
Pulse-to-pulse intensity variation	< 5%
Electron polarization, P_e	0.51 ± 0.06
Polarization reversal time	3 sec
Time between reversals	2 min
Intensity difference upon reversal	< 5%
Lifetime of lithium oven load	70 hr
Time to reload system	36 hr

TABLE II. Operating characteristics of polarized proton target.

Characteristic	Value
Magnetic field (longitudinal field of superconducting magnet)	50 kG
Temperature	1.05 K
Target material	25 cm^3 of butanol-porphyrexide beads (~1.7 mm diam)
Initial polarization of free protons[a]	0.50 to 0.65
Depolarizing dose (1/e)	$\sim 3\times 10^{14} e^-/cm^2$
Polarizing time (1/e)	~4 min
Anneal or target change time (including polarizing)	~45 min

[a]Improvements in target operation gave the larger polarization values in the later parts of the experiment.

monitored NMR signal normalized to a thermal equilibrium (TE) signal was used to determine the average target polarization P_p. The uncertainty, $\delta P_p/P_p = 10\%$, includes the errors in the TE measurements (8%) and the uncertainty in the correction for nonuniform irradiation of the target (5%). (Only ~70% of the total 2.5-cm×2.5-cm target cross-sectional area was illuminated by the rastered electron beam.)

The electron beam from the accelerator was momentum-analyzed by a transport system whose absolute momentum calibration was ~0.1%. A momentum slit in the transport system limited the beam energy spread to ±0.375%. Spin precession in the 24.5° bend of the beam switchyard determined that only electrons whose energies were integral multiples of 3.237 GeV had full longitudinal polarization. The electron beam charge per pulse was monitored with two precision toroidal charge monitors. Just upstream of the target, a microwave beam position monitor measured the beam position for each beam pulse with a sensitivity of ~0.1 mm. Computer-controlled vernier steering magnets 99 m upstream of the target were used in conjunction with this position monitor to keep the raster pattern of the beam centered on the target.

The scattered electrons were detected and their momentum and scattering angle were measured with the Stanford Linear Accelerator Center (SLAC) 8-GeV spectrometer. Electron identification was achieved with a gas threshold Cherenkov counter, a 3.25-radiation-length-thick lead glass counter array which sampled the buildup of the electromagnetic shower, and a lead-Isolite[9] shower counter. Less than one pion in 10^3 was misidentified as an electron by this system. An on-line XDS 9300 computer monitored the experiment and wrote data on magnetic tape.

Data were taken in a series of runs, each of which lasted about two hours. Runs were terminated when radiation damage reduced the target polarization to about half its initial value. The proton polarization direction was constant during a run and was reversed between runs. Each run was divided into cycles, with each cycle in turn comprising eight miniruns of about one-minute duration each. The electron polarization direction remained constant during a minirun and was varied in the pattern $--++--++$, where $-$ $(+)$ refers to the electron having negative (positive) helicity in the accelerator. This rapid modulation of the electron beam helicity was an important factor in avoiding systematic errors in the asymmetry measurement.

Each target raster pattern consisted of 313 points and was completed in 2.6 sec. An integral number of raster patterns was used for each minirun. The number of events taken in each minirun was normalized to the total charge measured by the toroids, and corrections were made for losses due to computer sampling, multiple hodoscope tracks, and dead time. The experimental asymmetry, Δ, is the quantity $\pm[(1256)-(3478)]/[(1256)+(3478)]$, where (1256) and (3478) refer to the sums of the corrected and normalized number of events in miniruns 1, 2, 5, 6 and 3, 4, 7, 8, respectively. The sign of Δ is chosen to give the antiparallel-minus-parallel asymmetry in accordance with Eq. (1). False asymmetries were measured with other combinations of miniruns.

Elastic scattering data were taken at the kinematic point for which $E = 6.473$ GeV, $E' = 6.066$ GeV, $\theta = 8.005°$, and $Q^2 = 0.765$ $(\mathrm{GeV}/c)^2$. A total of 2.1×10^6 electrons were detected with a typical

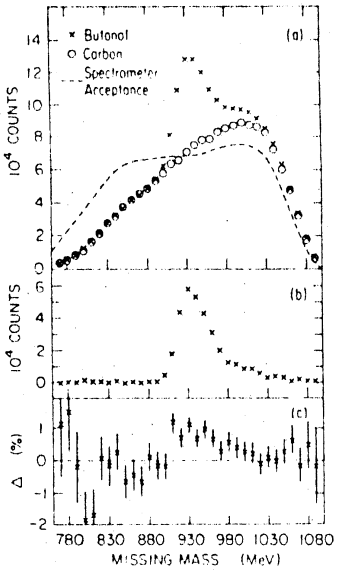

FIG. 1. Elastic scattering results for $E = 6.473$ GeV, $\theta = 8.005°$; (a) scattered electron counts versus missing mass with calculated spectrometer acceptance in arbitrary units; (b) scattered electron counts from free protons versus missing mass; (c) experimental asymmetry Δ versus missing mass.

counting rate of 0.25 scattered electrons per 1.5 μsec beam pulse. The combined missing mass (W) spectrum for electrons scattered from butanol for all runs independent of beam or target polarization is shown in Fig. 1(a), together with the background from electron-carbon scattering normalized to equal areas in the mass region $720 \leq W < 880$ MeV. Also shown in Fig. 1(a) is the spectrometer acceptance as determined from a Monte Carlo ray-tracing calculation. The free-proton spectrum (butanol minus background) versus missing mass is shown in Fig. 1(b). The experimental asymmetry, Δ, is shown plotted versus W in Fig. 1(c). The positive asymmetry associated with elastic scattering from free protons is apparent. Values of Δ for three missing-mass regions are given in Table III. Several false asymmetries, calculated over the complete missing-mass region 720 MeV $\leq W \leq$ 1120 MeV, are shown in Table IV, together with the χ^2 values for the agreement with zero of the measured false asymmetries for the 21 individual runs. No statistically significant false asymmetry was found.

The differential-cross-section asymmetry A of Eq. (1) is related to Δ by

$$\Delta = P_e P_p F A. \qquad (3)$$

Here F is the fraction of scattered electrons

TABLE III. Experimental asymmetry, Δ.

W (MeV)	Δ (%)
$720 \leq W < 890$	-0.36 ± 0.18
$890 \leq W < 1000$	$+0.63 \pm 0.10$
$1000 \leq W < 1120$[a]	$+0.15 \pm 0.13$

[a]Since a small fraction of the scattering events from free protons fall in this region, an asymmetry Δ of about +0.13% is expected.

within the elastic missing-mass region ($890 \leq W < 1000$ MeV) which originate from free protons. Using the normalized carbon spectrum to determine the bound-nucleon background, we obtained a value of $F = 0.27 \pm 0.02$. To obtain A, we could have used Eq. (3) with $P_e = 0.51$, the average value of $P_p \simeq 0.34$, and $\Delta = 0.0063 \pm 0.0010$ within the elastic region (Table III). Instead, we used a somewhat different method of calculation which took into account the gradual decrease of the target polarization during a run. Our final result is $A = 0.138 \pm 0.031$ (0.019), where the statistical counting error, shown in parentheses, is added in quadrature to the systematic errors in P_e, P_p, and F to determine the total uncertainty. The values obtained for Δ with the two different directions of proton polarization agree within statistical counting errors. This agreement provides an important test of the validity of our result. Systematic errors in Δ arising from a correlation of beam energy or angle with beam helicity are small compared to the statistical error, as is the error associated with the measurement of beam charge by the toroids. The effect of radiative corrections on A is expected to be small, and these corrections to the data have not yet been made.

The theoretical expression for A of Eq. (2) de-

TABLE IV. False asymmetries.

Combination of miniruns	Average asymmetry[a] (%)	$\chi^2(0)$ per degree of freedom
$\frac{(1234)-(5678)}{(1234)+(5678)}$	0.02 ± 0.07	13/21
$\frac{(1357)-(2468)}{(1357)+(2468)}$	0.01 ± 0.07	18/21
$\frac{(2367)-(1458)}{(2367)+(1458)}$	-0.08 ± 0.07	17/21

[a]Independent of sign of P_p.

pends on both the magnitude and sign of G_E/G_M. Unpolarized elastic scattering experiments determine G_E^2 and G_M^2, but not the sign of G_E/G_M.

For $Q^2 = 0.765$ (GeV/c)^2 these experiments[10] give $|\mu G_E/G_M| = 0.98 \pm 0.04$ in which $\mu = 2.79$. If G_E and G_M have the same sign, Eq. (2) yields $A = +0.112 \pm 0.001$, while if G_E and G_M have the opposite sign Eq. (2) gives $A = -0.017 \pm 0.002$. From our measured value of A we conclude that the theoretical and experimental values are in good agreement provided the signs of G_E and G_M are the same. The effect of proton structure on the hyperfine-structure interval in hydrogen involves an integral of the product of the proton structure functions and also gives the sign of G_E/G_M to be positive.[11]

The experimental method described in this Letter could in principle[2,12] be applied to determine G_E in the region $Q^2 \gtrsim 2$ (GeV/c)^2, where G_E is not well known, but its practical usefulness is limited by low counting rates.

We are happy to acknowledge the important contributions to this experiment by M. Browne, S. Dhawan, R. Eisele, Z. Farkas, R. Fong-Tom, H. Hogg, E. Garwin, R. Koontz, J. Sodja, S. St. Lorant, J. Wesley, and M. Zeller.

†Research supported in part by the U. S. Energy Research and Development Administration under Contract No. E(11-1)-3075 (Yale) and Contract No. E(04-3)-515, (Stanford Linear Accelerator Center), the German Federal Ministry of Research and Technology, and the University of Bielefeld, the Japan Society for the Promotion of Science, and the National Science Foundation.

[1]M. J. Alguard *et al.*, following Letter [Phys. Rev. Lett. 37, 1261 (1976)].

[2]N. Dombey, Rev. Mod. Phys. 41, 236 (1969). The methodology of this paper was used to derive Eq. (2).

[3]V. W. Hughes *et al.*, Phys. Rev. A 5, 195 (1972); M. J. Alguard *et al.*, in *Proceedings of the Ninth International Conference on High Energy Accelerators, Stanford Linear Accelerator Center, Stanford, California, 1974*, CONF-740 522 (National Technical Information Service, Springfield, Va., 1974), p. 309.

[4]P. S. Cooper *et al.*, Phys. Rev. Lett. 34, 1589 (1975).

[5]We thank the members of SLAC Group A for their invaluable help in making the electron polarization measurement by Møller scattering in March 1976.

[6]M. J. Alguard *et al.*, Bull. Am. Phys. Soc. 21, 98 (1976).

[7]W. W. Ash, in Proceedings of the Brookhaven National Laboratory Workshop in Physics with Polarized Targets, June 1974, BNL Report No. 20415 (unpublished), p. 309; W. W. Ash *et al.*, to be published.

[8]M. Borghini *et al.*, Nucl. Instrum. Methods 84, 168 (1970).

[9]Isolite is the name for a plastic formed by adding a wavelength-shifter to Lucite.

[10]Ch. Berger *et al.*, Phys. Lett. 35B, 87 (1971); W. Bartel *et al.*, Nucl. Phys. B 58, 429 (1973).

[11]H. Grotch and D. R. Yennie, Rev. Mod. Phys. 41, 350 (1969); C. Zemach, Phys. Rev. 104, 1771 (1956).

[12]A. I. Akhiezer *et al.*, Zh. Eksp. Teor. Fiz. 33, 765 (1957) [Sov. Phys. JETP 6, 588 (1958)].

VOLUME 37, NUMBER 19 PHYSICAL REVIEW LETTERS 8 NOVEMBER 1976

Deep Inelastic Scattering of Polarized Electrons by Polarized Protons*

M. J. Alguard, W. W. Ash, G. Baum, J. E. Clendenin, P. S. Cooper, D. H. Coward, R. D. Ehrlich, A. Etkin, V. W. Hughes, H. Kobayakawa, K. Kondo, M. S. Lubell, R. H. Miller, D. A. Palmer, W. Raith, N. Sasao, K. P. Schüler, D. J. Sherden, C. K. Sinclair, and P. A. Souder

University of Bielefeld, Bielefeld, West Germany, and City University of New York, New York, New York 10031, and Nagoya University, Nagoya, Japan, and Stanford Linear Accelerator Center, Stanford, California 94305, and University of Tsukuba, Ibaraki, Japan, and Yale University, New Haven, Connecticut 06520

(Received 5 August 1976)

We report measurements of the asymmetry in deep inelastic scattering of longitudinally polarized electrons by longitudinally polarized protons. The antiparallel-parallel asymmetries are positive and large in agreement with predictions of quark-parton models of the proton. A limit is obtained on parity nonconservation in the scattering of longitudinally polarized electrons by unpolarized nucleons.

Experimental and theoretical studies of deep inelastic electron scattering from protons and neutrons have led in the past eight years to the important discovery of scaling and to the quark-parton model of nucleon structure.[1] Deep inelastic muon[2] and neutrino[3] scattering have confirmed these general ideas.[4]

For deep inelastic electron-proton scattering,

accurate data have been obtained on the differential cross section $d^2\sigma/d\Omega dE'$ over a wide range of the energy loss, ν, of the electron and the square of the four-momentum transfer, q^2, to the proton. The two spin-averaged proton structure functions $W_1(\nu,q^2)$ and $W_2(\nu,q^2)$ have been determined from these data. Important, independent information is contained in two additional spin-dependent proton structure functions whose determination requires the measurement of spin correlation asymmetries.[5]

In this Letter we report the first results of an experiment done at the Stanford Linear Accelerator Center (SLAC) to measure the asymmetry, A, in the deep inelastic scattering of longitudinally polarized electrons by longitudinally polarized protons, where A is given by

$$A = [d\sigma(\uparrow\downarrow) - d\sigma(\uparrow\uparrow)]/[d\sigma(\uparrow\downarrow) + d\sigma(\uparrow\uparrow)], \quad (1)$$

with $d\sigma$ denoting the differential cross section $d^2\sigma(E,E',\theta)/d\Omega dE'$ for electrons of incident (scattered) energy E (E') and laboratory scattering angle θ, and the arrows denoting the antiparallel and parallel spin configurations.

If the scattering is described by the one-photon-exchange approximation, then for unpolarized electrons the virtual photons are linearly polarized, whereas for polarized electrons the photons are elliptically polarized. The differential cross section for the scattering of longitudinally polarized electrons by longitudinally polarized protons is

$$\frac{d^2\sigma}{d\Omega dE'} = \left(\frac{d\sigma}{d\Omega}\right)_M \left(\frac{1}{\epsilon(1+\nu^2/Q^2)}\right) W_1\{1 + \epsilon R \pm (1-\epsilon^2)^{1/2}\cos\psi A_1 \pm [2\epsilon(1-\epsilon)]^{1/2}\sin\psi A_2\}, \quad (2)$$

in which $(d\sigma/d\Omega)_M$ is the Mott differential cross section, $\epsilon = [1 + 2(1+\nu^2/Q^2)\tan^2\frac{1}{2}\theta]^{-1}$, $Q^2 = -q^2$, $R = \sigma_L/\sigma_T$ is the ratio of the cross sections for absorption of longitudinal and transverse virtual photons, and ψ is the angle between the directions of the virtual photon momentum and the proton spin. The + (−) signs in Eq. (2) refer to the antiparallel (parallel) spin configurations.

The spin-dependent terms A_1 and A_2 are two new measurable quantities which can be expressed in terms of two spin-dependent structure functions.[5,6] Equivalently, they can be expressed in terms of the total absorption cross sections of circularly polarized photons on polarized protons as

$$A_1 = (\sigma_{1/2} - \sigma_{3/2})/(\sigma_{1/2} + \sigma_{3/2}),$$
$$A_2 = 2\sigma_{TL}/(\sigma_{1/2} + \sigma_{3/2}), \quad (3)$$

where $\sigma_{1/2}$ ($\sigma_{3/2}$) is the total absorption cross section when the z component (z is the direction of the virtual photon momentum) of angular momentum of the virtual photon plus proton is $\frac{1}{2}$ ($\frac{3}{2}$), and σ_{TL}, which may be negative, is a term which arises from the interference between transverse and longitudinal photon-nucleon amplitudes. It should be noted that $\sigma_{1/2}$ and $\sigma_{3/2}$ are related to σ_T by $\sigma_{1/2} + \sigma_{3/2} = 2\sigma_T$.

For the case of protons polarized along the incident beam direction, the asymmetry A of Eq. (1) is

$$A = D(A_1 + \eta A_2), \quad (4)$$

where

$$D = (E - E'\epsilon)/E(1+\epsilon R)$$
$$= (1-\epsilon^2)^{1/2}\cos\psi/(1+\epsilon R), \quad (5)$$

and

$$\eta = \epsilon(Q^2)^{1/2}/(E - E'\epsilon)$$
$$= [2\epsilon/(1+\epsilon)]^{1/2}\tan\psi \simeq \tan\psi. \quad (6)$$

The quantity D can be regarded as a kinematic depolarization factor of the virtual photon and is ~0.3 for our kinematic points. Positivity limits imposed on A_1 and A_2 are[7]

$$|A_1| \le 1, \quad |A_2| \le \sqrt{R}. \quad (7)$$

In this experiment we determine the combination $A_1 + \eta A_2$ by dividing the measured electron-proton asymmetry A by the depolarization factor D. Although we do not separately determine A_1 and A_2, our result is dominated by A_1 because the kinematic factor η is small.

On the basis of a high-energy sum rule derived with the algebra of currents for a quark model, it has been predicted[8] that A_1 has a positive value greater than 0.2 over a large region of the deep inelastic continuum. Scaling relations are predicted for the spin-dependent proton structure functions, and hence also for A_1[9]:

$$A_1(\nu,Q^2) \to A_1(\omega) \text{ as } \nu, Q^2 \to \infty, \text{ with } \omega \text{ held constant} \quad (8)$$

($\omega = 2M\nu/Q^2$, M is the proton mass). Specific models of proton structure make widely varying predictions for A_1. The simplest quark-parton

TABLE I. Results of asymmetry measurements.

E (GeV)	θ (deg)	Q^2 [(GeV/c)^2]	W[a] (GeV)	ω	Δ (%)	A[b]	D[c]	$A_1+\eta A_2$[b]	$\lvert\eta A_2\rvert$
9.711	9.000	1.680	2.059	3	0.44 ± 0.11	0.191 ± 0.057 (0.044)	0.284	0.67 ± 0.20 (0.16)	< 0.146
12.948	9.000	2.735	2.519	3	0.50 ± 0.17	0.215 ± 0.089 (0.080)	0.352	0.61 ± 0.25 (0.23)	< 0.109
9.711	9.000	1.418	2.560	5	0.28 ± 0.11	0.141 ± 0.058 (0.051)	0.412	0.34 ± 0.14 (0.12)	< 0.087

[a] W is the missing mass of undetected hadron system.
[b] The total errors are the statistical counting errors added in quadrature to the systematic errors in P_e, P_p, and F; the numbers in parentheses are the 1-standard-deviation counting errors.
[c] D is obtained from Eq. (5) using $R = 0.14$.

model predicts that $A_1 - \frac{5}{9}$, and more elaborate models also predict large positive values for $A_1(\omega)$.[5,10]

The method of measuring the experimental asymmetry, Δ, for deep inelastic electron-proton scattering was the same as that described for elastic scattering in the preceding Letter.[11] For the inelastic case, the scattered electron counting rate was lower (0.02 to 0.06 electrons per pulse).

TABLE II. False asymmetries.[a]

Combination of miniruns	Average asymmetry[b] (%)	$\chi^2(0)$ per degree of freedom
	$\omega = 3$, $Q^2 = 1.680$	
$\frac{(1234)-(5678)}{(1234)+(5678)}$	0.04 ± 0.11	18/34
$\frac{(1357)-(2468)}{(1357)+(2468)}$	−0.04 ± 0.11	38/34
$\frac{(2367)-(1458)}{(2367)+(1458)}$	+0.14 ± 0.11	27/34
	$\omega = 3$, $Q^2 = 2.735$	
$\frac{(1234)-(5678)}{(1234)+(5678)}$	−0.30 ± 0.17	33/30
$\frac{(1357)-(2468)}{(1357)+(2468)}$	−0.03 ± 0.17	26/30
$\frac{(2367)-(1458)}{(2367)+(1458)}$	+0.24 ± 0.017	40/30
	$\omega = 5$, $Q^2 = 1.418$	
$\frac{(1234)-(5678)}{(1234)+(5678)}$	−0.12 ± 0.11	34/35
$\frac{(1357)-(2468)}{(1357)+(2468)}$	−0.10 ± 0.11	34/35
$\frac{(2367)-(1458)}{(2367)+(1458)}$	−0.03 ± 0.11	30/35

[a] See preceding Letter (Ref. 11) for definitions of false asymmetries.
[b] Irrespective of sign of target polarization.

Background due to misidentified pions was again negligible.

The antiparallel-parallel asymmetry Δ was measured for three deep inelastic kinematic points and the results are given in Table I. Several false asymmetries were also measured and are listed in Table II, together with the χ^2 values for the agreement with zero of the measured false asymmetries for the indicated degrees of freedom (number of individual runs). No statistically significant false asymmetries were found.

The asymmetry A of Eq. (1) is related to Δ by

$$\Delta = P_e P_p F A. \tag{9}$$

The electron polarization, P_e, was 0.51 ± 0.06, and the average target polarization, P_p, measured for each kinematic point, was $\simeq 0.40$ with 10% uncertainty. The quantity F is the fraction of detected electrons scattered from free protons. This is taken as the ratio of the number of free protons to the total number of nucleons in the target, including measured contributions from helium and other background sources. A small correction for the difference in scattering cross sections of neutrons and protons was also included. The value for F, determined for each point, was $\simeq 0.11$ with a 10% uncertainty.

The measured values of A are listed in Table I. The uncertainties are dominated by counting statistics. No radiative corrections have yet been made. Also listed are the quantities D (evaluated using $R = 0.14$),[1] $A/D = A_1 + \eta A_2$, and upper limits for $|\eta A_2|$ (taking $A_2 = \sqrt{R}$). From Table I it is seen that A/D is dominated by A_1. Furthermore, parton theories predict[12] that the interference term A_2 will be considerably smaller than its positivity limit $\sqrt{R}$. It is therefore valid to compare our measured value of A/D to theoretical predictions for A_1 as shown in Fig. 1.

With the explicit assumption that $A/D = A_1$, our

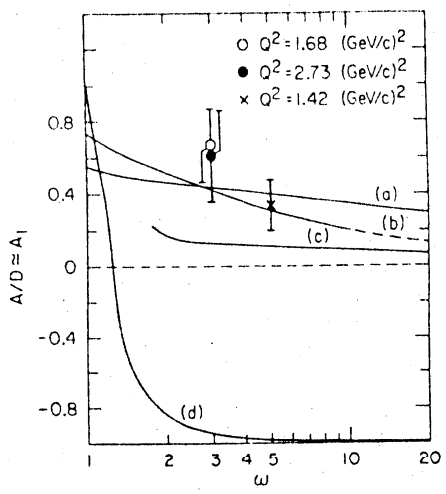

FIG. 1. Experimental values of $A/D \approx A_1$ and theoretical predictions of the virtual-photon–proton asymmetry A_1 versus ω. Theoretical curves a, b, c, and d are obtained from Refs. 5, 10, 13, and 14, respectively. For curve c the quark model with symmetry breaking is used: The model does not give values for A_1 in the range $1 < \omega < 2$, but rather gives $A_1(1) = 1$. For curve d the quantity $\mu^2/m_\rho{}^2$ in the theory is taken equal to 0.12.

values of A_1 are indeed positive and large in accord with early theoretical expectations from sum rules.[8] The two values for $\omega = 3$ agree within their errors, which is consistent with the expectation that A_1 satisfies the scaling relation, given by Eq. (8). Our data are consistent with the predictions of the quark-parton models shown as curves a [5] and b [10] in Fig. 1, but disagree strongly with the resonance model[13] (curve c) and the bare-nucleon–bare-meson model[14] (curve d). We note that the theoretical curves are all given for the scaling limit.

Data from this experiment can also be used to place a limit on parity nonconservation in the scattering of longitudinally polarized electrons from unpolarized nucleons, i.e., an interaction term of the form $\vec{\sigma}_e \cdot \vec{p}_e$ in which $\vec{\sigma}_e$ is the electron spin and $\vec{p}_e$ is the electron incident momentum. If we define Δ^+ (Δ^-) as the asymmetry for protons polarized along (against) the beam direction and if the magnitude of P_p is the same for both cases, then we can define an asymmetry, $\Delta_{\rm PNC}$, associated with parity nonconservation by[15]

$$\Delta_{\rm PNC} = (\Delta^+ - \Delta^-)/2 \equiv r P_e, \qquad (10)$$

in which $r = (d\sigma^- - d\sigma^+)/(d\sigma^- + d\sigma^+)$ is the asymmetry for electron polarization $P_e = 1$, and the minus and plus superscripts refer to the electron beam helicity. From the deep inelastic scattering data summarized in Table I for Q^2 between 1.4 and 2.7 $(\mathrm{GeV}/c)^2$, we find that r is consistent with zero. For the combined data we have an upper limit of $r < 5 \times 10^{-3}$ with a 95% confidence level. For the elastic scattering data reported in the preceding Letter,[11] again r is consistent with zero and its upper limit is less than 3×10^{-3} with a 95% confidence level. The gauge theories of weak and electromagnetic interactions, which contain parity nonconservation, predict[16,17] considerably smaller values of $r \approx (10^{-5}$ to $10^{-4}) Q^2/M^2$.

We are happy to acknowledge helpful and stimulating discussions with J. D. Bjorken, F. Gilman, and J. Kuti.

---

*Research supported in part by the U. S. Energy Research and Development Administration under Contract No. E(11-1)-3075 (Yale) and Contract No. E(04-3)-515 (Stanford Linear Accelerator Center), the German Federal Ministry of Research and Technology and the University of Bielefeld, the Japan Society for the Promotion of Science, and the National Science Foundation.

[1]R. E. Taylor, in *Proceedings of the International Symposium on Lepton and Photon Interactions at High Energies, Stanford, California, 1975*, edited by W. T. Kirk (Stanford Linear Accelerator Center, Stanford, Calif., 1975), p. 679. See also references therein.

[2]L. Mo, in *Proceedings of the International Symposium on Lepton and Photon Interactions at High Energies, Stanford, California, 1975*, edited by W. T. Kirk (Stanford Linear Accelerator Center, Stanford, Calif., 1975), p. 651.

[3]D. H. Perkins, in *Proceedings of the International Symposium on Lepton and Photon Interactions at High Energies, Stanford, California, 1975*, edited by W. T. Kirk (Stanford Linear Accelerator Center, Stanford, Calif., 1975), p. 571.

[4]C. H. Llewellyn-Smith, in *Proceedings of the International Symposium on Lepton and Photon Interactions at High Energies, Stanford, California, 1975*, edited by W. T. Kirk (Stanford Linear Accelerator Center, Stanford, Calif., 1975), p. 709. See also references therein.

[5]J. Kuti and V. F. Weisskopf, Phys. Rev. D 4, 3418 (1971).

[6]F. Gilman, Phys. Rep. 4, 95 (1972); F. Gilman, SLAC Report No. SLAC-167, 1973 (unpublished), Vol. I, p. 71.

[7]M. G. Doncel and E. de Rafael, Nuovo Cimento 4A, 363 (1971).

[8]J. D. Bjorken, Phys. Rev. D 1, 1376 (1970).

[9]L. Galfi *et al.*, Phys. Lett. 31B, 465 (1970).

[10]F. Close, Nucl. Phys. B80, 269 (1974), and references therein.

[11]M. J. Alguard *et al.*, preceding Letter [Phys. Rev.

Lett. 37, 1258 (1976)].
[12]J. D. Bjorken and F. Gilman, private communication.
[13]G. Domokos *et al.*, Phys. Rev. D 3, 1191 (1971).
[14]S. D. Drell and T. D. Lee, Phys. Rev. D 5, 1738 (1972).
[15]In the actual analysis, target polarization differences were included. Since $P_p FA \simeq 0.01$ is small, these differences have little effect.
[16]S. M. Berman and J. R. Primack, Phys. Rev. D 9, 2171 (1974).
[17]G. Feinberg, Phys. Rev. D 12, 3575 (1975).

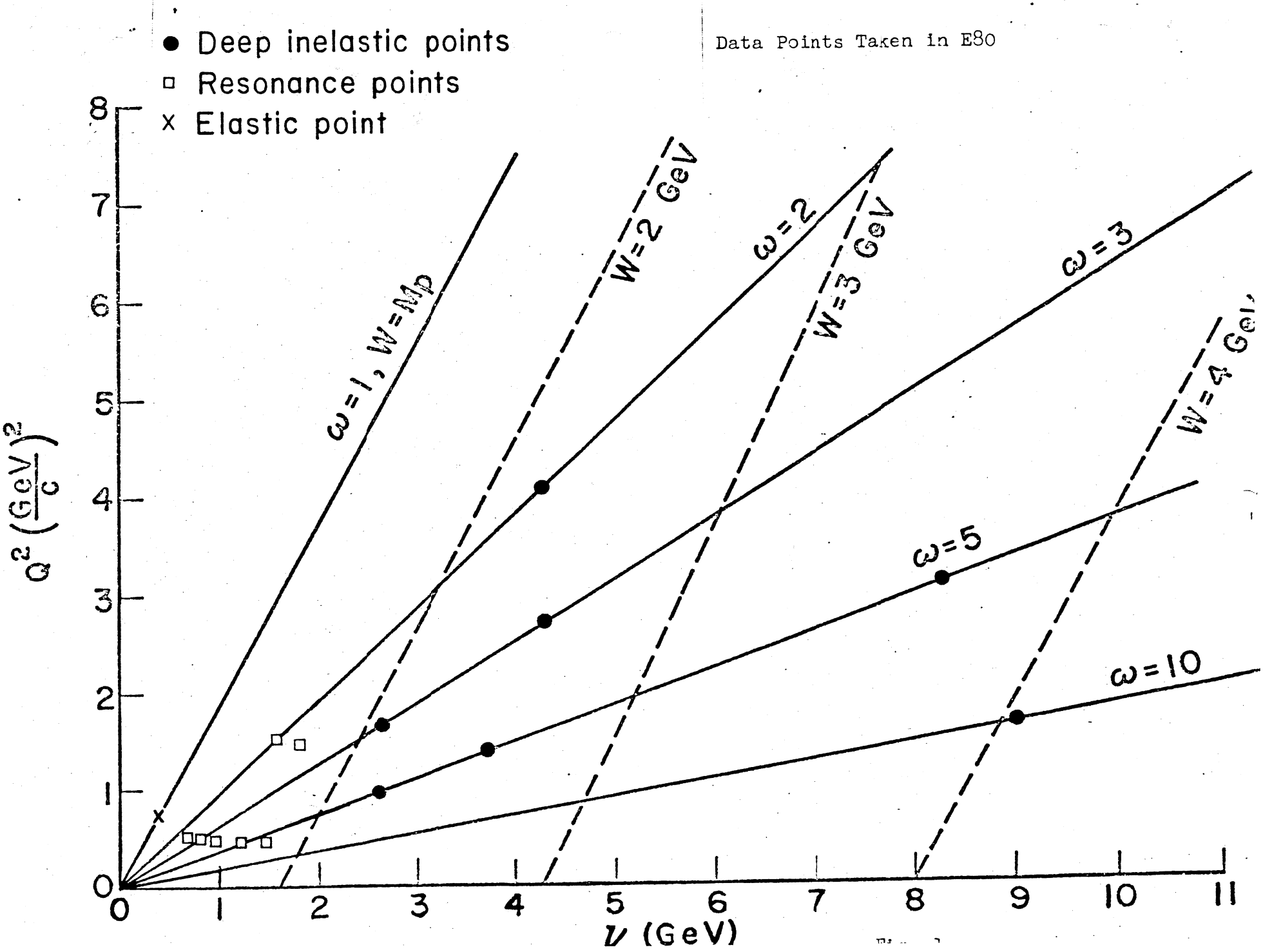
Deep inelastic points
Resonance points
Elastic point
Data Points Taken in E80
$Q^2\left(\frac{GeV}{c}\right)^2$
ν (GeV)
$\omega=1$, $W=M_p$
$W=2$ GeV
$\omega=2$
$W=3$ GeV
$\omega=3$
$W=4$ GeV
$\omega=5$
$\omega=10$
0
1
2
3
4
5
6
7
8
9
10
11

Table Results of Asymmetry Measurements in De Inelastic Scattering (Data taken in 19[illegible] [Published in Phys. Rev. Lett. 37, 1261 (1976)]

E (GeV)	θ (deg)	Q^2 $(GeV/c)^2$	W (GeV)	ω	$\Delta(\%)$	$A^{a)}$	$D^{b)}$	$A_1 + \eta A_2{}^{a)}$	$\lvert\eta A_2\rvert^{c)}$
9.71	9°	1.680	2.059	3	0.44±0.11	0.191±0.057(0.044)	0.284	0.67±0.20(0.16)	<0.146
12.95	9°	2.735	2.519	3	0.50±0.17	0.215±0.089(0.080)	0.352	0.61±0.25(0.23)	<0.109
9.71	9°	1.413	2.560	5	0.28±0.11	0.141±0.058(0.051)	0.412	0.34±0.14(0.12)	<0.087

Preliminary On-line Results (Data taken in 1976)

E (GeV)	θ (deg)	Q^2 $(GeV/c)^2$	W (GeV)	ω	$\Delta(\%)$	$A^{a)}$	$D^{b)}$	$A_1 + \eta A_2{}^{a)}$	$\lvert\eta A_2\rvert^{c)}$
12.95	11°	4.09	2.22	2	1.03±0.27	0.173±0.054(0.0452)	0.35	0.49±0.15(0.13)	0.133
9.71	9°	1.68	2.06	3	0.72±0.19	0.173±0.054(0.045)	0.284	0.61±0.19(0.16)	0.146
12.95	9°	2.74	2.52	3	0.80±0.34	0.192±0.088(0.082)	0.352	0.55±0.25(0.23)	0.109
9.71	7°	1.02	2.20	4.9	0.34±0.11	0.086±0.031(0.027)	0.277	0.31±0.11(0.10)	0.117
16.18	8.5°	2.95	3.56	5	1.00±0.34	0.251±0.096(0.086)	0.527	0.48±0.18(0.16)	0.055
16.18	7°	1.70	4.04	10	0.46±0.18	0.115±0.050(0.045)	0.619	0.19±0.08(0.07)	0.032

a) The total errors are the statistical counting errors added in quadrature to the systematic errors in P_e, P_p and F; the numbers in parentheses are the one standard deviation counting errors.

b) $D = (E-E'\varepsilon)/E(1+\varepsilon R)$ with $R = 0.14$.

c) Upper limits for $|\eta A_2|$ taking $A_2 = \sqrt{R}$.

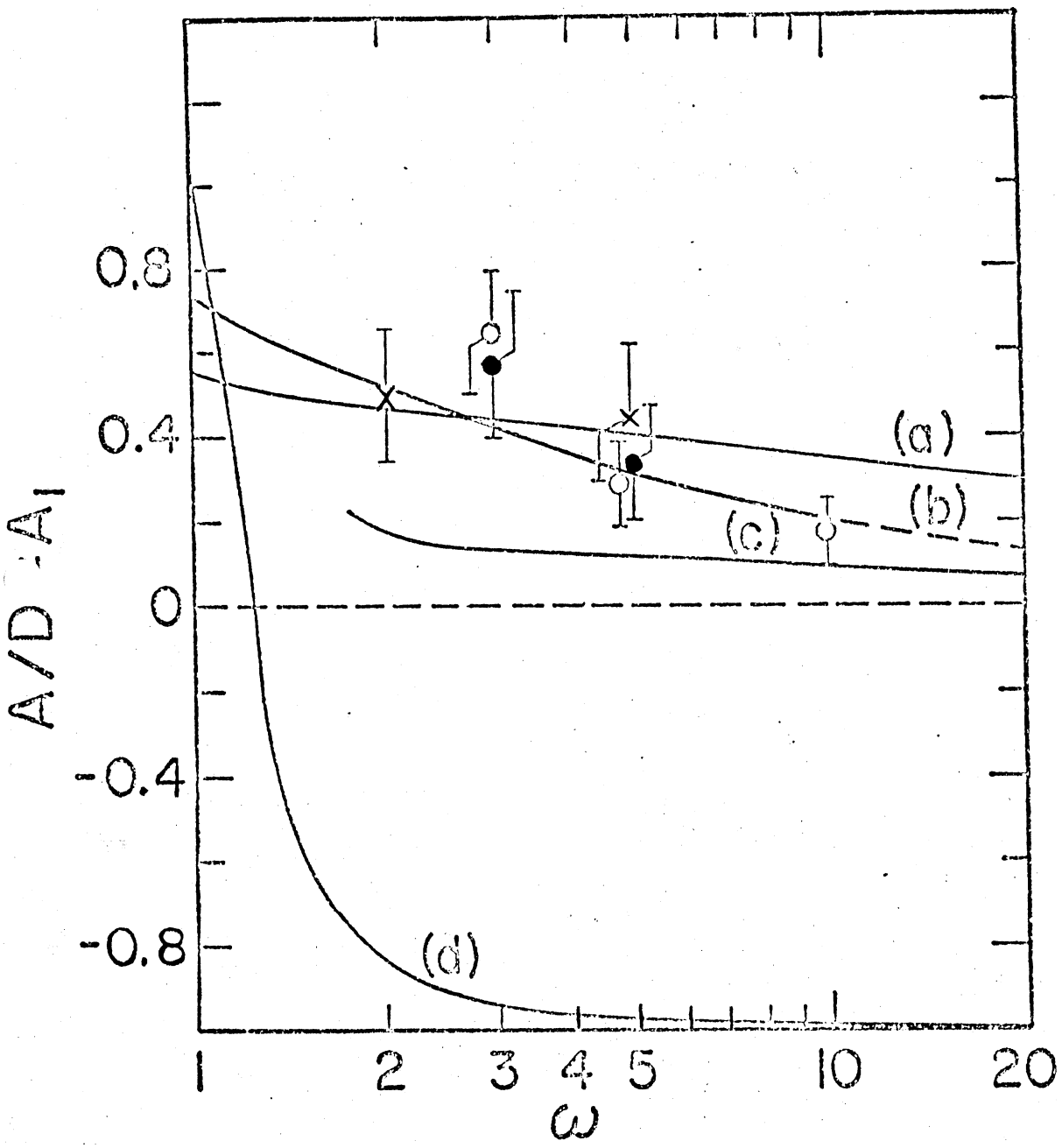

(See Fig. 1 of Phys. Rev. Lett. 37, 1261 (1976)
and Table 1, p. 8 of this proposal)

Fig. 2

Bjorken's sum rule

The Bjorken sum rule is an important general consequence of the quark-parton model of the nucleon and of the assumption that the weak current for quarks has the same form as that for leptons. (Bjorken, 1966, 1970; Feynman, 1972) It can be written

$$\int_0^1 \frac{dx}{x}\left[A_1^p(x) \cdot \nu W_2^p(x) - A_1^n(x) \cdot \nu W_2^n(x)\right] = \frac{1}{3}\left|\frac{g_A}{g_V}\right| \simeq 0.4 \qquad (1)$$

where g_A/g_V is the ratio of axial to vector weak coupling constants, and is about 1.2 experimentally.

In order to evaluate the left hand side of the above equation, we assume

$$A_1^n(x) = 0 \qquad \text{(neutron asymmetry)}$$

and use a fit for νW_2^p obtained from the SLAC-MIT experiments. We use our measured values of $A_1^p(x)$ as given in Table 1 and assume further that scaling is valid so that A_1^p depends only on x. Hence we obtain for the range of x from 0.1 to 0.5

$$\int_{0.1}^{0.5} \frac{dx}{x}\left[A_1^p(x)\ \nu W_2^p(x)\right] = 0.19 \pm 0.03$$

Fig. 3 shows νW_2^p, $\nu W_2^p/x$ and our data points for $A_1^p(x)$ as a function of x.

It is obvious that the integral is very sensitive to the lower limit but not to the upper limit. If we assume $A_1^p(x) = 1$ for the range from 0.5 to 1.0, then the contribution to the integral from this region is about 0.02. Therefore, roughly speaking, about 50% of the sum rule is saturated by the contribution from the proton in the range x = 0.1 ~ 1.0.

J.D. Bjorken, Phys. Rev. 148, 1467 (1966).
J.D. Bjorken, Phys. Rev. D 1, 1376 (1970).
R.P. Feynman, Photon-Hadron Interactions (W.A. Benjamin, Inc., 1972).

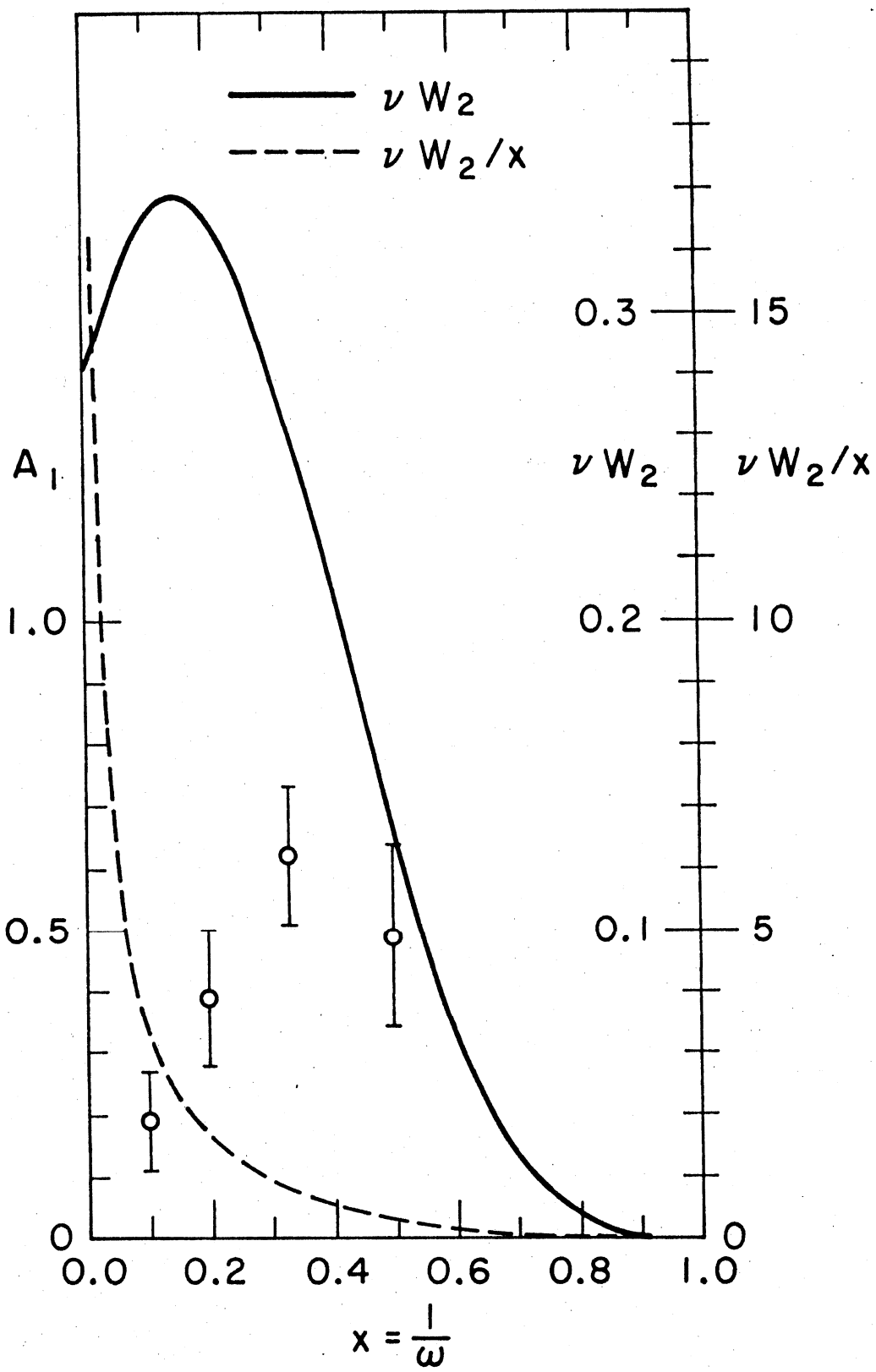

Graph relevant to Bjorken sum rule.

Fig. 3

Table 2. Preliminary On-line Results of Asymmetry Measurements in Resonance Region (Data Taken in 1976)

E (GeV)	θ (deg)	Q^2 $(GeV/c)^2$	W (GeV)	ω	Δ(%)	A^a	D^b	$A_1 + \eta A_2{}^a$
.47	7°	0.56	1.234	2.1	0.07±0.06	0.0135±0.0121(0.0110)	0.11	0.12±0.11(0.10)
.47	7°	0.55	1.376	2.9	0.27±0.11	0.0541±0.0243(0.0218)	0.14	0.38±0.17(0.15)
.47	7°	0.52	1.522	3.7	0.40±0.09	0.0799±0.0233(0.0180)	0.18	0.44±0.13(0.10)
.47	7°	0.50	1.688	5.0	0.26±0.08	0.0485±0.0175(0.0148)	0.23	0.21±0.08(0.06)
.47	7°	0.48	1.820	6.1	0.29±0.12	0.0541±0.0251(0.0228)	0.27	0.20±0.09(0.08)
.71	8°	1.54	1.522	1.9	0.58±0.13	0.1168±0.0339(0.0265)	0.18	0.64±0.18(0.14)
.71	8°	1.49	1.688	2.3	0.66±0.14	0.1085±0.0294(0.0228)	0.22	0.51±0.14(0.11)

a. The total errors are the statistical counting errors added in quadrature to the systematic errors in P_e, P_p and F; the number in parentheses are the one standard deviation counting errors.

b. $D = (E-E'\varepsilon)/E$; R is assumed to be 0.

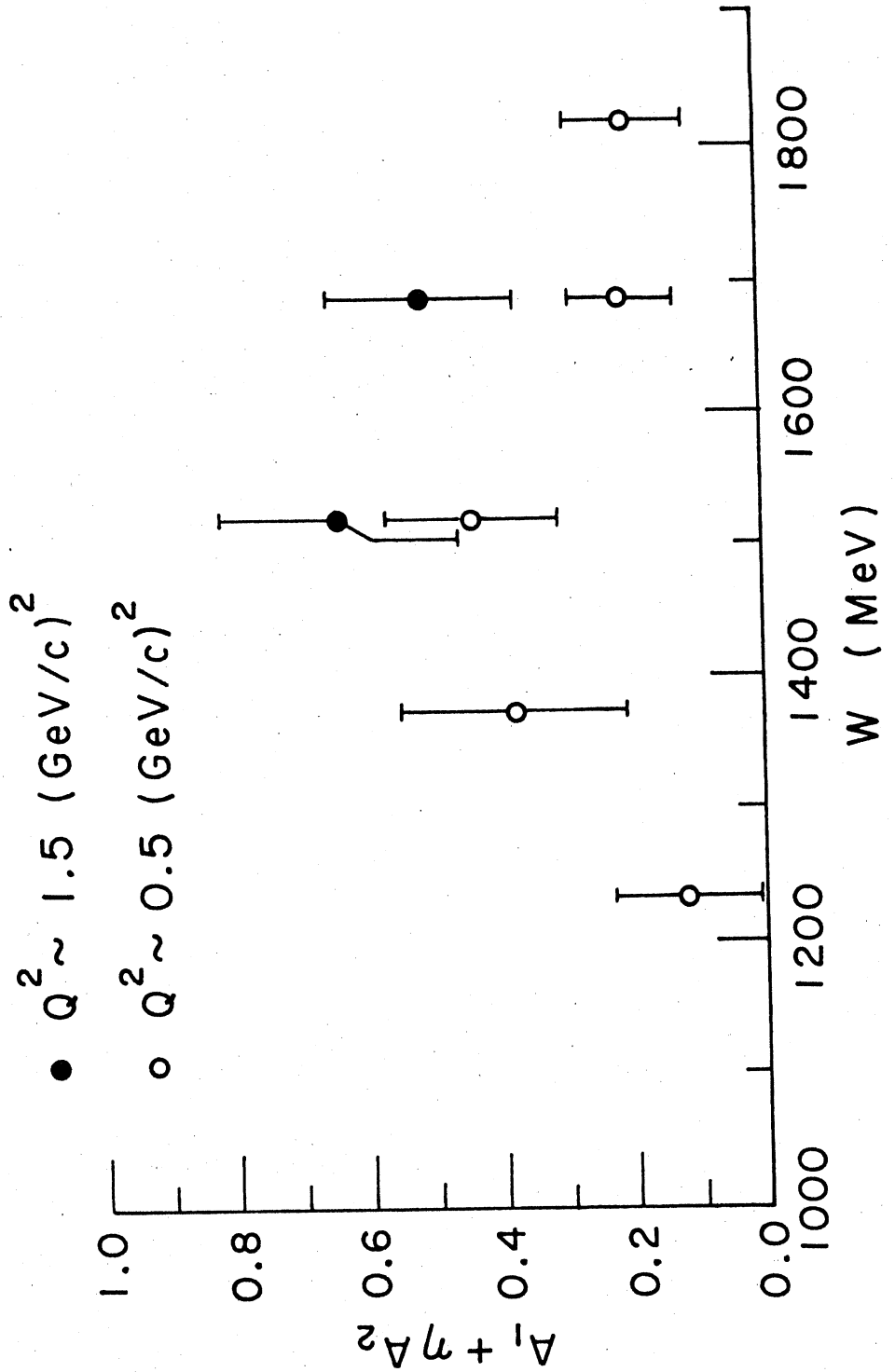

Fig. 4

One-Line Results in Resonance Region from E80.

II. Motivation

The principal scientific objectives of this proposal are

(1) To increase the precision (~a factor of 3) and extend the kinematic range (ω ~ 1.5 to 13 and Q^2 up to 9 $(GeV/c)^2$) of measurement of the virtual photon-proton asymmetry A_1^p. These measurements will significantly improve the test of scaling for spin-dependent quantities and will provide useful results for distinguishing models of proton structure.

(2) To measure for the first time the virtual photon-neutron asymmetry A_1^n. Values of A_1^n very different from those of A_1^p are predicted by the theories of nucleon structure and will be tested by our measurements. Furthermore an improved test of the Bjorken sum rule (Eq.(1), p. 10) can be made when neutron data are available.

A new large acceptance spectrometer operating up to 18 GeV/c together with improvements in the beam intensity and target polarization will result in an effective increase in data accumulation rate by more than an order of magnitude. The statistical error in the counting rate asymmetry $\Delta(\Delta=P_e P_p F A)$ for a particular kinematic point will be reduced by a factor of 3 to 4 compared to E80, and data over a wide kinematic range will be obtained simultaneously (Section III).

Measurements of the neutron asymmetry A^n (or A_1^n) can be deduced from measurements on the deuteron and on the proton. With adequate precision the deuteron magnetic moment can be taken as the sum o the proton and neutron magnetic moments (The effect of the ^3D state

admixture in the deuteron can be neglected.), and hence $\Delta_n = \Delta_d - \Delta_p = P_e P_n F_n A^n$, where $P_n \sim P_d$. Since the neutron asymmetry A^n must be obtained essentially by subtraction of the proton asymmetry from the deuteron asymmetry, and since, furthermore, achievable deuteron polarizations in targets are about 22% whereas proton polarizations are about 80%, the measurement of neutron asymmetry is difficult and the projected statistical accuracies are $\Delta A_1^n \simeq 0.05$ to 0.1. (See Table 10)

(1) The Bjorken sum rule is given in Eq. (1) on p. 10. This important relation was derived from the quark-parton model of the nucleon and the assumption that the weak current for quarks has the same form as that for leptons. We give on p.10 the present state of the test of this relation based on our measurements of proton asymmetry A_1^p. The main contribution that our proposed E130 experiment will make to an improved test of the Bjorken sum rule will be in providing data on A_1^n, which appears in a term of the sum rule. The new values of A_1^p will be of higher precision and will cover a slightly larger range in ω than the E80 data, and hence will be of some value to the accurate evaluation of the integral, particularly when they are combined later with values of A_1^p at high ω from the planned CERN muon deep inelastic polarization experiment.

(2) Violation of Bjorken scaling for the spin independent nucleon structure functions, has been observed both in electron (Taylor, 1975) and in muon (Mo 1975) deep inelastic scattering. This is a topic of great theoretical importance (Llewellyn-Smith, 1975). Scaling relations are also predicted for the spin dependent proton structure functions [e.g., $A_1^p(\nu, Q^2) \underset{\nu \to \infty ;\ Q^2 \to \infty}{=} A_1^p(\omega)$]. Since the spin dependent proton structure functions are independent of the spin-averaged structure functions, the scaling relation for A_1^p is a new, independent relation. Scaling violation for spin-dependent structure functions may occur due to parton structure

(Colglazier and Rajaraman, 1974), as a logarithmic violation in gauge theory (Ahmen and Ross, 1975), or through use of the wrong scaling variable It will be useful to have a more precise test of scaling for A_1^p, which E130 dat should provide. Furthermore, eventually the combination of precise E130 data with the CERN polarized muon data at high Q^2 will also be very valuable.

(3) Theoretical predictions for A_1^p and A_1^n are given in Figures 5 and 6 from a number of classes of quark-parton models of the nucleon.

Curve 1. A relativistic symmetric valence quark model (Kuti-Weisskopf, 1971)

Curves 2. Models of Kuti-Weisskopf type using other recent experimental da from e-p, e-n and ν-N scattering and dilepton production in pp collisions, and improved quark distribution functions. [(a) Blankenbecler et al., 1975: (b) McElhaney and Tuan, 1973: (c) Barger and Phillips, 1974.]

Curve 3. Unsymmetrical model for which $A^n \to 1$ as $x \to 1$ with single parton carrying the entire nucleon momentum (Feynman, 1972, Close, 1973). See also Flume-Gorczyca and Kitakado (1974) and Farrar and Jackson (1975). Farrar and Jackson emohasize the importance of polarized e-p scattering near x=1.

Curve 4. Nucleon model incorporating the Melosh transformation which distinguishes between constituent and current quarks (Close, 1974).

Curve 5. Asymmetry prediction based on source theory which does not use a parton picture. (Schwinger, 1976, 1977)

The usefulness of the new higher precision proton asymmetry data we propose as regards the proton models can be discussed for three different regions of x values.

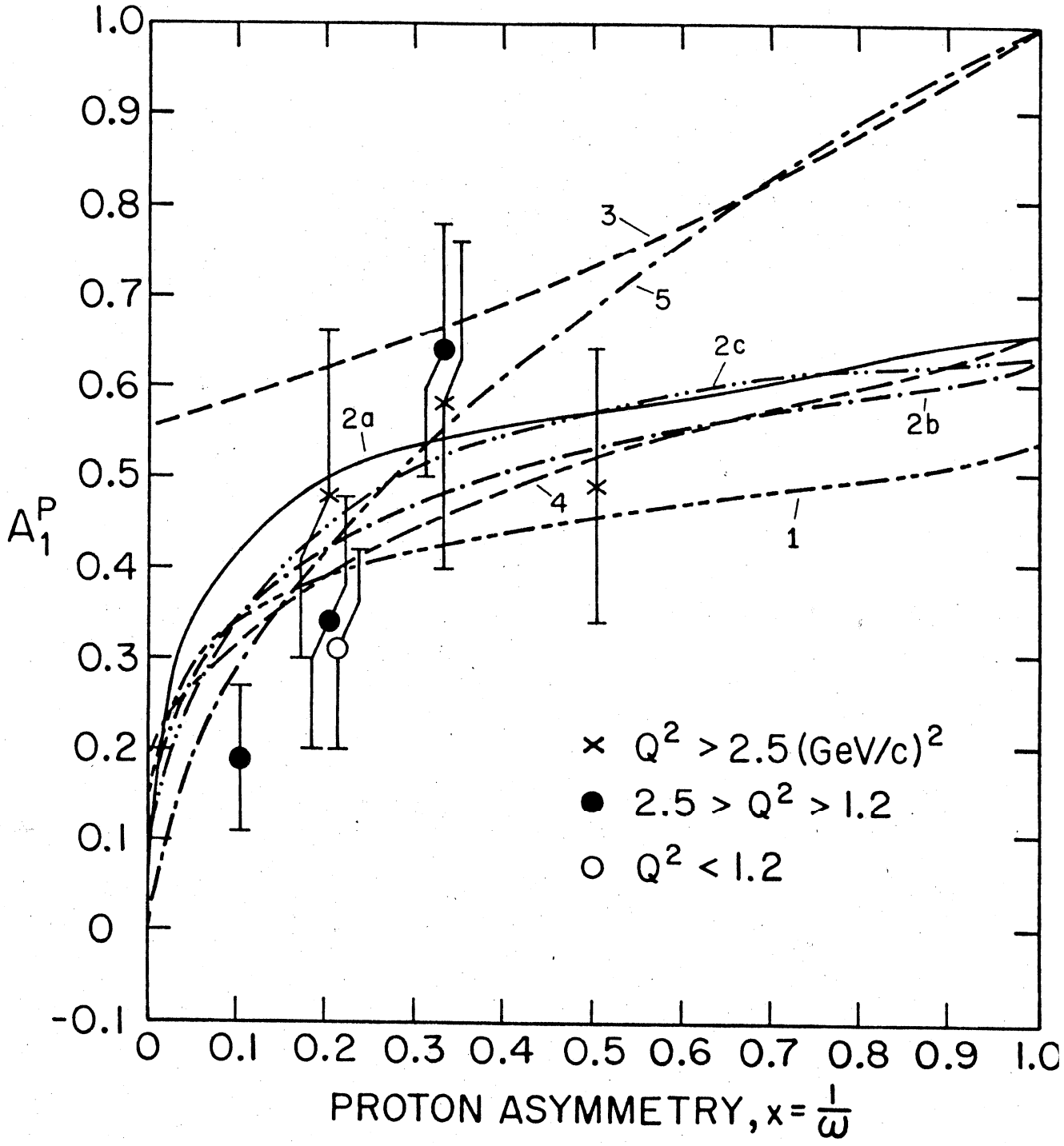
1.0
0.9
0.8
0.7
0.6
0.5
0.4
0.3
0.2
0.1
0
-0.1
A_1^P
0
0.1
0.2
0.3
0.4
0.5
0.6
0.7
0.8
0.9
1.0
PROTON ASYMMETRY, $x = \frac{1}{\omega}$
3
5
2c
2a
2b
4
1
× $Q^2 > 2.5$ (GeV/c)^2
● $2.5 > Q^2 > 1.2$
○ $Q^2 < 1.2$

Fig. 5

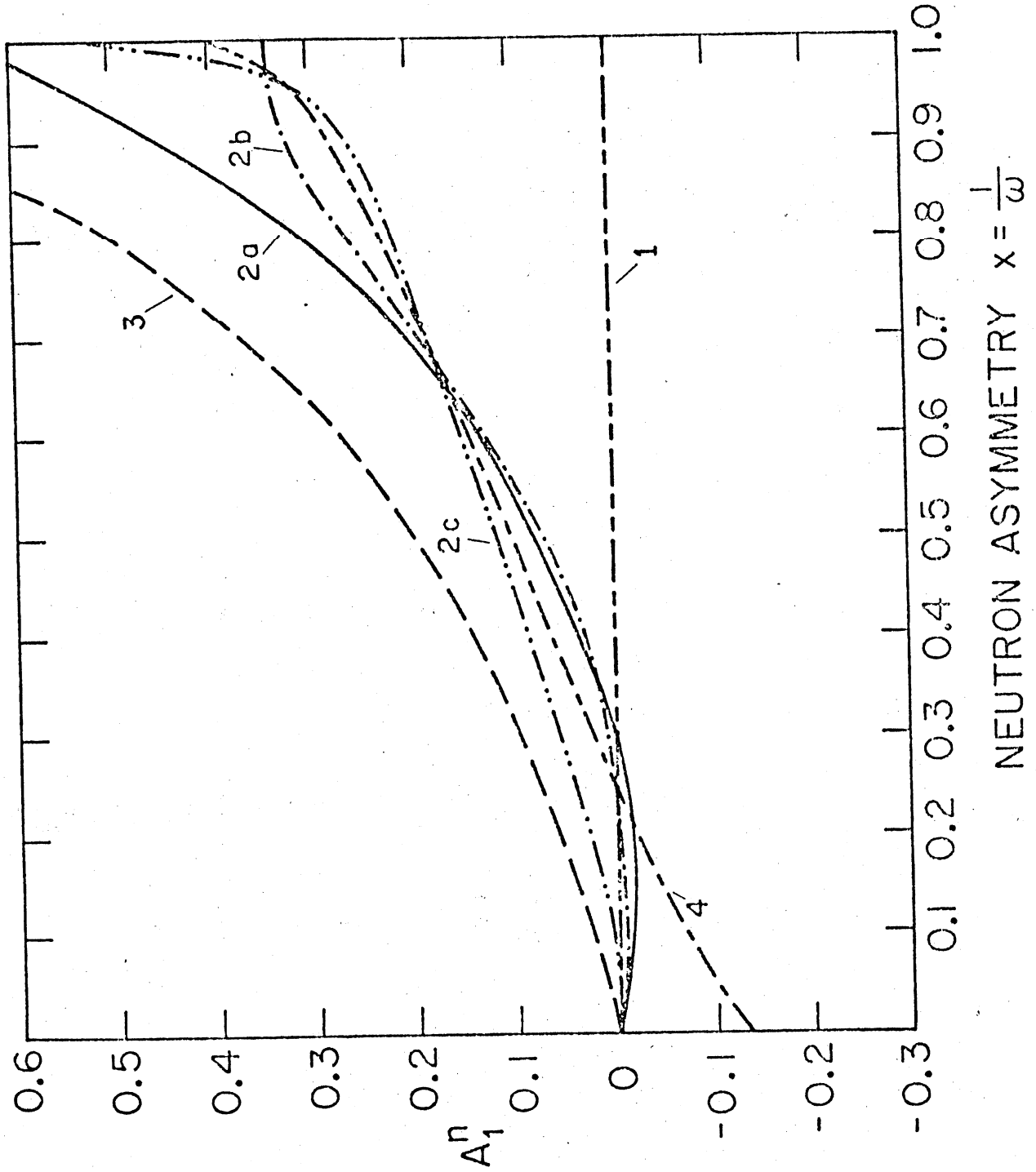
0.6
0.5
0.4
0.3
0.2
0.1
0
-0.1
-0.2
-0.3
A_1^n
0.1 0.2 0.3 0.4 0.5 0.6 0.7 0.8 0.9 1.0
NEUTRON ASYMMETRY $x = \frac{1}{\omega}$
1
2a
2b
2c
3
4

Fig. 6

1. $x \to 1$ region $(0.5 \leq x \leq 1.0)$

There are two classes of theories as seen in Fig. 5 which give

I. $A^p \to 0.6 \pm 0.05$

II. $A^p \to 1$

It will clearly be very valuable to obtain A_1^p values with higher accuracies in the range of $x = 0.5$ as proposed (Table 9). Such data could be important in the choice between these two classes of models.

2. Central region $(0.2 \leq x < 0.5)$

Experimental data are most easily obtained here. Improved accuracies with $\Delta A^p \simeq 0.03$ will be useful in establishing small differences between model predictions. Data can be obtained over a wide range of Q^2 for a test of scaling. Furthermore, it is in this region that the neutron asymmetry will be measured, and accurate proton data are required in order to determine A_1^n from asymmetry data on the deuteron.

3. $x \to 0$ region $(0 \leq x < 0.2)$

Predictions of the models are less certain and even the sign of the asymmetry is an open question. Improved data out to $\omega \sim 13$ should be very useful. Radiative corrections will be important.

Data on the neutron asymmetry A^n will be exploratory and will test the qualitative predictions of the quark-parton models. In the central region $0.1 \leq x < 0.4$ where we propose to measure A_1^n to $\sim \pm 0.05$, the models predict that A_1^n will have a small positive value.

As we point out in our Physical Review Letter (M.J. Alguard et al., Phys. Rev. Lett. 37, 1261 (1976) our experimental data on the asymmetry in the scattering of longitudinally polarized electrons by longitudinally polarized protons determines only the virtual photon proton asymmetry ($A_1^p + \eta A_2^p$). The kinematic factor η is relatively small and, taken together with the positivity limit $|A_2^p| < \sqrt{R}$, the upper limit on ηA_2^p is about equal to the statistical errors for our E80 data. Furthermore, quark-parton models predict that A_2^p will be smaller than its positivity limit. Hence we have neglected this term in comparisons of our measured asymmetry values with theoretical values for A_1^p.

With the improved precision in values of A_1^p proposed here, the above approximation may no longer be valid and it will be important to obtain experimental data on A_2^p in order to determine A_1^p alone. Although the asymmetry $A_2^p = \frac{\sigma_{TL}}{\sigma_T}$ arises from an interference between longitudinal and transverse photons and does not appear to be a crucial quantity for the theories at present, it would still be valuable to test the general qualitative theoretical prediction that A_2^p is very small.

Measurements of A_2^p can be made with transverse polarization of the proton target. We have the major items of a suitable transversely polarized proton target from experiments with a polarized target at Brookhaven. The PEGGY source and spectrometer would be applicable.

We may at a later date submit a proposal to do measurements of A_2^p, which will require about 300 hrs of data-taking time.

A major experiment is being planned and prepared for the SPS at CERN (European Muon Collaboration) to measure the asymmetry A in deep inelastic scattering of polarized muons by polarized protons. Their data will be obtained at much higher ν and Q^2 than our SLAC data; the ω range to be covered extends from $\omega \simeq 1.5$ to $\omega \simeq 20$. Their projected statistical accuracies are comparable to our SLAC E80 results and hence a factor of 3 to 4 worse than our projected E130 results. The SLAC and CERN experiments will particularly usefully complement one another in providing a test for scaling of A_1^p. It is of course always useful to study a process both with electrons and with muons and thus be able to test μe universality.

As a general conclusion we emphasize that the polarized e-p and e-n scattering experiments provide a unique type of data, which can test the general concepts of sum rules and scaling and also provide information about the spin structure of the nucleon.

European Muon Collaboration, CERN proposal July 1, 1974; Addendum September, 1976.

References

J. Kuti and V.F. Weisskopf, Phys. Rev. D 4, 3418 (1971).

R. Blankenbecler et al., SLAC-PUB-1531 (1975).
See also G.R. Farrar, Nucl. Phys. B 77, 429 (1974).

R. McElhaney and S.F. Tuan, Phys. Rev. D 8, 2267 (1973).
J.T. Dankin and G.J. Feldman, Phys. Rev. D 8, 2862 (1973);
See also G. Altarelli, N. Cabibbo, L. Maiani, and R. Petronzio, Nucl. Phys. B 69, 531 (1974). J. Okada, S. Pakvasa and S.F. Tuan, Lett. Nuovo Cimento 16, 555 (1976).
V. Barger and R.J.N. Phillips, Nucl. Phys. B 73, 269 (1974).
See also H.P. Paar and E.A. Paschos, Phys. Rev. D 10, 1502 (1974).

R. Feynman, Photon and Hadron Interactions, (W.A. Benjamin, Reading, Mass., 1972)

F.E. Close, Phys. Lett. 43B, 422 (1973).
Flume-Gorczyca and S. Kitakado, DESY Report 74/48 (1974).
G.R. Farrar and D.R. Jackson, Phys. Rev. Lett. 35, 1416 (1975).

J. Schwinger, Proc. Nat. Acad. Sci. 72, 1 (1975).

J. Schwinger, Proc. Natl. Acad. Sci. 73, 3351 (1976).

J. Schwinger, "Deep Inelastic Sum Rules in Source Theory," preprint, 1977.

E.W. Colglazier and R. Rajaraman, Phys. Rev. D 10, 334 (1974).

M.A. Ahmed and G.G. Ross, Phys. Lett. 56B, 385 (1975).

L.W. Mo, Proceedings of the 1975 Intern. Symposium on Lepton and Photon Interactions at High Energies, Stanford University, ed. W.T. Kirk (Stanford Linear Accel. Center, Stanford, Calif., 1975), p. 651;
C. Chang et al., Phys. Rev. Lett. 35, 901 (1975).

R.E. Taylor, Proceedings of the 1975 Intern. Symposium on Lepton and Photo Interactions at High Energies, Stanford University, ed. W.T. Kirk (Stanford Linear Accel. Center, Stanford, Calif., 1975), p. 679.

C.H. Lewellyn-Smith, Proceedings of the 1975 Intern. Symp. on Lepton and Photon Interactions at High Energies, Stanford University, ed. W.T. Kirk (Stanford Linear Accel. Center, Stanford, Calif., 1975), p. 709.

III. Description of Experiment

Introduction

The principles and techniques of our proposed experiment are essentially the same as for our SLAC E80 experiment. PEGGY will be used as the polarized electron source and our present polarized target, still operating at $1^{\circ}K$, will also be used. Modest modifications in PEGGY will result in an increase in beam intensity by a factor of 2. Modest changes in the target will achieve higher proton polarization, and provide polarized deuterons. The major improvement over E80 will be obtained with a new fixed-angle large-acceptance spectrometer operating at a momentum up to 18 GeV/c. It will have lower angular and momentum resolutions than the 8 GeV/c spectrometer, but the resolutions will be quite adequate for our deep inelastic studies. The spectrometer will have an acceptance 7.5 times that of the 8 GeV/c spectrometer, and at the higher operating energies more favorable kinetic points provide an additional improvement factor of 3.

The new spectrometer, together with the modest modifications in PEGGY and in the polarized target, should thus increase our effective data acquisition rate by about a factor of 40.

Polarized Electron Source

The Yale-SLAC polarized electron source, PEGGY, was continually improved (Alguard et al., 1977) throughout the duration of E80 to the point where an average intensity of 0.88×10^9 e^-/pulse at GeV energies was achieved during the last two weeks of running. In fact, during periods lasting several hours, intensities of 1.1×10^9 e^-/pulse were sustained. At the same time, the overall availability of PEGGY was increased to 75%. All of the pertinent operating characteristics of PEGGY are summarized in Table 3.

Although the performance characteristics of PEGGY were quite satisfactory for E80, several improvements in the source are possible without major modification. As a result of improved uv optical technology it will be possible to remove the uv interference filter (which rejects the 670.8 nm Li resonance radiation) and the existing aluminized MgF_2 overcoated diagonal mirror and to replace this combination with a single dielectric mirror. The reflectivity of the dielectric mirror over the relevant bandwidth (180 nm-230 nm) is estimated by Acton Research to be 0.85; virtually all 670.8 nm radiation will be rejected. This reflectivity is to be contrasted with the effective optical efficiency of 0.39 for the existing filter and mirror combination. Thus a gain of a factor of 2.2 in electron intensity can be expected. An additional gain in electron intensity of a factor of 1.2 is expected from refurbishing of the ellipsoidal mirror, giving an overall gain of 2.6.

We therefore anticipate that PEGGY will be able to provide ~2.8 x 10^9 e^-/pulse at GeV energies with no degradation in electron polarization. Since radiation damage of the target will restrict useful operation to ~1.5x10^9 e^-/pulse we expect to be able to reduce the intensity of the Li atomic beam thereby extending the lifetime of the Li oven load to >200 hrs and increasing the availability of the source to 85%, as indicated in Table 3. Should higher electron intensities be required at any time, we are modifying the oven and collimator system to produce an atomic beam with an intensity about 1.5 times greater than the existing beam. This will provide the capability of producing an electron intensity of ~4x10^9 e^-/pulse on target with a Li oven load lifetime of ~150 hrs. All the improvements require minimal modification and could be implemented by the fall of 1977. The anticipated PEGGY characteristics for E130 are summarized in Table 3.

M.J. Alguard et al., SLAC-PUB-1902, 1977, submitted to 1977 Particle Accelerator Conference, Chicago, Illinois, March 16-18, 1977.

Table 3. Operating Characteristics of Polarized Electron Beam

Characteristics	Experimental Value 12/76	Projected Value For E130
Pulse length	1.5 μs	No change
Repetition rate[a]	180 pps	No change
Electron intensity at GeV energies		
Average	0.88×10^9 e^-/pulse[b]	$>2 \times 10^9$ e/pulse
Maximum	1.1×10^9 e^-/pulse[c]	
Pulse to pulse intensity variation	<5%	<5%
Electron polarization	0.85	0.85
Polarization reversal time	3s	3s
Intensity difference upon reversal[d]	<5%	~1%
Lifetime of lithium oven load[e]	175 h	200 h
Time to reload lithium	43 h	36 h
Overall availability	75%	85%

[a]Modulator and flash lamp are usually operated at a repetition rate of 180 pps with 120 pps injected into accelerator and 60 pps used for polarization measurement at low energy.

[b]Based upon final two weeks of E80.

[c]Sustained for periods of several hours.

[d]During E95 it was shown that the intensity difference can be reduced to <1%.

[e]Based upon 740g capacity of oven.

Polarized Target

The existing Yale-SLAC polarized target can be used for the experimer without major modifications. Either normal or deuterated butanol can be polarized in the same apparatus, since both protons and deuterons interact with the electron spin reservoir in exactly the same way. (Borghir and Scheffler, 1971) For a given spin temperature T_s, deuteron polarizations are much lower than proton polarizations; a deuteron polarization of 22% corresponds to the 80% proton polarizations projected for E-130 for unirradiated target material. The only hardware addition required for deuterons is a 32 MHz DMR system for measuring the polarization.

Our main effort on the target will be devoted to improving the proton polarization to 80% and the polarizing times to 2 min, as has been achieved at other laboratories (Borghini et al., 1971; Hartman et al., 197 with 50 kG - $1^{\circ}K$ targets albeit with smaller target volumes. Projected target operating characteristics are listed in Table 4.

The main performance limitation of our target in E80 was inadequate microwave power. Only ~5% of the generated microwave power was delivered to the target material; we hope to double this efficiency. Also, oscillators with twice the power output of our carcinotron are now commerically available. Improving the cryogenics will lower the temperature, accomodate more microwave power, and also significantly reduce the microwave power needed to achieve a given T_s. We are now setting up the target in the cryogenics building and will search for possible heat leaks, constrictions, oscillations, etc., that may be

reducing the cryostat's performance but can be eliminated once isolated. Should a further reduction in temperature be desirable, additional pumping capacity could be procured and installed without difficulty.

The deuteron polarization will be determined by techniques based on measuring the lineshape and measuring T_s through the polarization of the ~2% free protons present in the sample (Guckelsburger and Udo, 1976). In addition, the method of weighing individual targets will give an independent measurement. Both methods should be accurate to ~5%.

M. Borghini and K. Scheffler, Nucl. Instr. and Method. 95, 93 (1971).

M. Borghini, et al., Nucl. Instr. and Meth. 97, 577 (1971).

K. Guckelsberger and F. Udo, to be published.

G. Hartman, et al., Nucl. Instr. and Meth. 106, 9 (1973).

Table 4: Operating Characteristics for Polarized Target

	E-80	E-130 Proposed	CERN (Borghini et al., 19
Temperature	1.05°K	1.0°K	1.0°K
Magnetic field	50 kG	50 kG	50 kG
Cooling power	~700 mW	~700 mW	
Volume	25 cm^3	25 cm^3	0.25 cm^3
Beam heat load	~125 mW at 100 μA	~190 mW at 150 μA	
Microwave power	100-200 mW	~500 mW	~200 mW/cm
Annealing time	45 min.	30 min.	
Polarizing time			
Protons	4 min.	2 min.	
Deuterons		5 min.	5 min.
Polarization (no radiation damage)			
Protons	68%	75-80%	86±4%
Deuterons		16-22%	26±2%
Average polarization (including radiation damage)			
Protons	50%	55%	
Deuterons		12%	

Beam Energy

19.4 GeV is at present the highest one of the magic energies at which the electrons arrive at the pivot with longitudinal polarization after precessing through the 24.5° bend from the accelerator. However, with a small additional bend we can shift the magic energy. For kinematic reasons we like to run at the highest practical beam energy. Our plan is to use 22 GeV with an additional bend of 13 mrad in the beam achieved with a deflector magnet (5D36) just upstream of the polarized target (Fig. 7). The PEGGY beam can be dumped in the SEQ, as during E80. However, it should be located at the end of ESA far away from the detectors, and it should be well shielded in order to minimize background. An energy of 19.4 GeV could be a satisfactory fall back value.

New Spectrometer

Data taking for E80 has been limited by very low event rate, which was as low as 0.002 events/pulse for our most difficult point at $\omega=2$, $Q^2=4$. The polarized target can not be exposed to a much greater dose of electrons because of the radiation damage that goes along with it. Therefore a spectrometer that has a much greater acceptance than the 8 GeV spectrometer is required.

Basically the spectrometer can be simple because we do not require high momentum or angular resolution. We had originally proposed to adopt the E122 spectrometer design (Sato, 1976) which features three magnets (B201, Q82, B81) of the 8 GeV and 20 GeV spectrometers. Since we cannot take advantage of the focusing property of the quadrupole, we have studied the simpler configuration with only the two bending magnets B201 and B81 (Figs. 9,10, 11). This gives us a further gain in solid angle by a factor of 1.5 as compared to the E122 scheme while it still covers a large (50%) momentum bite. Overall we gain a factor of 7.5 in acceptance $\Delta\Omega$ $\Delta p/p$ as compared to the 8 GeV spectrometer used in E80 (Table 5).

Table 9 gives several kinematic points in the continuum that would be obtained with this spectrometer. The large momentum acceptance is well matched to the entire ω range of interest from 2.5 to 13. Thus all these data would come from one spectrometer setting ($\theta=5^\circ$), and indeed fluctuations in target polarization, for example, would have no effect on the ω dependence. Table 8 covers the low ω, high Q^2 range that would be obtained with a $\theta = 10^\circ$ setting.

T. Sato, "The Spectrometer for E122," 8/3/76, Group A Engineering Note 66.

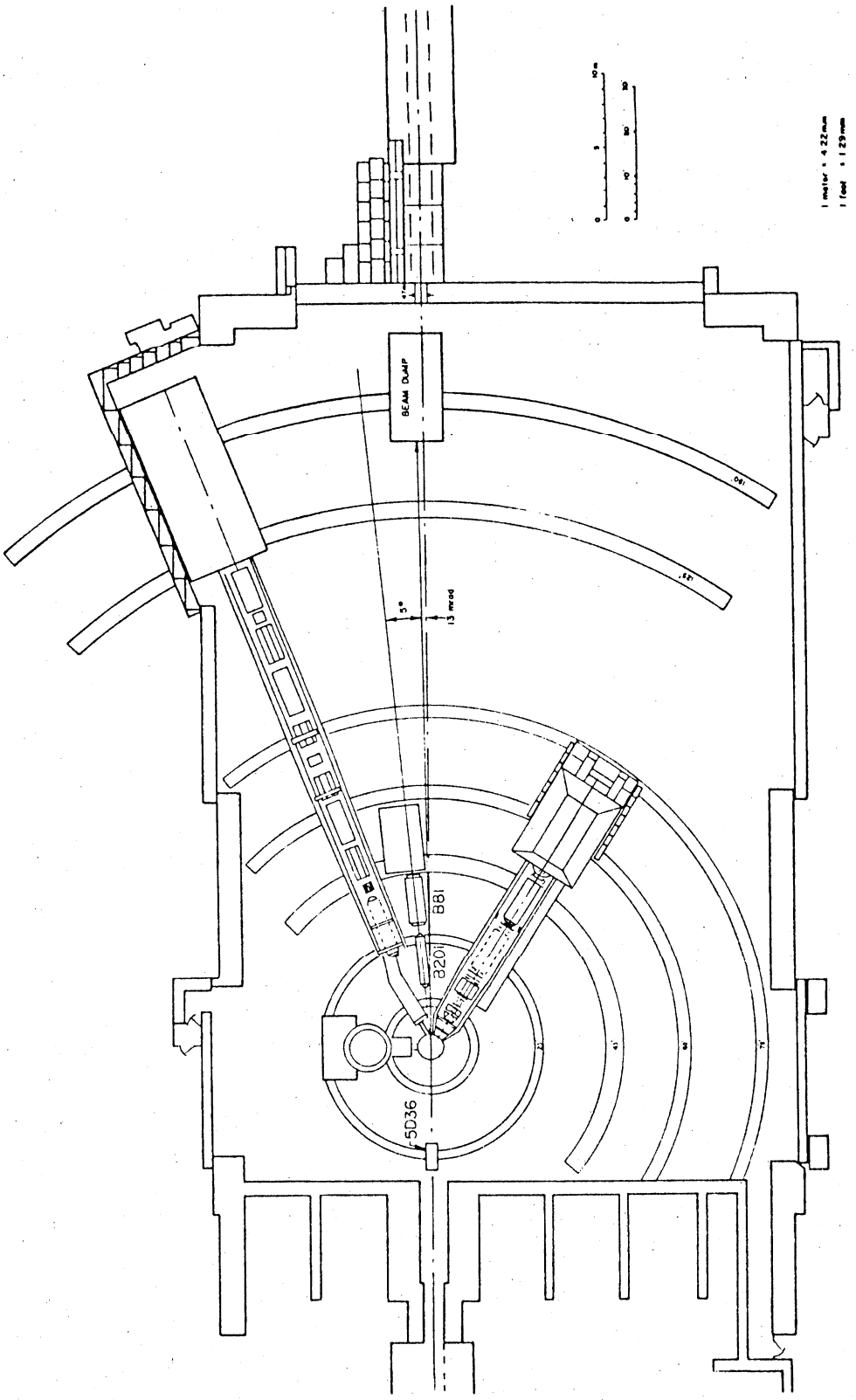

Fig. 7

Table 5: Spectrometer

	E130 Spectrometer	8 GeV spectrometer (for comparison)
$\Delta p/p$	±25%	±2%
$\Delta\theta$	±7.5 mrad	±7 mrad
$\Delta\phi$	±15 mrad	±27 mrad
$\Delta\Omega$	0.45 msr	0.75 msr
$\int\Delta\Omega\,\Delta p/p$	0.22 msr	0.03 msr

Fig. 8 shows a layout of the spectrometer. The scattering angle ϑ is recorded in the horizontal plane. Momentum dispersion is in the vertical plane, orthogonal to ϑ. The bending angle of $2x7^{\circ}$ is sufficient to block the straight line of sight between target and detector Yet the required excitation of the magnets at 15 GeV/c is modest and the field inhomogeneities are less than 1% across the used gapwidth. The trajectories are recorded in four planes of proportional wire chambers (PWC) and determine momentum and scattering angle to an accuracy of $\Delta p/p = \pm 1\%$ and $\Delta\vartheta = \pm 0.1$ mrad. At our kinematic settings (Table 8 to 10) this translates into resolutions for ω and Q^2 of $\Delta\omega/\omega \approx \pm$ (2 to 5)% and $\Delta Q^2/Q^2 \approx \pm 1\%$, which is adequate.

Electrons are identified with a preradiator (P) - shower counter (S) combination with an expected pion rejection of at least 50 to 1. Pion contamination essentially originates from pion photoproduction and becomes worrysome only at the lower momentum bins where the π^-/e^- ratio can exceed 1. We have estimated the π^-/e^- ratios for E130 on the basis of data from SLAC experiment E89 (Table 6). In order to improve the pion rejection further we plan the addition of a long N_2-Cerenkov counter (C) operated at 0.25 atm with a pion threshold of about 12 GeV/c. Even a few GeV/c above threshold such a counter still maintains useful discriminatory power. A Cerenkov counter with an even higher threshold would become either too long or drop below 99% efficiency. Finally, there are two aperture defining counters (F,R). With the exception of the PWC's the detector arrangement is very similar to the situation in E80 (Table 7).

The multiwire proportional chambers are to be constructed with 2 mm wire spacing and are of conventional design. We are planning to have a prototype ready by August 1977.

Our group has built and owns readout electronics for 20 chamber planes which is being used in the E-61 polarization experiment at Fermilab. This readout uses serial (Dhawan,1974) transmission using one coax cable to transfer datawords between a chamber plane and a CAMAC module. This system is very flexible and adaptable to use in ESA.

The mechanical construction of the spectrometer requires that a massive fixed angle support frame be built for the two magnets and the detector housing. Helium bags rather than vacuum chambers will be used with the magnets. A detector house has to be assembled from concrete blocks. Moving from the 5° to the 10° setting will require dissassembly and reassembly of the spectrometer components. Substantial experience with regard to the cost and labor aspect of the spectrometer setup should be gained from SLAC experiment E122 which requires quite similar operations.

S. Dhawan, "A Fast readout and Geometrical Reconstruction System for Proportional Wire Chambers," IEEE Transactions on Nuclear Science, Vol. NS-21, No. 1, 1974.

Table 6: Estimated π^-/e^- ratio

p (GeV/c)	$\theta=5^o$ π^-/e^-	$\theta=10^o$ π^-/e^-
10	<6	<1.6
11	3	<1.0
12	1.5	<1.0
13	0.6	<1.0
14	0.3	<1.0
>15	<0.1	<1.0

Table 7: Detectors and Related Hardware

Qty.	Type	Proposed Deliverer
1	Lead glass shower counter (36×100 cm^2) with four phototubes (existing)	SLAC
1	Preradiator: already used in E80 with phototubes (existing)	SLAC
1	N_2-Cerenkov counter: $0.5 \times 0.9 \times 4.5$ m^3, to be operated at ~0.25 atm.	Yale
1	Cerenkov N_2 gas supply, pump and pressure controls (existing)	SLAC
2	Front and rear trigger counters	Yale
10	Proportional wire chambers: four X, four Y and two tilted chambers (35 x 85 cm each, 2 mm wire spacing); amplifiers; readout electronics and computer interface for ca. 3000 channels; magic gas supply. The readout electronics is already existing.	Yale

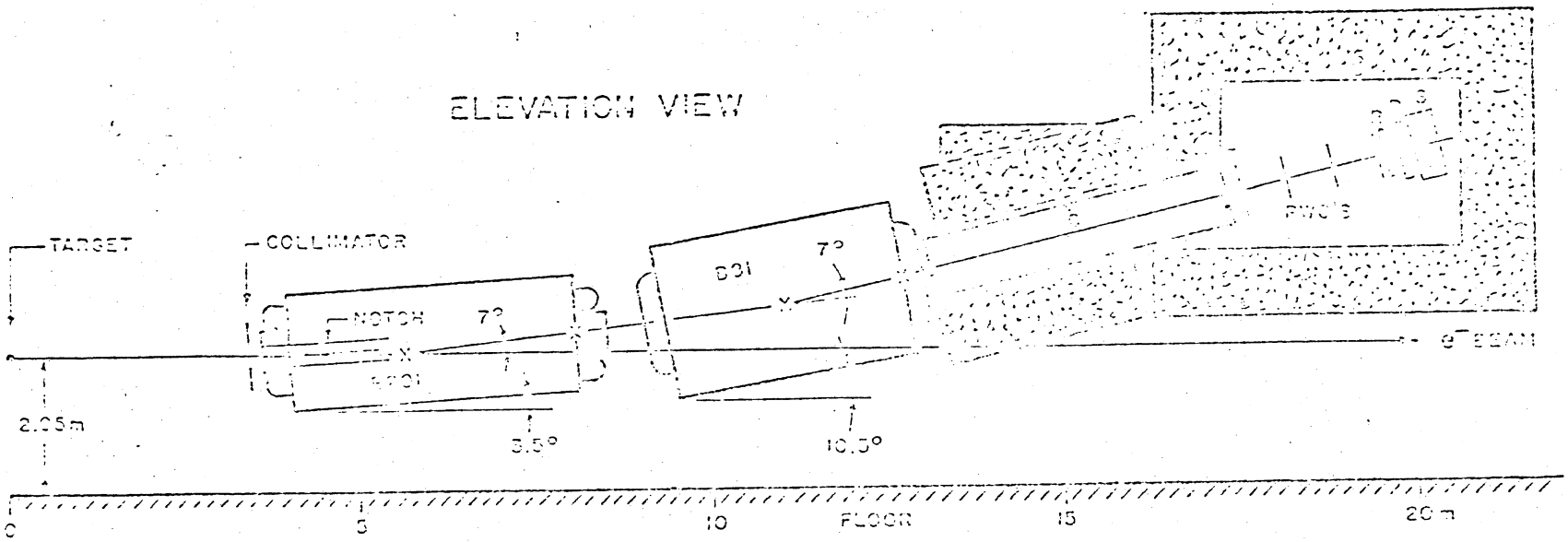

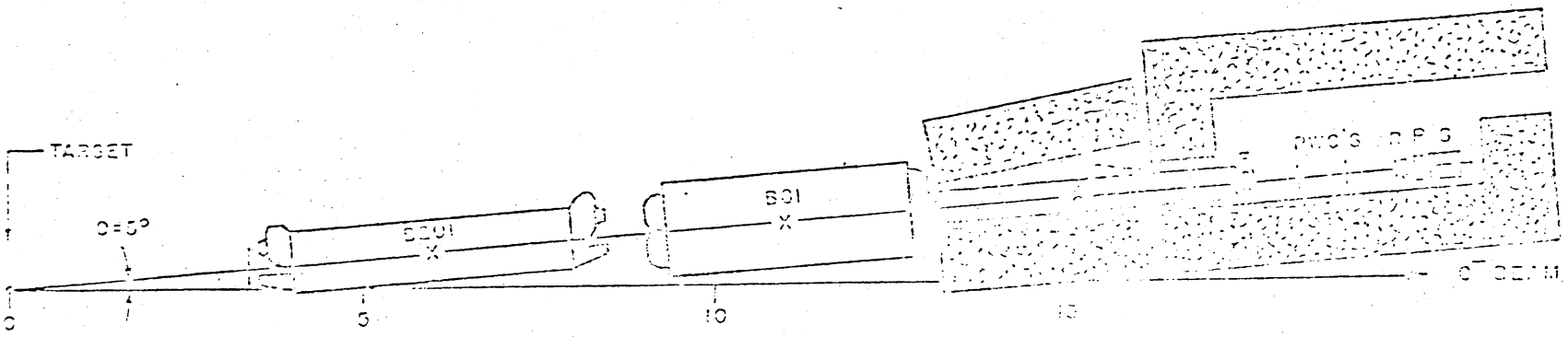

PLAN VIEW

Fig. 8

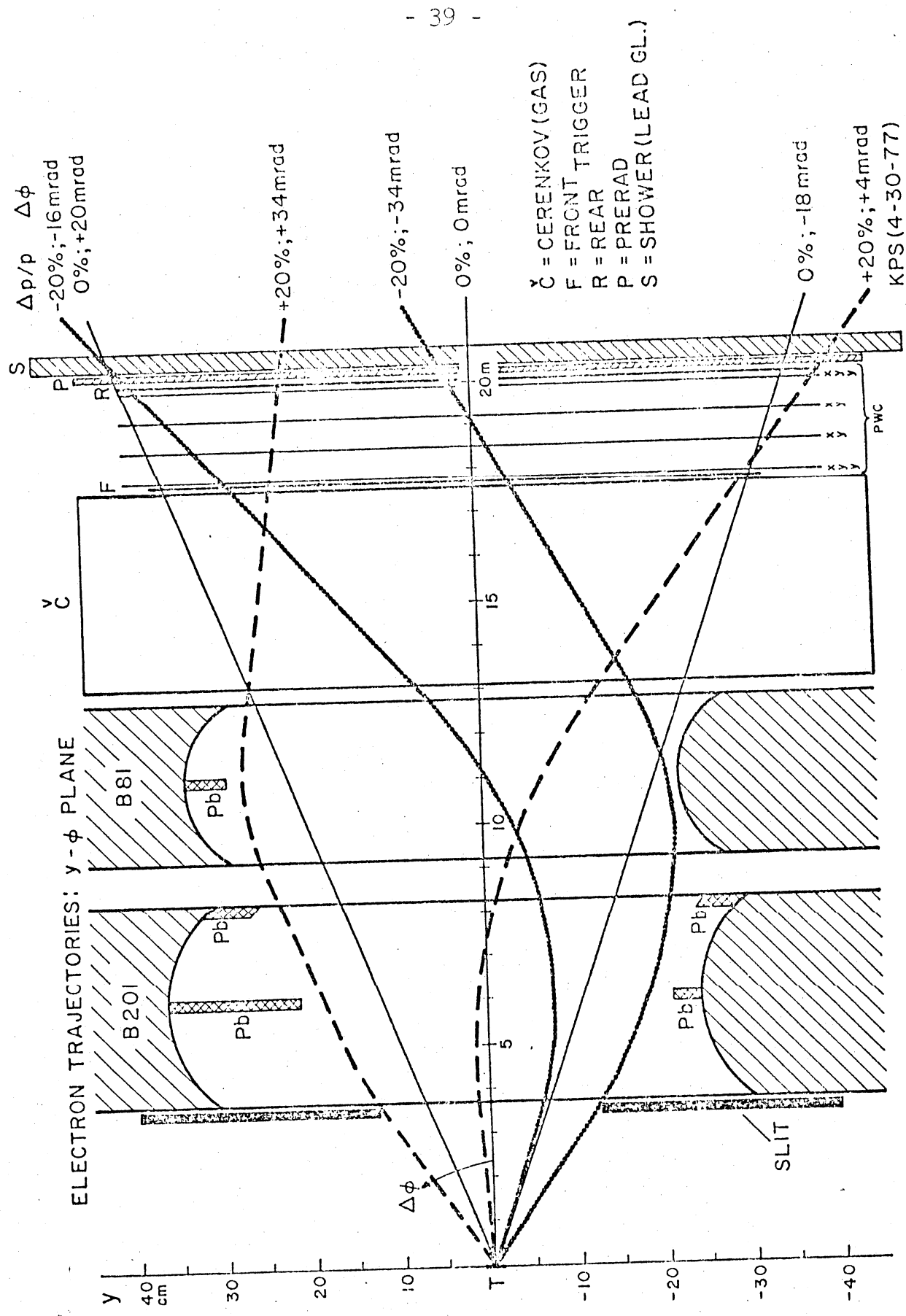
ELECTRON TRAJECTORIES: y-φ PLANE
Δp/p Δφ
-20%;-16mrad
0%;+20mrad
+20%;+34mrad
-20%;-34mrad
0%; 0mrad
0%; -18mrad
+20%;+4mrad
KPS(4-30-77)
Č = CERENKOV(GAS)
F = FRONT TRIGGER
R = REAR
P = PRERAD
S = SHOWER(LEAD GL.)
S
P
R
F
Č
20 m
PWC
B81
B201
Pb
SLIT
Δφ
y
40 cm
30
20
10
T
-10
-20
-30
-40
15
10
5

Fig. 9

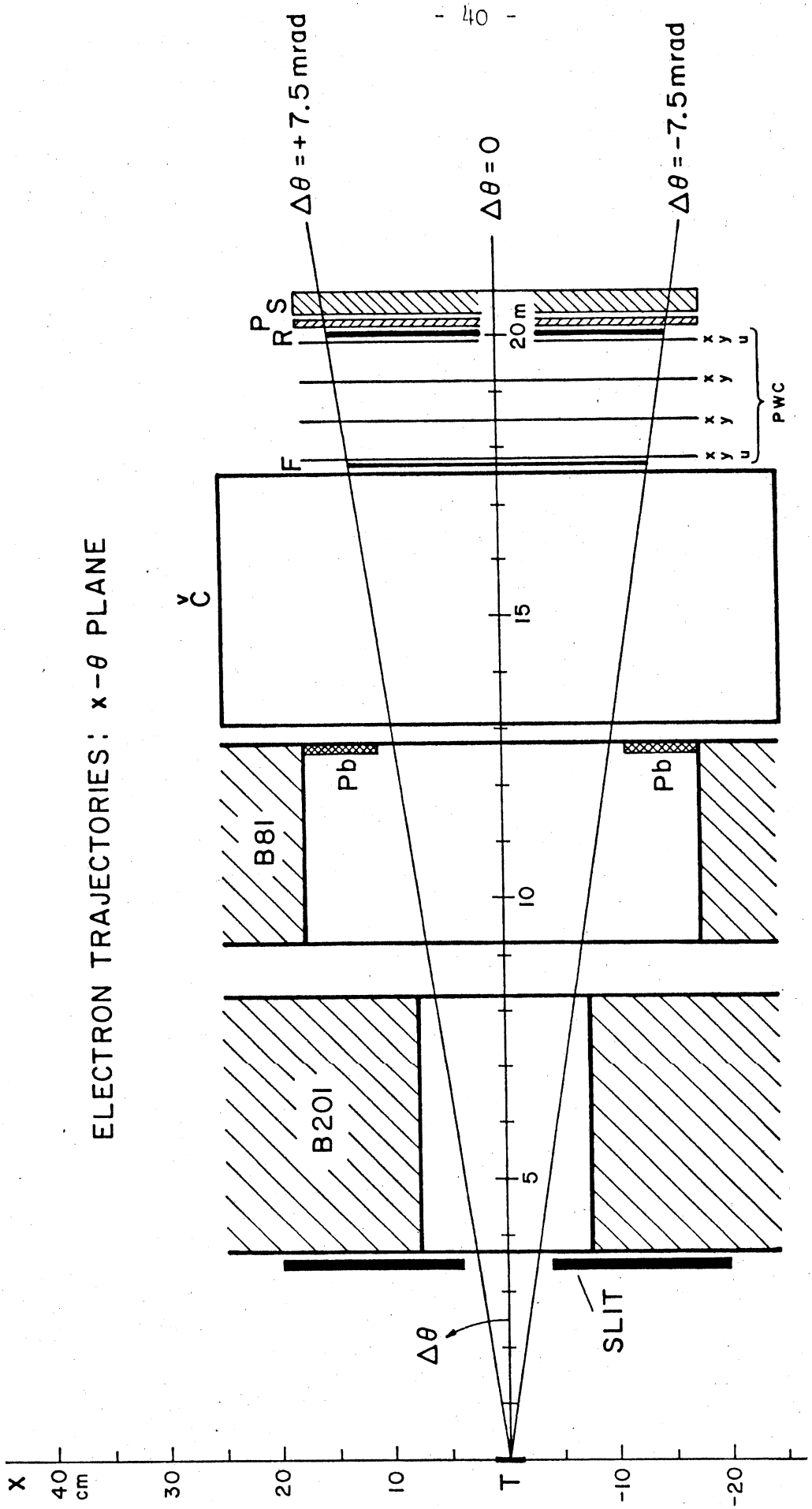
ELECTRON TRAJECTORIES: x-θ PLANE
Δθ = +7.5 mrad
Δθ = 0
Δθ = -7.5 mrad
P
S
R
20 m
x x y u
x x y y
x x y y
x y y u
PWC
F
C
15
Pb
Pb
B81
10
B201
5
Δθ
SLIT
X
40
cm
30
20
10
T
-10
-20

Fig. 10

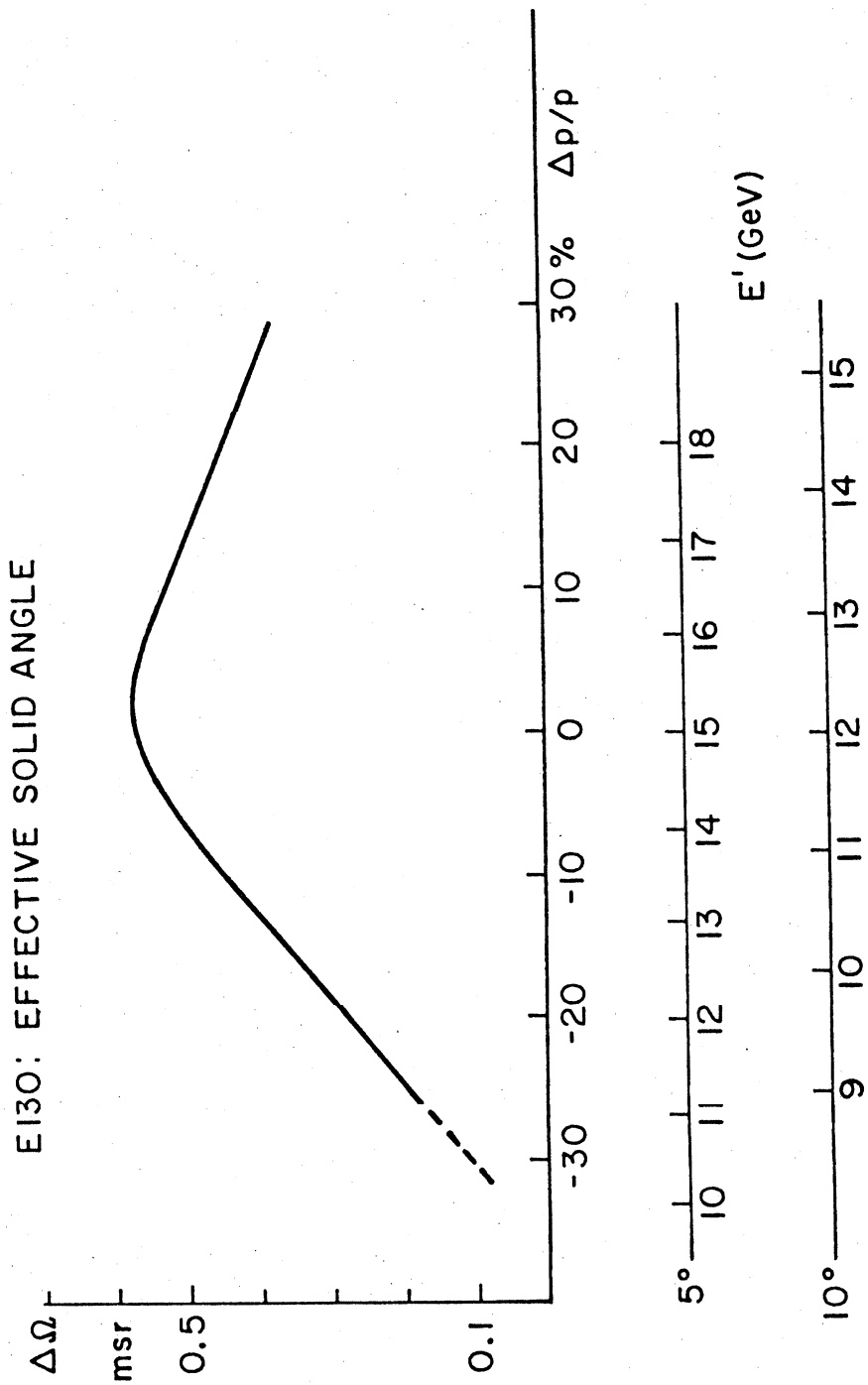
E130: EFFECTIVE SOLID ANGLE
ΔΩ
msr
0.5
0.1
-30
-20
-10
0
10
20
30 %
Δp/p
5°
10°
E'(GeV)

Fig. 11

Data to be Obtained

We propose to obtain data for two settings of the spectrometer, first with $\theta = 10^{\circ}$ and second $\theta = 5^{\circ}$. The predictions for the data to be obtained are given in Tables 8, 9, and 10. Only the statistical errors are given in the Tables.

With regard to systematic errors we plan to determine the beam polarization P_e to about ±5% by Möller scattering. The proton and deuteron polarizations will be determined to about ±5% as well. Finally the fraction F will also be determined to about ±5%. These systematic errors amount to about 10% and occur as a multiplicative scale factor uncertainty.

The running time required is indicated in Table 11. We propose to measure first the proton asymmetries for $\theta = 10^{\circ}$ in one cycle of machine operation. In a subsequent cycle we will measure the proton and deuteron asymmetries for $\theta = 5^{\circ}$.

TABLE 8: Kinematics for Proton Low ω and High Q^2

$E = 22$ GeV

$\theta = 10^{o}$

E' GeV	ν GeV	Q^2 $(GeV/c)^2$	W GeV	ω	D	$\frac{d^2\sigma}{d\Omega dE'/E'}$ $(10^{-30} cm^2/Sr)$	M[a]	events/pulse $x10^{-3}$ [b]	events/300 hrs $x10^{6}$	Error in Δ $(x10^{-2})$ [c]	Error in A_1^p [d]
15	7	10	2.0	1.3	.32	.010	.02	0.9	0.17	0.24	0.14
14	8	9.4	2.6	1.6	.37	.024	.06	2.2	0.43	0.15	0.08
13	9	8.7	3.0	1.9	.42	.040	.13	3.7	0.72	0.12	0.05
12	10	8.0	3.4	2.3	.48	.052	.20	4.5	0.87	0.11	0.05
11	11	7.4	3.8	2.8	.53	.058	.29	3.9	0.76	0.11	0.04
10	12	6.7	4.1	3.4	.58	.059	.36	2.8	0.55	0.13	0.05
9	13	6.0	4.4	4.1	.64	.058	.43				

(a) M is the figure of merit $D^2 \, d^2\sigma/d\Omega dE'/E'$, which is inversely proportional to running time for a given error in A_1^p. For the $\omega=3$, $Q^2=2.7$ $(GeV/c)^2$ point of E80, we take M=1.

(b) Assumes $1.5x10^9$ e^-/pulse, a 3.8 cm target of density 0.7 g/cm^3 and a 20% loss due to beam rastering.

(c) $\Delta = P_e P_p F A^p$ is the raw counting rate asymmetry.

(d) Assumes $A_1^p = A^p/D = \Delta/(P_e P_p F D)$ with $P_e=0.85$, $P_p=0.55$, $F=0.1$, and $nA_2^p=0$.

TABLE 9: Kinematics for Precision Proton Data

E = 22 GeV

$\theta = 5.0^{o}$

E' (GeV)	ν (GeV)	Q^2 $(GeV/c)^2$	W GeV	ω	D	$\frac{d^2\sigma}{d\Omega dE'/E'}$ $(x10^{-30}cm^2)$	M	events/pulse	events/100 hrs $(x10^6)$	Error in Δ $(x10^{-4})$	Error in A_1^p
18	4	3.0	2.3	2.5	0.17	3.3	1.7	0.15	9.7	3.2	0.035
17	5	2.9	2.7	3.3	0.22	3.2	2.7	0.17	11.0	3.0	0.026
16	6	2.7	3.1	4.2	0.27	2.8	3.6	0.17	11.0	3.0	0.021
15	7	2.5	3.4	5.2	0.32	2.4	4.2	0.15	9.7	3.2	0.020
14	8	2.3	3.7	6.4	0.37	2.0	4.9	0.12	7.8	3.6	0.020
13	9	2.2	4.0	7.8	0.41	1.7	5.5	0.07	4.5	4.7	0.023
12	10	2.0	4.2	9.3	0.47	1.4	5.8	0.04	2.6	6.2	0.026
11	11	1.8	4.4	11.2	0.53	1.2	6.3	0.02	1.3	8.8	0.035
10	12	1.7	4.7	13.4	0.58	1.1	6.6				

TABLE 10: Kinematics for Deuterons

E = 22 GeV

$\theta = 5.0^{\circ}$

E' (GeV)	ν (GeV)	Q^2 $(GeV/c)^2$	W GeV	ω	D	$\frac{d^2\sigma}{d\Omega dE'/E'}$ $\times 10^{-30} cm^2/sr$	M[b]	events/pulse	events/200 hrs $(\times 10^6)$	Error in Δ $(\times 10^{-4})$	Error$_d$[a] in A_1	Error in A_1^n
18	4	3.0	2.3	2.5	.17	2.7	0.6					
								0.28	36	1.7	0.038	0.10
16	6	2.7	3.1	4.2	.27	2.5	2.1					
								0.29	37	1.6	0.025	0.06
14	8	2.3	3.7	6.4	.37	1.9	3.5					
								0.18	26	2.0	0.024	0.05
12	10	2.0	4.2	9.3	.47	1.4	4.6					
								0.06	8	3.6	0.035	0.08
10	12	1.7	4.7	13.4	.58	1.0	5.6					

a Assume $P_e P_D F = 0.02$ [P_e=0.85, P_D=0.12, F=0.2].

b A factor of $(1-1/\omega)^2$ is included to account for the smaller neutron cross section.

Table 11. Running Time

Data Collection	Factored Hours
Proton (10°) (Table 8)	300
Proton (5°) (Table 9)	100
Deuteron (5°) (Table 10)	200
	600

Check out, background, and Möller measurement

250 hrs at 10 to 30 pps

Our plan of data-taking is to obtain the $\theta = 10^{\circ}$ data in one cycle and the $\theta = 5^{\circ}$ data in a subsequent cycle.

Group Proposing Experiment

Yale

V.W. Hughes	Professor
M.S. Lubell	Associate Professor
M.E. Zeller	Associate Professor
P.A. Souder	Assistant Professor
M.J. Alguard	Research Associate and Lecturer
J.E. Clendenin	Research Associate
K.P. Schüler	Research Associate
T. Sasao	Research Staff Physicist
M.R. Bergstrom	Graduate Student
R.F. Oppenheim	Graduate Student
D.A. Palmer	Graduate Student
G. Dhawan	Electronics Engineer
R. Fong-Tom	Microwave Engineer

SLAC

R.H. Miller

S.J. St Lorant

University of Bielefeld, Germany

W. Raith	Professor
G. Baum	

University of Tsukuba and KEK, Japan

K. Kondo	Professor
S. Miyashita	
K. Morimoto	

VOLUME 37, NUMBER 19 PHYSICAL REVIEW LETTERS 8 NOVEMBER 1976

Elastic Scattering of Polarized Electrons by Polarized Protons*

M. J. Alguard, W. W. Ash, G. Baum, J. E. Clendenin, P. S. Cooper, D. H. Coward, R. D. Ehrlich, A. Etkin, V. W. Hughes, H. Kobayakawa, K. Kondo, M. S. Lubell, R. H. Miller, D. A. Palmer, W. Raith, N. Sasao, K. P. Schüler, D. J. Sherden, C. K. Sinclair, and P. A. Souder

University of Bielefeld, Bielefeld, West Germany, and City University of New York, New York, New York 10031, and Nagoya University, Nagoya, Japan, and Stanford Linear Accelerator Center, Stanford, California 94305, and University of Tsukuba, Ibaraki, Japan, and Yale University, New Haven, Connecticut 06520

(Received 5 August 1976)

We report on a new type of high-energy electron-proton scattering experiment in which longitudinally polarized electrons are scattered from longitudinally polarized protons. The asymmetry in elastic scattering at $Q^2 = 0.765$ (GeV/c)^2 was measured; our result agrees with the theoretical asymmetry and determines the sign of G_E/G_M to be positive.

In this Letter we describe a high-energy electron-proton scattering experiment in which polarized electrons are scattered from polarized protons, and present the first results for elastic scattering. Our first results for deep inelastic scattering are reported in the following Letter.[1]

The momentum and scattering angle of the scattered electrons were measured when longitudinally polarized electrons were scattered from longitudinally polarized protons. The basic quantity measured was the antiparallel-parallel asymmetry A in the differential cross sections given by

$$A = \frac{d\sigma(\uparrow\downarrow) - d\sigma(\uparrow\uparrow)}{d\sigma(\uparrow\downarrow) + d\sigma(\uparrow\uparrow)}, \tag{1}$$

in which $d\sigma$ denotes the differential cross section $d\sigma(E, \theta)/d\Omega$ for incident electron energy E and laboratory scattering angle θ, and the arrows denote the antiparallel and parallel spin configurations.

If elastic scattering is described by the one-photon-exchange approximation, then the asymmetry can be expressed as[2]

$$A = \frac{\tau G_M}{G_E}\left\{\frac{2M}{E} + \frac{G_M}{G_E}\left[\frac{2\tau M}{E} + 2(1+\tau)\tan^2\frac{\theta}{2}\right]\right\} \times \left\{1 + \tau\left(\frac{G_M}{G_E}\right)^2\left[1 + 2(1+\tau)\tan^2\frac{\theta}{2}\right]\right\}^{-1}, \tag{2}$$

in which $\tau = Q^2/4M^2$, $q^2 = -Q^2 = -4EE'\sin^2(\theta/2)$ is the square of the four-momentum of the virtual photon, M is the proton mass, E' is the scattered electron energy, and G_E and G_M are the electric and magnetic elastic form factors of the proton. The electron mass has been neglected. We chose to measure A for elastic scattering primarily to test the validity of our experimental method. Alternatively, we can regard our measurement as a test of Eq. (2) and as a determination of the sign of G_E/G_M.

The polarized electron source (PEGGY), which serves as an injector to the 20-GeV Stanford linear accelerator, is based on photoionization of a polarized Li^6 atomic beam by a pulsed uv light source.[3] Typical characteristics of the polarized electron beam are given in Table I. The electron polarization, P_e, was measured by Mott scattering at the output of PEGGY and by Møller scattering at high energy. The value given for P_e is based on the Møller scattering measurements.[4,5] The uncertainty, $\delta P_e/P_e = 12\%$, includes counting statistics (10%) and the uncertainty in the uv light intensity for photoionization. (The polarization depends upon light intensity through a depolarizing resonant two-photon ionization process.[5])

Protons were polarized by the method of dynamic nuclear orientation in a butanol target doped with 1.4% porphyrexide.[7] Typical operating conditions are given in Table II. The techniques of beam rastering and target annealing[8] were used to reduce the effects of radiation damage to an acceptable level. Targets were annealed about every two hours and replaced after about five exposures to the beam. The continuously

TABLE I. Characteristics of polarized electron beam.

Characteristic	Value
Pulse length	1.5 μsec
Repetition rate	120 pulses/sec
Electron intensity (at high energy)	$\sim 10^9 e^-$/pulse
Pulse-to-pulse intensity variation	< 5%
Electron polarization, P_e	0.51 ± 0.06
Polarization reversal time	3 sec
Time between reversals	2 min
Intensity difference upon reversal	< 5%
Lifetime of lithium oven load	70 hr
Time to reload system	36 hr

TABLE II. Operating characteristics of polarized proton target.

Characteristic	Value
Magnetic field (longitudinal field of superconducting magnet)	50 kG
Temperature	1.05°K
Target material	25 cm^3 of butanol-porphyrexide beads (~1.7 mm diam)
Initial polarization of free protons[a]	0.50 to 0.65
Depolarizing dose (1/e)	$\sim 3\times 10^{14} e^-/cm^2$
Polarizing time (1/e)	~4 min
Anneal or target change time (including polarizing)	~45 min

[a]Improvements in target operation gave the larger polarization values in the later parts of the experiment.

monitored NMR signal normalized to a thermal equilibrium (TE) signal was used to determine the average target polarization P_p. The uncertainty, $\delta P_p/P_p = 10\%$, includes the errors in the TE measurements (8%) and the uncertainty in the correction for nonuniform irradiation of the target (5%). (Only ~70% of the total 2.5-cm×2.5-cm target cross-sectional area was illuminated by the rastered electron beam.)

The electron beam from the accelerator was momentum-analyzed by a transport system whose absolute momentum calibration was ~0.1%. A momentum slit in the transport system limited the beam energy spread to ±0.375%. Spin precession in the 24.5° bend of the beam switchyard determined that only electrons whose energies were integral multiples of 3.237 GeV had full longitudinal polarization. The electron beam charge per pulse was monitored with two precision toroidal charge monitors. Just upstream of the target, a microwave beam position monitor measured the beam position for each beam pulse with a sensitivity of ~0.1 mm. Computer-controlled vernier steering magnets 99 m upstream of the target were used in conjunction with this position monitor to keep the raster pattern of the beam centered on the target.

The scattered electrons were detected and their momentum and scattering angle were measured with the Stanford Linear Accelerator Center (SLAC) 8-GeV spectrometer. Electron identification was achieved with a gas threshold Cherenkov counter, a 3.25-radiation-length-thick lead glass counter array which sampled the buildup of the electromagnetic shower, and a lead-Isolite[9] shower counter. Less than one pion in 10^3 was misidentified as an electron by this system. An online XDS 9300 computer monitored the experiment and wrote data on magnetic tape.

Data were taken in a series of runs, each of which lasted about two hours. Runs were terminated when radiation damage reduced the target polarization to about half its initial value. The proton polarization direction was constant during a run and was reversed between runs. Each run was divided into cylces, with each cycle in turn comprising eight miniruns of about one-minute duration each. The electron polarization direction remained constant during a minirun and was varied in the pattern $--++--++$, where $-$ ($+$) refers to the electron having negative (positive) helicity in the accelerator. This rapid modulation of the electron beam helicity was an important factor in avoiding systematic errors in the asymmetry measurement.

Each target raster pattern consisted of 313 points and was completed in 2.6 sec. An integral number of raster patterns was used for each minirun. The number of events taken in each minirun was normalized to the total charge measured by the toroids, and corrections were made for losses due to computer sampling, multiple hodoscope tracks, and dead time. The experimental asymmetry, Δ, is the quantity $\pm[(1256)-(3478)]/[(1256)+(3478)]$, where (1256) and (3478) refer to the sums of the corrected and normalized number of events in miniruns 1, 2, 5, 6 and 3, 4, 7, 8, respectively. The sign of Δ is chosen to give the antiparallel-minus-parallel asymmetry in accordance with Eq. (1). False asymmetries were measured with other combinations of miniruns.

Elastic scattering data were taken at the kinematic point for which $E = 6.473$ GeV, $E' = 6.066$ GeV, $\theta = 8.005°$, and $Q^2 = 0.765$ $(\mathrm{GeV}/c)^2$. A total of 2.1×10^6 electrons were detected with a typical

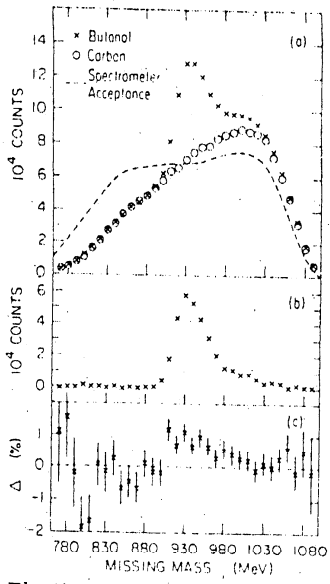

FIG. 1. Elastic scattering results for $E = 6.473$ GeV, $\theta = 8.005°$; (a) scattered electron counts versus missing mass with calculated spectrometer acceptance in arbitrary units; (b) scattered electron counts from free protons versus missing mass; (c) experimental asymmetry Δ versus missing mass.

counting rate of 0.25 scattered electrons per 1.5 μsec beam pulse. The combined missing mass (W) spectrum for electrons scattered from butanol for all runs independent of beam or target polarization is shown in Fig. 1(a), together with the background from electron-carbon scattering normalized to equal areas in the mass region $720 \leq W < 880$ MeV. Also shown in Fig. 1(a) is the spectrometer acceptance as determined from a Monte Carlo ray-tracing calculation. The free-proton spectrum (butanol minus background) versus missing mass is shown in Fig. 1(b). The experimental asymmetry, Δ, is shown plotted versus W in Fig. 1(c). The positive asymmetry associated with elastic scattering from free protons is apparent. Values of Δ for three missing-mass regions are given in Table III. Several false asymmetries, calculated over the complete missing-mass region 720 MeV $\leq W \leq$ 1120 MeV, are shown in Table IV, together with the χ^2 values for the agreement with zero of the measured false asymmetries for the 21 individual runs. No statistically significant false asymmetry was found.

The differential-cross-section asymmetry A of Eq. (1) is related to Δ by

$$\Delta = P_e P_p F A. \tag{3}$$

Here F is the fraction of scattered electrons

TABLE III. Experimental asymmetry, Δ.

W (MeV)	Δ (%)
$720 \leq W < 890$	-0.36 ± 0.18
$890 \leq W < 1000$	$+0.63 \pm 0.10$
$1000 \leq W < 1120$[a]	$+0.15 \pm 0.13$

[a]Since a small fraction of the scattering events from free protons fall in this region, an asymmetry Δ of about +0.13% is expected.

within the elastic missing-mass region ($890 \leq W < 1000$ MeV) which originate from free protons. Using the normalized carbon spectrum to determine the bound-nucleon background, we obtained a value of $F = 0.27 \pm 0.02$. To obtain A, we could have used Eq. (3) with $P_e = 0.51$, the average value of $P_p \simeq 0.34$, and $\Delta = 0.0063 \pm 0.0010$ within the elastic region (Table III). Instead, we used a somewhat different method of calculation which took into account the gradual decrease of the target polarization during a run. Our final result is $A = 0.138 \pm 0.031$ (0.019), where the statistical counting error, shown in parentheses, is added in quadrature to the systematic errors in P_e, P_p, and F to determine the total uncertainty. The values obtained for Δ with the two different directions of proton polarization agree within statistical counting errors. This agreement provides an important test of the validity of our result. Systematic errors in Δ arising from a correlation of beam energy or angle with beam helicity are small compared to the statistical error, as is the error associated with the measurement of beam charge by the toroids. The effect of radiative corrections on A is expected to be small, and these corrections to the data have not yet been made.

The theoretical expression for A of Eq. (2) de-

TABLE IV. False asymmetries.

Combination of miniruns	Average asymmetry[a] (%)	$\chi^2(0)$ per degree of freedom
$\frac{(1234)-(5678)}{(1234)+(5678)}$	0.02 ± 0.07	13/21
$\frac{(1357)-(2468)}{(1357)+(2468)}$	0.01 ± 0.07	18/21
$\frac{(2367)-(1458)}{(2367)+(1458)}$	-0.08 ± 0.07	17/21

[a]Independent of sign of P_p.

pends on both the magnitude and sign of G_E/G_M. Unpolarized elastic scattering experiments determine G_E^2 and G_M^2, but not the sign of G_E/G_M. For $Q^2 = 0.765$ (GeV/c)^2 these experiments[10] give $|\mu G_E/G_M| = 0.98 \pm 0.04$ in which $\mu = 2.79$. If G_E and G_M have the same sign, Eq. (2) yields $A = +0.112 \pm 0.001$, while if G_E and G_M have the opposite sign Eq. (2) gives $A = -0.017 \pm 0.002$. From our measured value of A we conclude that the theoretical and experimental values are in good agreement provided the signs of G_E and G_M are the same. The effect of proton structure on the hyperfine-structure interval in hydrogen involves an integral of the product of the proton structure functions and also gives the sign of G_E/G_M to be positive.[11]

The experimental method described in this Letter could in principle[2,12] be applied to determine G_E in the region $Q^2 \approx 2$ (GeV/c)^2, where G_E is not well known, but its practical usefulness is limited by low counting rates.

We are happy to acknowledge the important contributions to this experiment by M. Browne, S. Dhawan, R. Eisele, Z. Farkas, R. Fong-Tom, H. Hogg, E. Garwin, R. Koontz, J. Sodja, S. St. Lorant, J. Wesley, and M. Zeller.

*Research supported in part by the U. S. Energy Research and Development Administration under Contract No. E(11-1)-3075 (Yale) and Contract No. E(04-3)-515, (Stanford Linear Accelerator Center), the German Federal Ministry of Research and Technology, and the University of Bielefeld, the Japan Society for the Promotion of Science, and the National Science Foundation.

[1]M. J. Alguard *et al.*, following Letter [Phys. Rev. Lett. 37, 1261 (1976)].

[2]N. Dombey, Rev. Mod. Phys. 41, 236 (1969). The methodology of this paper was used to derive Eq. (2).

[3]V. W. Hughes *et al.*, Phys. Rev. A 5, 195 (1972); M. J. Alguard *et al.*, in *Proceedings of the Ninth International Conference on High Energy Accelerators, Stanford Linear Accelerator Center, Stanford, California, 1974*, CONF-740 522 (National Technical Information Service, Springfield, Va., 1974), p. 309.

[4]P. S. Cooper *et al.*, Phys. Rev. Lett. 34, 1589 (1975).

[5]We thank the members of SLAC Group A for their invaluable help in making the electron polarization measurement by Møller scattering in March 1976.

[6]M. J. Alguard *et al.*, Bull. Am. Phys. Soc. 21, 98 (1976).

[7]W. W. Ash, in Proceedings of the Brookhaven National Laboratory Workshop in Physics with Polarized Targets, June 1974, BNL Report No. 20415 (unpublished), p. 309; W. W. Ash *et al.*, to be published.

[8]M. Borghini *et al.*, Nucl. Instrum. Methods 84, 168 (1970).

[9]Isolite is the name for a plastic formed by adding a wavelength-shifter to Lucite.

[10]Ch. Berger *et al.*, Phys. Lett. 35B, 87 (1971); W. Bartel *et al.*, Nucl. Phys. B 58, 429 (1973).

[11]H. Grotch and D. R. Yennie, Rev. Mod. Phys. 41, 350 (1969); C. Zemach, Phys. Rev. 104, 1771 (1956).

[12]A. I. Akhiezer *et al.*, Zh. Eksp. Teor. Fiz. 33, 765 (1957) [Sov. Phys. JETP 6, 588 (1958)].

APPENDIX III

Deep Inelastic Scattering of Polarized Electrons by Polarized Protons*

M. J. Alguard, W. W. Ash, G. Baum, J. E. Clendenin, P. S. Cooper, D. H. Coward, R. D. Ehrlich, A. Etkin, V. W. Hughes, H. Kobayakawa, K. Kondo, M. S. Lubell, R. H. Miller, D. A. Palmer, W. Raith, N. Sasao, K. P. Schüler, D. J. Sherden, C. K. Sinclair, and P. A. Souder

University of Bielefeld, Bielefeld, West Germany, and City University of New York, New York, New York 10031, and Nagoya University, Nagoya, Japan, and Stanford Linear Accelerator Center, Stanford, California 94305, and University of Tsukuba, Ibaraki, Japan, and Yale University, New Haven, Connecticut 06520

(Received 5 August 1976)

We report measurements of the asymmetry in deep inelastic scattering of longitudinally polarized electrons by longitudinally polarized protons. The antiparallel-parallel asymmetries are positive and large in agreement with predictions of quark-parton models of the proton. A limit is obtained on parity nonconservation in the scattering of longitudinally polarized electrons by unpolarized nucleons.

Experimental and theoretical studies of deep inelastic electron scattering from protons and neutrons have led in the past eight years to the important discovery of scaling and to the quark-parton model of nucleon structure.[1] Deep inelastic muon[2] and neutrino[3] scattering have confirmed these general ideas.[4]

For deep inelastic electron-proton scattering,

accurate data have been obtained on the differential cross section $d^2\sigma/d\Omega dE'$ over a wide range of the energy loss, ν, of the electron and the square of the four-momentum transfer, q^2, to the proton. The two spin-averaged proton structure functions $W_1(\nu,q^2)$ and $W_2(\nu,q^2)$ have been determined from these data. Important, independent information is contained in two additional spin-dependent proton structure functions whose determination requires the measurement of spin correlation asymmetries.[5]

In this Letter we report the first results of an experiment done at the Stanford Linear Accelerator Center (SLAC) to measure the asymmetry, A, in the deep inelastic scattering of longitudinally polarized electrons by longitudinally polarized protons, where A is given by

$$A=[d\sigma(\downarrow\uparrow)-d\sigma(\uparrow\uparrow)]/[d\sigma(\downarrow\uparrow)+d\sigma(\uparrow\uparrow)], \tag{1}$$

with $d\sigma$ denoting the differential cross section $d^2\sigma(E,E',\theta)/d\Omega dE'$ for electrons of incident (scattered) energy E (E') and laboratory scattering angle θ, and the arrows denoting the antiparallel and parallel spin configurations.

If the scattering is described by the one-photon-exchange approximation, then for unpolarized electrons the virtual photons are linearly polarized, whereas for polarized electrons the photons are elliptically polarized. The differential cross section for the scattering of longitudinally polarized electrons by longitudinally polarized protons is

$$\frac{d^2\sigma}{d\Omega dE'}=\left(\frac{d\sigma}{d\Omega}\right)_M\left(\frac{1}{\epsilon(1+\nu^2/Q^2)}\right)W_1\{1+\epsilon R\pm(1-\epsilon^2)^{1/2}\cos\psi A_1\pm[2\epsilon(1-\epsilon)]^{1/2}\sin\psi A_2\}, \tag{2}$$

in which $(d\sigma/d\Omega)_M$ is the Mott differential cross section, $\epsilon=[1+2(1+\nu^2/Q^2)\tan^2\frac{1}{2}\theta]^{-1}$, $Q^2=-q^2$, $R=\sigma_L/\sigma_T$ is the ratio of the cross sections for absorption of longitudinal and transverse virtual photons, and ψ is the angle between the directions of the virtual photon momentum and the proton spin. The + (−) signs in Eq. (2) refer to the antiparallel (parallel) spin configurations.

The spin-dependent terms A_1 and A_2 are two new measurable quantities which can be expressed in terms of two spin-dependent structure functions.[5,6] Equivalently, they can be expressed in terms of the total absorption cross sections of circularly polarized photons on polarized protons as

$$A_1=(\sigma_{1/2}-\sigma_{3/2})/(\sigma_{1/2}+\sigma_{3/2}),$$
$$A_2=2\sigma_{TL}/(\sigma_{1/2}+\sigma_{3/2}), \tag{3}$$

where $\sigma_{1/2}$ ($\sigma_{3/2}$) is the total absorption cross section when the z component (z is the direction of the virtual photon momentum) of angular momentum of the virtual photon plus proton is $\frac{1}{2}$ ($\frac{3}{2}$), and σ_{TL}, which may be negative, is a term which arises from the interference between transverse and longitudinal photon-nucleon amplitudes. It should be noted that $\sigma_{1/2}$ and $\sigma_{3/2}$ are related to σ_T by $\sigma_{1/2}+\sigma_{3/2}=2\sigma_T$.

For the case of protons polarized along the incident beam direction, the asymmetry A of Eq. (1) is

$$A=D(A_1+\eta A_2), \tag{4}$$

where

$$D=(E-E'\epsilon)/E(1+\epsilon R)$$
$$=(1-\epsilon^2)^{1/2}\cos\psi/(1+\epsilon R), \tag{5}$$

and

$$\eta=\epsilon(Q^2)^{1/2}/(E-E'\epsilon)$$
$$=[2\epsilon/(1+\epsilon)]^{1/2}\tan\psi\approx\tan\psi. \tag{6}$$

The quantity D can be regarded as a kinematic depolarization factor of the virtual photon and is ~0.3 for our kinematic points. Positivity limits imposed on A_1 and A_2 are[7]

$$|A_1|\le 1,\quad |A_2|\le\sqrt{R}. \tag{7}$$

In this experiment we determine the combination $A_1+\eta A_2$ by dividing the measured electron-proton asymmetry A by the depolarization factor D. Although we do not separately determine A_1 and A_2, our result is dominated by A_1 because the kinematic factor η is small.

On the basis of a high-energy sum rule derived with the algebra of currents for a quark model, it has been predicted[8] that A_1 has a positive value greater than 0.2 over a large region of the deep inelastic continuum. Scaling relations are predicted for the spin-dependent proton structure functions, and hence also for A_1[9]:

$$A_1(\nu,Q^2)\to A_1(\omega)\ \text{as}\ \nu,Q^2\to\infty,\ \text{with}\ \omega\ \text{held constant} \tag{8}$$

($\omega=2M\nu/Q^2$, M is the proton mass). Specific models of proton structure make widely varying predictions for A_1. The simplest quark-parton

TABLE I. Results of asymmetry measurements.

E (GeV)	θ (deg)	Q^2 [(GeV/c)^2]	W[a] (GeV)	ω	Δ (%)	A[b]	D[c]	$A_1+\eta A_2$[b]	$\lvert\eta A_2\rvert$
9.711	9.000	1.680	2.059	3	0.44 ± 0.11	0.191 ± 0.057 (0.044)	0.284	0.67 ± 0.20 (0.16)	<0.146
12.948	9.000	2.735	2.519	3	0.50 ± 0.17	0.215 ± 0.089 (0.080)	0.352	0.61 ± 0.25 (0.23)	<0.109
9.711	9.000	1.418	2.560	3	0.28 ± 0.11	0.141 ± 0.058 (0.051)	0.412	0.34 ± 0.14 (0.12)	<0.087

[a] W is the missing mass of undetected hadron system.
[b] The total errors are the statistical counting errors added in quadrature to the systematic errors in P_e, P_p, and F; the numbers in parentheses are the 1-standard-deviation counting errors.
[c] D is obtained from Eq. (5) using $R=0.14$.

model predicts that $A_1=\frac{5}{9}$, and more elaborate models also predict large positive values for $A_1(\omega)$.[5,10]

The method of measuring the experimental asymmetry, Δ, for deep inelastic electron-proton scattering was the same as that described for elastic scattering in the preceding Letter.[11] For the inelastic case, the scattered electron counting rate was lower (0.02 to 0.06 electrons per pulse).

TABLE II. False asymmetries.[a]

Combination of miniruns	Average asymmetry[b] (%)	$\chi^2(0)$ per degree of freedom
	$\omega=3$, $Q^2=1.680$	
$\frac{(1234)-(5678)}{(1234)+(5678)}$	0.04 ± 0.11	18/34
$\frac{(1357)-(2468)}{(1357)+(2468)}$	-0.04 ± 0.11	38/34
$\frac{(2367)-(1458)}{(2367)+(1458)}$	$+0.14\pm0.11$	27/34
	$\omega=3$, $Q^2=2.735$	
$\frac{(1234)-(5678)}{(1234)+(5678)}$	-0.30 ± 0.17	33/30
$\frac{(1357)-(2468)}{(1357)+(2468)}$	-0.03 ± 0.17	26/30
$\frac{(2367)-(1458)}{(2367)+(1458)}$	$+0.24\pm0.017$	40/30
	$\omega=5$, $Q^2=1.418$	
$\frac{(1234)-(5678)}{(1234)+(5678)}$	-0.12 ± 0.11	34/35
$\frac{(1357)-(2468)}{(1357)+(2468)}$	-0.10 ± 0.11	34/35
$\frac{(2367)-(1458)}{(2367)+(1458)}$	-0.03 ± 0.11	30/35

[a] See preceding Letter (Ref. 11) for definitions of false asymmetries.
[b] Irrespective of sign of target polarization.

Background due to misidentified pions was again negligible.

The antiparallel-parallel asymmetry Δ was measured for three deep inelastic kinematic points and the results are given in Table I. Several false asymmetries were also measured and are listed in Table II, together with the χ^2 values for the agreement with zero of the measured false asymmetries for the indicated degrees of freedom (number of individual runs). No statistically significant false asymmetries were found.

The asymmetry A of Eq. (1) is related to Δ by

$$\Delta = P_e P_p F A. \tag{9}$$

The electron polarization, P_e, was 0.51 ± 0.06, and the average target polarization, P_p, measured for each kinematic point, was ~ 0.40 with 10% uncertainty. The quantity F is the fraction of detected electrons scattered from free protons. This is taken as the ratio of the number of free protons to the total number of nucleons in the target, including measured contributions from helium and other background sources. A small correction for the difference in scattering cross sections of neutrons and protons was also included. The value for F, determined for each point, was $\simeq 0.11$ with a 10% uncertainty.

The measured values of A are listed in Table I. The uncertainties are dominated by counting statistics. No radiative corrections have yet been made. Also listed are the quantities D (evaluated using $R=0.14$),[1] $A/D=A_1+\eta A_2$, and upper limits for $|\eta A_2|$ (taking $A_2=\sqrt{R}$). From Table I it is seen that A/D is dominated by A_1. Furthermore, parton theories predict[12] that the interference term A_2 will be considerably smaller than its positivity limit $\sqrt{R}$. It is therefore valid to compare our measured value of A/D to theoretical predictions for A_1 as shown in Fig. 1.

With the explicit assumption that $A/D=A_1$, our

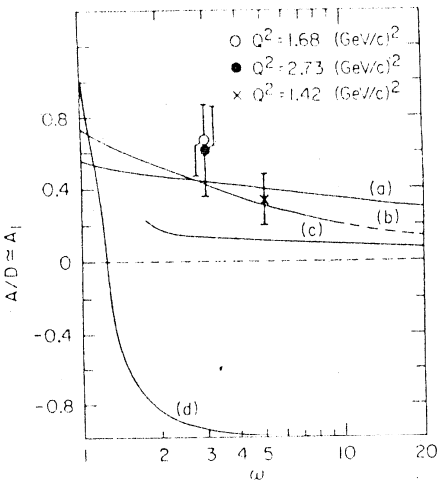

FIG. 1. Experimental values of $A/D \approx A_1$ and theoretical predictions of the virtual-photon–proton asymmetry A_1 versus ω. Theoretical curves a, b, c, and d are obtained from Refs. 5, 10, 13, and 14, respectively. For curve c the quark model with symmetry breaking is used: The model does not give values for A_1 in the range $1<\omega<2$, but rather gives $A_1(1)=1$. For curve d the quantity $\mu^2/m_p{}^2$ in the theory is taken equal to 0.12.

values of A_1 are indeed positive and large in accord with early theoretical expectations from sum rules.[8] The two values for $\omega=3$ agree within their errors, which is consistent with the expectation that A_1 satisfies the scaling relation, given by Eq. (8). Our data are consistent with the predictions of the quark-parton models shown as curves a[5] and b[10] in Fig. 1, but disagree strongly with the resonance model[13] (curve c) and the bare-nucleon–bare-meson model[14] (curve d). We note that the theoretical curves are all given for the scaling limit.

Data from this experiment can also be used to place a limit on parity nonconservation in the scattering of longitudinally polarized electrons from unpolarized nucleons, i.e., an interaction term of the form $\vec{\sigma}_e\cdot\vec{p}_e$ in which $\vec{\sigma}_e$ is the electron spin and $\vec{p}_e$ is the electron incident momentum. If we define Δ^+ (Δ^-) as the asymmetry for protons polarized along (against) the beam direction and if the magnitude of P_p is the same for both cases, then we can define an asymmetry, Δ_{PNC}, associated with parity nonconservation by[15]

$$\Delta_{PNC}=(\Delta^+-\Delta^-)/2\equiv rP_e, \tag{10}$$

in which $r=(d\sigma^- - d\sigma^+)/(d\sigma^- + d\sigma^+)$ is the asymmetry for electron polarization $P_e=1$, and the minus and plus superscripts refer to the electron beam helicity. From the deep inelastic scattering data summarized in Table I for Q^2 between 1.4 and 2.7 $(\mathrm{GeV}/c)^2$, we find that r is consistent with zero. For the combined data we have an upper limit of $r<5\times10^{-3}$ with a 95% confidence level. For the elastic scattering data reported in the preceding Letter,[11] again r is consistent with zero and its upper limit is less than 3×10^{-3} with a 95% confidence level. The gauge theories of weak and electromagnetic interactions, which contain parity nonconservation, predict[16,17] considerably smaller values of $r\simeq(10^{-5}$ to $10^{-4})Q^2/M^2$.

We are happy to acknowledge helpful and stimulating discussions with J. D. Bjorken, F. Gilman, and J. Kuti.

*Research supported in part by the U. S. Energy Research and Development Administration under Contract No. E(11-1)-3075 (Yale) and Contract No. E(04-3)-515 (Stanford Linear Accelerator Center), the German Federal Ministry of Research and Technology and the University of Bielefeld, the Japan Society for the Promotion of Science, and the National Science Foundation.

[1]R. E. Taylor, in *Proceedings of the International Symposium on Lepton and Photon Interactions at High Energies, Stanford, California, 1975*, edited by W. T. Kirk (Stanford Linear Accelerator Center, Stanford, Calif., 1975), p. 679. See also references therein.

[2]L. Mo, in *Proceedings of the International Symposium on Lepton and Photon Interactions at High Energies, Stanford, California, 1975*, edited by W. T. Kirk (Stanford Linear Accelerator Center, Stanford, Calif., 1975), p. 651.

[3]D. H. Perkins, in *Proceedings of the International Symposium on Lepton and Photon Interactions at High Energies, Stanford, California, 1975*, edited by W. T. Kirk (Stanford Linear Accelerator Center, Stanford, Calif., 1975), p. 571.

[4]C. H. Llewellyn-Smith, in *Proceedings of the International Symposium on Lepton and Photon Interactions at High Energies, Stanford, California, 1975*, edited by W. T. Kirk (Stanford Linear Accelerator Center, Stanford, Calif., 1975), p. 709. See also references therein.

[5]J. Kuti and V. F. Weisskopf, Phys. Rev. D 4, 3418 (1971).

[6]F. Gilman, Phys. Rep. 4, 95 (1972); F. Gilman, SLAC Report No. SLAC-167, 1973 (unpublished), Vol. I, p. 71.

[7]M. G. Doncel and E. de Rafael, Nuovo Cimento 4A, 363 (1971).

[8]J. D. Bjorken, Phys. Rev. D 1, 1376 (1970).

[9]L. Galfi *et al.*, Phys. Lett. 31B, 465 (1970).

[10]F. Close, Nucl. Phys. B80, 269 (1974), and references therein.

[11]M. J. Alguard *et al.*, preceding Letter [Phys. Rev.

Lett. 37, 1258 (1976)].
[12]J. D. Bjorken and F. Gilman, private communication.
[13]G. Domokos *et al.*, Phys. Rev. D 3, 1191 (1971).
[14]S. D. Drell and T. D. Lee, Phys. Rev. D 5, 1738 (1972).
[15]In the actual analysis, target polarization differences were included. Since $P_p FA \simeq 0.01$ is small, these differences have little effect.
[16]S. M. Berman and J. R. Primack, Phys. Rev. D 9, 2171 (1974).
[17]G. Feinberg, Phys. Rev. D 12, 3575 (1975).

Appendix IV

VOLUME 41, NUMBER 2 PHYSICAL REVIEW LETTERS 10 JULY 1978

Deep-Inelastic *e-p* Asymmetry Measurements and Comparison with the Bjorken Sum Rule and Models of Proton Spin Structure

M. J. Alguard, W. W. Ash, G. Baum, M. R. Bergstrom, J. E. Clendenin, P. S. Cooper, D. H. Coward, R. D. Ehrlich, V. W. Hughes, K. Kondo, M. S. Lubell, R. H. Miller, S. Miyashita, D. A. Palmer, W. Raith, N. Sasao, K. P. Schüler, D. J. Sherden, P. A. Souder, and M. E. Zeller

University of Bielefeld, Bielefeld, West Germany, and Stanford Linear Accelerator Center, Stanford, California 94035, and University of Tsukuba, Ibaraki, Japan, and Yale University, New Haven, Connecticut 06520

(Received 26 April 1978)

We report new measurements of the asymmetry in the deep-inelastic scattering of longitudinally polarized electrons by longitudinally polarized protons in the kinematic range $2 \leq \omega \leq 10$, $1 \leq Q^2 \leq 4$ (GeV/c)^2, and $2 \leq W \leq 4$ GeV. We compare our results with the Bjorken sum rule and with several theoretical models of the internal spin structure of the proton.

We have previously reported[1-3] on an experiment in which longitudinally polarized electrons were scattered from longitudinally polarized protons and have presented the first data on the asymmetry in deep-inelastic *e-p* scattering. In this Letter we report new asymmetry data, make appropriate radiative corrections, and discuss the theoretical implications of the results.

The basic quantity determined is the asymmetry $A = [d\sigma(\uparrow\downarrow) - d\sigma(\uparrow\uparrow)]/[d\sigma(\uparrow\downarrow) + d\sigma(\uparrow\uparrow)]$, in which $d\sigma$ denotes the differential cross section $d^2\sigma(E,E',\theta)/d\Omega\, dE'$ for electrons of incident (scattered) energy E (E') and laboratory scattering angle θ, and the arrows denote the antiparallel and parallel longitudinal spin configurations. The momentum and scattering angle of the scattered electrons are observed, and the experimental asymmetry $\Delta = P_e P_p F A$ is measured, in which P_e is the electron-beam polarization, P_p is the proton-target polarization, and F is the fraction of detected electrons scattered from the free (polarizable) protons in the complex target.

The experimental method was essentially the same as that reported previously, but some significant improvements in operating conditions were achieved. We increased P_e to 0.85 ± 0.08 by elimination of a multistep photoionization process.[4] Improvements in the target microwave system increased the average value of P_p to 0.50 with a smaller systematic uncertainty of ± 0.04. Reduction of extraneous material increased F to ~ 0.13. The electron beam was rastered over an area somewhat greater than that of the target, giving uniform radiation damage and hence uniform polarization over the target volume. However, only data for which the beam was within a fiducial region of the target were used for the results. As a test of the experimental method, the asymmetry in elastic scattering at $E = 6.47$ GeV, $\theta = 8.0°$, $Q^2 = 0.765$ (GeV/c)^2 was measured giving $A = 0.092 \pm 0.017$, in reasonable agreement with the theoretical value $A = 0.112 \pm 0.001$ and the previously measured value[1] of $A = 0.138 \pm 0.031$.

The results of our asymmetry measurements for seven deep-inelastic kinematic points are given in Table I. Additional kinematic information for each point is given in Table II. The variables used in Table I are defined in Ref. 2. The depolarizing factor D depends on the value of $R = \sigma_L/\sigma_T$. Here we use the current value[5] of $R = 0.25$ and change our earlier results accordingly. In addition to Δ and A, we give the radiatively corrected values for A and for the virtual-photon-proton asymmetry $A/D = A_1 + \eta A_2$. The quantity A_1 equals $(\sigma_{1/2} - \sigma_{3/2})/(\sigma_{1/2} + \sigma_{3/2})$, in which $\sigma_{1/2}$ ($\sigma_{3/2}$) is the total absorption cross section when the z component (z is the direction of the virtual photon momentum) of angular momentum of the virtual photon plus proton is $\frac{1}{2}$ ($\frac{3}{2}$). The quantity ηA_2 is a small interference term whose calculated upper limits are shown in Table I. We shall approximate A_1 by A/D.

We have made radiative corrections to our measured asymmetries using the extensive data available on the spin-averaged cross sections,[6] our measured A values (Table I), and the calculated values of A for elastic scattering. In order to unfold the asymmetries we chose several trial functions for $A(\nu, Q^2)$ in the relevant kinematic region and used each of these together with the spin-averaged cross sections to generate $d^2\sigma(\uparrow\uparrow)/d\Omega\, dE'$ and $d^2\sigma(\uparrow\downarrow)/d\Omega\, dE'$. For each kinemat-

TABLE I: Results of asymmetry measurements.

ω	Q^2 (GeV/c)^2	ν (GeV)	W (GeV)	Δ (%)	A[b]	D	A[c]	A_1+A_2[c,d]	$\lvert\eta A_2\rvert$[e]
2.0	4.09	4.35	2.22	1.28 ± 0.26	$0.211\pm0.051(0.042)$	0.33	0.213 ± 0.057	0.67 ± 0.18	<0.18
3.0	1.68	2.69	2.06	0.51 ± 0.18	$0.009\pm0.037(0.034)$				
3.0[a]	1.68	2.69	2.06	0.44 ± 0.11	$0.191\pm0.057(0.044)$	0.26	0.131 ± 0.039	0.52 ± 0.15	<0.20
3.0	2.74	4.37	2.52	0.95 ± 0.35	$0.166\pm0.065(0.060)$	0.32	0.188 ± 0.066	0.60 ± 0.21	<0.15
3.0[a]	2.74	4.37	2.52	0.50 ± 0.17	$0.215\pm0.089(0.080)$				
4.9	1.02	2.65	2.20	0.29 ± 0.11	$0.058\pm0.023(0.022)$	0.25	0.062 ± 0.031	0.25 ± 0.13	<0.16
5.0[a]	1.42	3.78	2.56	0.28 ± 0.11	$0.141\pm0.058(0.051)$	0.38	0.148 ± 0.073	0.41 ± 0.20	<0.12
5.0	2.95	7.87	3.56	0.63 ± 0.33	$0.099\pm0.062(0.061)$	0.49	0.109 ± 0.081	0.23 ± 0.17	<0.07
10.0	1.70	9.12	4.04	0.42 ± 0.19	$0.100\pm0.038(0.035)$	0.58	0.117 ± 0.057	0.22 ± 0.11	<0.04

[a]Values previously reported in Ref. 2.

[b]Measured values without radiative corrections. The total errors are statistical counting errors added in quadrature to the systematic errors in P_e, P_p, and F; the numbers in parentheses are the 1-standard-deviation counting errors.

[c]Radiatively corrected values (see Table II).

[d]Calculated using weighted average of D.

[e]Calculated upper limits using $R=0.25$.

ic point these cross sections were radiated using the equivalent radiator method.[7] Then asymmetries were formed and compared with the measured asymmetries. Thus we were able to obtain a number of functions consistent with our data. These functions were compared with preliminary results[8] in the resonance region and were found to be consistent. Radiative contributions to a given kinematic point come from a kinematic region with lower ω and lower missing mass W. For each point we chose a cut in ω so as to exclude contributions from the resonance region and then used our functions for $A(\nu, Q^2)$ to correct our asymmetries. The corrected values for A were insensitive to the choice of function. The elastic tail contributes only a few percent to the cross section in our kinematic region. We note that corrected values of $A_1+\eta A_2$ in Table II are larger than the uncorrected value by no more than 0.05. The statistical errors are increased by factors from 1.2 to 1.7 because 14% to 34% of the events originated from regions below the ω cuts. Systematic errors associated with radiative corrections are small compared to statistical errors. The final asymmetry value corresponds to a range of ω values and can be associated with a weighted average value of ω.

Our radiatively corrected values of $A/D \simeq A_1$ from Tables I and II are plotted versus $x=1/\omega$ in Fig. 1. For a given ω, the $A/D \simeq A_1$ values for different Q^2 agree within their errors, which is consistent with the predicted[9] scaling relation $A_1(\nu, Q^2) \to A_1(\omega)$ as $\nu, Q^2 \to \infty$ with ω held constant. Henceforth we shall assume scaling and at each

TABLE II. Kinematics and radiative corrections.

ω	Q^2 (GeV/c)^2	E (GeV)	θ (deg)	Range of ω	Weighted average of ω	Fraction of events inside cuts	Radiative correction[a]	$A_1+\eta A_2$ corrected
2.0	4.09	12.95	11.0	1.7–2.0	1.95	0.86	+0.02	0.67 ± 0.18
3.0	1.68	9.71	9.0	2.5–3.0	2.93	0.75	+0.02	0.52 ± 0.15
3.0	2.74	12.95	9.0	2.5–3.0	2.92	0.77	+0.03	0.60 ± 0.21
4.9	1.02	9.71	7.0	3.5–4.9	4.63	0.73	+0.03	0.25 ± 0.13
5.0	1.42	9.71	9.0	3.5–5.0	4.73	0.75	+0.04	0.41 ± 0.20
5.0	2.95	16.18	8.5	3.5–5.0	4.72	0.77	+0.03	0.23 ± 0.17
10.0	1.70	16.18	7.0	6.0–10.0	9.21	0.66	+0.05	0.22 ± 0.11

[a] $(A_1+\eta A_2)_{\text{corrected}} - (A_1+\eta A_2)_{\text{uncorrected}}$.

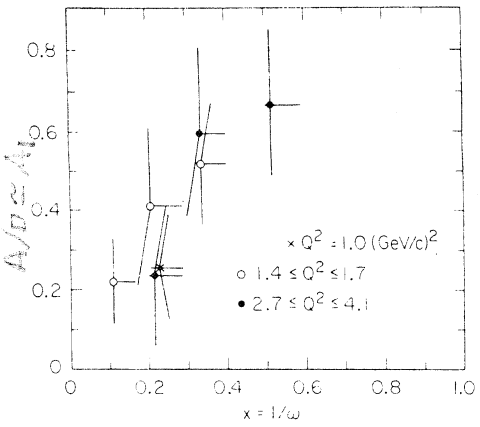

FIG. 1. Experimental values of $A/D \simeq A_1$ vs x. The horizontal bars give the range in x associated with the radiative corrections.

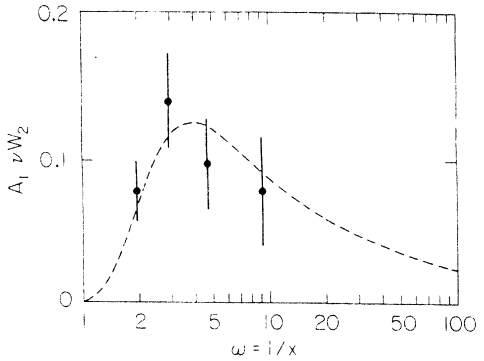

FIG. 2. Experimental values of $A_1 \nu W_2$ vs ω. The dashed curve uses $A_1 = 0.78\omega^{-1/2}$.

ω point take the weighted average of the $A_1(\nu, Q^2)$ values to give $A_1(\omega)$.

The Bjorken sum rule for polarized electroproduction is an important general consequence of quark current algebra.[10] It applies in the scaling limit and reads

$$\int_{\omega=1}^{\infty} d\omega \omega^{-1}(A_1^p \nu W_2^p - A_1^n \nu W_2^n) = \tfrac{1}{3}|g_A/g_V| = 0.417 \pm 0.003, \quad (1)$$

where W_2 is the nucleon structure function, p and n refer to proton and neutron, and g_A (g_V) is the axial (vector) weak coupling constant of β decay. The experimental value[11] for $|g_A/g_V|$ is used in Eq. (1). In the absence of experimental information on A_1^n we approximate $A_1^n = 0$, since quark-parton models of the neutron predict that A_1^n is small. Values of νW_2^p were obtained from cross-section measurements.[12] Figure 2 shows $A_1 \nu W_2 \equiv A_1^p \nu W_2^p$ plotted versus ω. The value of the integral from $\omega = 1.95$ to $\omega = 9.21$ obtained from our data is 0.16 ± 0.03, saturating 40% of the sum rule. Evaluation of the complete integral requires extrapolation to large and small values of ω, the more significant uncertainty coming from the large-ω contribution. We fit our asymmetry data to the form $A_1 = c\omega^{-1/2}$, obtaining a value $c = 0.78 \pm 0.13$. This form, suggested by Regge theory[13] for large ω, represents a satisfactory fit to our data over the entire measured range. The dashed curve in Fig. 2 shows the resulting values of $A_1 \nu W_2$ for this parametrization and gives a value for the full integral of 0.34 ± 0.05 which is consistent with the sum rule. An alternative approach is to assume the validity of the Bjorken sum rule to place limits on the large-ω behavior of the asymmetry. If the asymmetry A_1 at large ω is assumed to be proportional to ω^{-k}, then our data require $0 < k \lesssim 1$.

The predictions for A_1 in the scaling limit from several quark-parton models as well as that from source theory are shown as a function of x in Fig. 3, together with our measured values of $A/D \simeq A_1$. These predictions are in qualitative agreement with the experimental data. Clearly, more accurate data, particularly for lower ω, are required to distinguish among these models.

As discussed in Ref. 2 our data place a limit on parity nonconservation in the scattering of

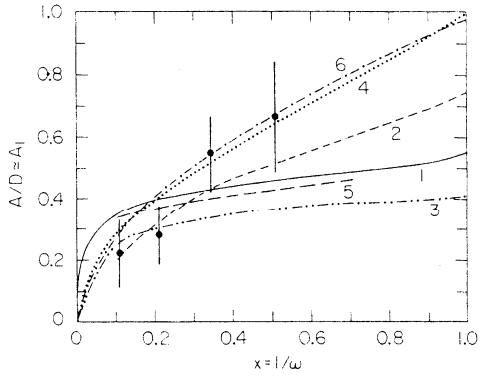

FIG. 3. Experimental values of $A/D \simeq A_1$ compared to theoretical predictions for A_1. The models are as follows: (1) a relativistic symmetric valence-quark model of the proton (Ref. 14); (2) a model incorporating the Melosh transformation which distiguishes between constituents and current quarks (Ref. 15); (3) a model introducing nonvanishing quark orbital angular momentum (Ref. 16); (4) an unsymmetrical model in which the entire spin of the nucleon is carried by a single quark in the limit of $x = 1$ (Ref. 17); (5) the MIT bag model of quark confinement (Ref. 18); (6) source theory (Ref. 19).

longitudinally polarized electrons from unpolarized nucleons by measuring the asymmetry $r = (d\sigma^- - d\sigma^+)/(d\sigma^- + d\sigma^+)$ in which the superscripts refer to the electron helicity for a fully polarized electron beam. From the data in Table I for Q^2 between 1 and 4 $(\mathrm{GeV}/c)^2$, we have $|r| < 3 \times 10^{-3}$ at a 95% confidence level.

We are indebted to L. Boyer, M. Browne, S. Dhawan, S. Dyer, R. Eisele, R. Fong-Tom, W. Kapica, H. Martin, J. Sodja, and L. Trudell for their exceptional efforts in the prepration and running of this experiment. This research was supported in part by the U. S. Department of Energy under Contracts No. EY-76-C-02-3075 and No. EY-76-C-03-0515, the German Federal Ministry of Research and Technology, and the Japan Society for the Promotion of Science.

[1]M. J. Alguard *et al.*, Phys. Rev. Lett. 37, 1258 (1976).

[2]M. J. Alguard *et al.*, Phys. Rev. Lett. 37, 1261 (1976). (There is a typographical error in Table I: In the last row, $\omega = 3$ should read $\omega = 5$.)

[3]N. Sasao, Ph.D. thesis, Yale University, 1977 (unpublished).

[4]M. J. Alguard *et al.*, Phys. Rev. A 16, 209 (1977).

[5]L. N. Hand, in *Proceedings of the International Symposium on Lepton and Photon Interactions at High Energies, Hamburg, 1977*, edited by F. Gutbrod (Deutsches Electronen-Synchrotron, Hamburg, Germany, 1977), p. 417.

[6]A. Bodek *et al.*, Phys. Lett. 51B, 417 (1974), and references quoted therein; A. Bodek *et al.*, to be published.

[7]L. W. Mo and Y. S. Tsai, Rev. Mod. Phys. 41, 205 (1969); Y. S. Tsai, SLAC Report No. SLAC-PUB-848, 1971 (unpublished).

[8]M. R. Bergstrom *et al.*, Bull. Am. Phys. Soc. 23, 529 (1978).

[9]L. Galfi *et al.*, Phys. Lett. 31B, 465 (1970).

[10]J. D. Bjorken, Phys. Rev. D 1, 1376 (1970).

[11]T. G. Trippe *et al.*, Rev. Mod. Phys. 48, No. 2, Pt. 2, S51 (1976).

[12]S. Stein *et al.*, Phys. Rev. D 12, 1884 (1975).

[13]R. L. Heimann, Nucl. Phys. B64, 429 (1973).

[14]J. Kuti and V. W. Weisskopf, Phys. Rev. D 4, 3418 (1971).

[15]F. E. Close, Nucl. Phys. B80, 269 (1974).

[16]G. W. Look and E. Fischbach, Phys. Rev. D 16, 211 (1977); L. M. Sehgal, Phys. Rev. D 10, 1663 (1974).

[17]R. Carlitz and J. Kaur, Phys. Rev. Lett. 38, 673, 1102(E) (1977); J. Kaur, Nucl. Phys. B128, 219 (1977).

[18]R. J. Hughes, Phys. Rev. D 16, 622 (1977); R. L. Jaffe, Phys. Rev. D 11, 1953 (1975).

[19]J. Schwinger, Nucl. Phys. B123, 223 (1977).

APPENDIX V

(Submitted to Physical Review Letters July 22 1980)

SLAC-PUB 2557
July 1980

MEASUREMENT OF ASYMMETRY IN SPIN-DEPENDENT e-p RESONANCE REGION SCATTERING

G. Baum, M. R. Bergström, J. E. Clendenin, R. D. Ehrlich,[a]
V. W. Hughes, K. Kondo, M. S. Lubell, S. Miyashita, R. H. Miller,
D. A. Palmer,[b] W. Raith, N. Sasao,[c] K. P. Schüler,
and P. A. Souder
University of Bielefeld, Bielefeld, West Germany
Stanford Linear Accelerator Center, Stanford, California 94305
University of Tsukuba, Ibaraki, Japan
Yale University, New Haven, Connecticut 06520

ABSTRACT

We report the first measurements of the asymmetry in resonance region scattering of longitudinally polarized electrons by longitudinally polarized protons. Data have been obtained at $Q^2 = 0.5$ and 1.5 $(\mathrm{GeV}/c)^2$ in the missing mass range $W = 1.1$ to 1.9 GeV. Results are compatible with a multipole analysis of single pion electroproduction. The spin-dependent behavior is consistent with a duality mechanism as in the unpolarized case.

We have previously reported measurements of the asymmetry in spin-dependent elastic and deep inelastic e-p scattering.[1-3] We report here the first resonance region measurements[4] of the asymmetry in the scattering of longitudinally polarized electrons from longitudinally polarized protons. Such data are of considerable interest to duality theory and to quark models of nucleon resonances, as well as to multipole analyses of electroproduction. Furthermore, we can learn how the scaling behavior of the spin-dependent structure function, which we have observed in the deep inelastic region,[2,3,5] is approached at the rather small four-momentum transfers studied in this experiment.

The basic quantity determined is the asymmetry $A = (d\sigma(\uparrow\downarrow) - d\sigma(\uparrow\uparrow))/(d\sigma(\uparrow\downarrow) + d\sigma(\uparrow\uparrow))$, in which $d\sigma$ denotes the inclusive differential cross section $d^2\sigma(E,E',\theta)/d\Omega dE'$ for electrons of incident (scattered) energy $E(E')$ and laboratory scattering angle θ, and the arrows denote the antiparallel and parallel longitudinal spin configurations. The asymmetry A is obtained from the experimental asymmetry $A = P_e P_p F A$, in which P_e is the electron beam polarization, P_p is the proton target polarization, and F is the fraction of detected electrons scattered from the free (polarizable) protons in the complex target.

The experiment was performed at the Stanford Linear Accelerator Center using the 8-GeV/c spectrometer and an experimental method reported previously.[1-3] The magnitudes of P_e and $\langle P_p \rangle$ were 0.85 ± 0.08 and 0.50 ± 0.04, respectively, and F varied over the kinematic range from 0.08 to 0.21.

The kinematic points at which our measurements of A were made are listed in Table I. With E = 6.47 GeV and $\theta = 7.0^{\circ}$, five different momentum settings of the spectrometer from E' = 4.92 to 5.83 GeV covered continuously the missing mass region W from 1.090 to 1.872 GeV for $Q^2 = 0.5$ $(GeV/c)^2$. With E = 9.71 GeV and $\theta = 8.0^{\circ}$, two E' settings of 7.87 and 8.13 GeV continuously covered the region W = 1.360 to 1.840 GeV for $Q^2 = 1.5$ $(GeV/c)^2$.

Radiative corrections associated with elastic and inelastic scattering are calculated by the same methods as those employed for deep inelastic asymmetry data.[3,6] The effect of the elastic tail is removed by expressing the inelastic asymmetry, A^{ie}, in the form $A = f^{ie}A^{ie} + f^{e}A^{e}$, where A^{e} is the calculated elastic asymmetry[1] and $f^{ie}(f^{e})$ is the fraction of the events due to inelastic (elastic) scattering (Table I). The fractions f are deduced from a parametrization of unpolarized cross section data[7] equivalently radiated[8] for our target thickness of 0.1 radiation lengths. The radiative corrections due to contaminations from inelastic domains appear in Table II. Contributions from inside the W bin under consideration (f_{cuts}) were treated as the true signal from which the radiatively corrected asymmetries were formed.[9] The statistical errors in the asymmetries are increased by factors of 1 to 1.6 because 0 to 60% of the events originated outside the W cuts.

The completely corrected results are given in Table II with variables the same as those defined in Ref. 2. The depolarizing factor D depends on the value of $R = \sigma_L/\sigma_T$ taken to be 0.1.[10] In addition to the electron asymmetry A, we show the resulting virtual photon - proton asymmetry $A/D = A_1 + \eta A_2$, where $A_1 = (\sigma_{1/2} - \sigma_{3/2})/(\sigma_{1/2} + \sigma_{3/2})$, with $\sigma_{1/2}(\sigma_{3/2})$

the total absorption cross section for the net spin component of the virtual photon plus proton along the photon direction of motion equal to 1/2(3/2). The quantity ηA_2 is an interference term bounded by $|A_2| \leq R^{1/2}$. The uncertainties shown are dominated by statistical errors.

The radiatively corrected values of $A/D = A_1 + \eta A_2$ from Table II are plotted versus W in Fig. 1(a) with two previously published data-points also shown just outside the resonance region.[3] Except in the region of the $\Delta(1232)$ resonance, the values of $A_1 + \eta A_2$ are predominantly large and positive throughout the entire range in W. Extraction of values for individual resonances is complicated by the presence of a large nonresonant background, as is easily seen from Fig. 1(b) which shows all the contributions at $Q^2 = 0.5$ $(GeV/c)^2$. The proportion of inelastic events not due to the resonances is given in the last column of Table II.

The contribution to the asymmetry $A_1 + \eta A_2$, which arises from the two channels $ep \rightarrow en\pi^+$ and $ep \rightarrow ep\pi^0$, has been calculated[11] for our kinematic points. This calculation is based on a multipole analysis[12] of extensive electroproduction data in the resonance region and does not use our data. The results of these calculations are displayed in Fig. 2 for the cases of "a" Born term asymmetries alone, "b" Born term plus $\Delta(1232)$ asymmetries, and "c" Born term plus all resonance asymmetries. It is not surprising that case "a" shows asymmetries beginning near zero at low W instead of near +1 (which an s-wave assumption would dictate) since the presence of the charged channels requires[13] the retention of the pion pole term (which contains all partial waves). Thus angular momentum barrier arguments are ruled out, even this close to threshold. Although single pion electroproduction accounts for only about one-half of the total inelastic cross section in our kinematic region, good agreement is obtained with our data. Thus the net asymmetry contributed by the other channels cannot be very different from our measured asymmetries.

At the center of the $\Delta(1232)$, the dominant A_1 component of A/D is expected to be -0.5 for the P_{33} partial wave, which is known to be essentially pure M1 excitation and which contributes 74% to our data point at W = 1.240 GeV. The P_{33} partial wave is still very strong throughout the second and third resonance peaks, but the associated asymmetry changes sign outside the central region of the first resonance, as shown by curve "b" in Fig. 2.

Theoretical predictions about the asymmetry of the $D_{13}(1520)$ and $F_{15}(1688)$ resonances are more uncertain. Symmetric quark models,[14] for example, predict a rapid change of the asymmetry from negative to positive as Q^2 varies from 0.5 to 1.5 $(GeV/c)^2$. As a consequence of the strong nonresonant background more precise asymmetry data are required for the isolation of these individual resonance asymmetries.

The global effect of the spin-dependent behavior of all the s-channel resonances has been studied in the framework of a symmetrical quark model.[15] Somewhat surprisingly, the polarization asymmetry of the summed resonances duplicates the result of the naive quark model for the deep inelastic region $(A_1 = 5/9)$. The resonance region asymmetries must be predominantly negative in the photoproduction limit $(Q^2 = 0)$, as can be inferred from the Drell-Hearn-Gerasimov sum rule,[16] and our data show that the asymmetry has already changed sign at $Q^2 = 0.5(GeV/c)^2$. In the unpolarized case, it is well known that the structure function νW_2 scales throughout much of the resonance region and that at least a form of global duality holds between the resonance region and the deep inelastic region.[17] In order to test whether such a correspondence exists in the polarized case as well, we have plotted in Fig. 3 our resonance data

against the scaling variable $\omega = 2M\nu/Q^2$. The curve shown ($0.78\omega^{-1/2}$) is a fit to our deep inelastic data.[3] At the first resonance, a major oscillation away from the deep inelastic curve occurs, but otherwise scaling seems to apply for all resonance points. The situation does not change if we use slightly different scaling variables which have been suggested.[17] We conclude that the spin dependent behavior is also consistent with a duality mechanism, in analogy to the unpolarized case.

Acknowledgements

We are indebted to R. Devenish and V. Gerhardt for the multipole calculations. We also thank R. Devenish and F. Gilman for valuable discussions. The research was supported in part by the U.S. Department of Energy under Contract Nos. DE-AC02-76ER03075 (Yale University) and DE-AC03-76SF00515 (SLAC), the German Federal Ministry of Research and Technology, and the Japan Society for the Promotion of Science.

REFERENCES

(a) Present address: Cornell University, Ithaca, NY 14850.

(b) Present address: University of California, Santa Barbara, CA 93106

(c) Present address: Kyoto University, Kyoto, Japan

1. M.J. Alguard et al., Phys. Rev. Lett. 37, 1258 (1976).
2. M.J. Alguard et al., Phys. Rev. Lett. 37, 1261 (1976).
3. M.J. Alguard et al., Phys. Rev. Lett. 41, 70 (1978).
4. M.R. Bergström et al., Bull. Am. Phys. Soc. 23, 529 (1978).
5. G. Baum et al., paper submitted to XX International Conference on High Energy Physics, Madison, Wisconsin (1980).
6. K.P. Schüler, in High Energy Physics with Polarized Beams and Polarized Targets, Argonne, 1978, edited by G.H. Thomas (American Institute of Physics, New York, 1979), p. 217.
7. S. Stein et al., Phys. Rev. D 10, 1884 (1975).
8. L.W. Mo and Y.S. Tsai, Rev. Mod. Phys. 41, 205 (1969); Y.S. Tsai, SLAC Report No. SLAC-PUB-848, 1971 (unpublished).
9. M.R. Bergström, Ph.D. thesis, Yale University, 1979 (unpublished).
10. F.W. Brasse et al., Nucl. Phys. B 110, 413 (1976).
11. R.C.E. Devenish and V. Gerhardt, private communication.
12. R.C.E. Devenish and D.H. Lyth, Nucl. Phys. B 93, 109 (1975).
13. R.L. Walker, Phys. Rev. 182, 1729 (1969).
14. F. Ravndal, Phys. Rev. D 4, 1466 (1971); S. Ono, Nucl. Phys. B 107, 522 (1976); for a dual model see J.G. Körner, DESY Report No. DESY 75/57, 1975 (unpublished).
15. F.E. Close et al., Phys. Rev. D 6, 2533 (1972); F.E. Close and F.J. Gilman, Phys. Rev. D 7, 2258 (1973).

16. S.D. Drell and A.C. Hearn, Phys. Rev. Lett. 16, 908 (1966); S.B. Gerasimov, Sov. J. Nucl. Phys. 2, 430 (1966); I. Karliner, Phys. Rev. D 7, 2717 (1973).

17. E.D. Bloom and F.J. Gilman, Phys. Rev. D 4, 2901 (1971); V. Rittenberg and H.R. Rubinstein, Phys. Lett. B 35, 50 (1971).

TABLE I: ELECTRON ASYMMETRY DATA AND ELASTIC TAIL SUBTRACTION

W (GeV)	Q^2 $(GeV/c)^2$	E (GeV)	θ (deg)	ϵ	A (Measured electron asymmetry)	A^{ee}	f^{ie} (Inelastic fraction)	A^{ie} (Electron asymmetry after elastic tail subtraction)
1.168	0.57	6.47	7.0	0.127 ± 0.148	0.031 ± 0.035	0.049 ± 0.001	0.46	-0.030 ± 0.073
1.247	0.56	6.47	7.0	-0.078 ± 0.079	-0.012 ± 0.011	0.023 ± 0.001	0.75	-0.045 ± 0.015
1.386	0.54	6.47	7.0	0.305 ± 0.083	0.052 ± 0.017	0.021 ± 0.001	0.76	0.041 ± 0.022
1.527	0.52	6.47	7.0	0.392 ± 0.088	0.069 ± 0.017	0.015 ± 0.001	0.83	0.065 ± 0.021
1.623	0.51	6.47	7.0	0.223 ± 0.156	0.042 ± 0.029	0.015 ± 0.002	0.83	0.033 ± 0.033
1.709	0.49	6.47	7.0	0.305 ± 0.086	0.045 ± 0.014	0.013 ± 0.001	0.85	0.038 ± 0.018
1.824	0.48	6.47	7.0	0.451 ± 0.122	0.075 ± 0.021	0.014 ± 0.001	0.83	0.074 ± 0.026
1.419	1.56	9.71	8.0	-0.166 ± 0.356	-0.024 ± 0.046	0.015 ± 0.003	0.89	-0.045 ± 0.052
1.512	1.34	9.71	8.0	0.629 ± 0.215	0.130 ± 0.037	0.010 ± 0.002	0.82	0.110 ± 0.040
1.613	1.21	9.71	8.0	0.724 ± 0.146	0.096 ± 0.025	0.009 ± 0.001	0.83	0.093 ± 0.027
1.716	1.08	9.71	8.0	0.719 ± 0.170	0.095 ± 0.026	0.007 ± 0.002	0.85	0.093 ± 0.027
1.794	1.45	9.71	8.0	0.870 ± 0.265	0.093 ± 0.036	0.007 ± 0.004	0.85	-0.007 ± 0.059

TABLE II: INELASTIC RADIATIVE CORRECTIONS AND COMPLETELY CORRECTED ELECTRON AND PHOTON ASYMMETRY RESULTS

Range of W (GeV)	W (GeV)	Q^2 $(GeV/c)^2$	A (Corrected electron asymmetry)	D (for R = 0.1)	$A_1 + \eta A_2$ (Corrected photon asymmetry)	Inelastic Radiative Correction[a]	$\lvert \eta A_2 \rvert$ (Upper limit for R = 0.1)	f_{cuts} [b]	f_{bkgd} [c]
1.090-1.184	1.158	0.57	−0.080 ± 0.074	0.088	−0.34 ± 0.33	0.00	0.38	1.00	0.35
1.184-1.312	1.247	0.56	−0.145 ± 0.217	0.103	−0.44 ± 0.16	0.00	0.32	0.42	0.29
1.312-1.472	1.386	0.54	0.057 ± 0.034	0.132	0.30 ± 0.26	+0.20	0.24	0.65	0.54
1.472-1.584	1.527	0.52	0.082 ± 0.031	0.165	0.49 ± 0.18	+0.10	0.19	0.68	0.56
1.584-1.648	1.623	0.51	0.042 ± 0.065	0.191	0.22 ± 0.34	+0.04	0.16	0.81	0.76
1.648-1.776	1.709	0.49	0.045 ± 0.027	0.215	0.21 ± 0.12	+0.03	0.14	0.81	0.70
1.776-1.872	1.824	0.48	0.096 ± 0.053	0.250	0.38 ± 0.21	+0.03	0.12	0.48	0.39
1.360-1.472	1.419	1.56	−0.017 ± 0.077	0.152	−0.11 ± 0.51	+0.16	0.24	0.87	0.76
1.472-1.552	1.512	1.54	0.151 ± 0.057	0.169	0.91 ± 0.35	+0.12	0.22	0.69	0.59
1.552-1.664	1.613	1.51	0.153 ± 0.043	0.183	0.82 ± 0.23	+0.11	0.19	0.83	0.81
1.664-1.776	1.716	1.48	0.103 ± 0.041	0.201	0.51 ± 0.21	+0.05	0.17	0.95	0.72
1.776-1.840	1.794	1.46	−0.035 ± 0.128	−0.220	−0.16 ± 0.69	−0.13	0.26	1.00	0.87

(a) $(A_1 + \eta A_2)^{corrected} - (A_1 + \eta A_2)^{uncorrected}$

(b) fraction of events inside cuts, used for inelastic radiative corrections

(c) fraction of nonresonant background present in corrected asymmetries

FIGURE CAPTIONS

1. (a) Asymmetry versus missing mass W.

   (b) Differential cross section versus W. Also shown is a decomposition into individual resonances and the background.

2. (a) Asymmetry data at $Q^2 = 0.5$ $(GeV/c)^2$ compared with a multipole analysis performed by Devenish and Gerhardt: "a" Born terms alone, "b" Born terms plus $\Delta(1232)$, "c" Born terms plus all resonances.

   (b) Same for $Q^2 = 1.5$ $(GeV/c)^2$.

3. Asymmetry versus scaling variable ω. The curve $0.78\omega^{-1/2}$ is a fit to deep inelastic data ($W > 2$ GeV). The data points are the resonance region results ($W < 2$ GeV) of this work.

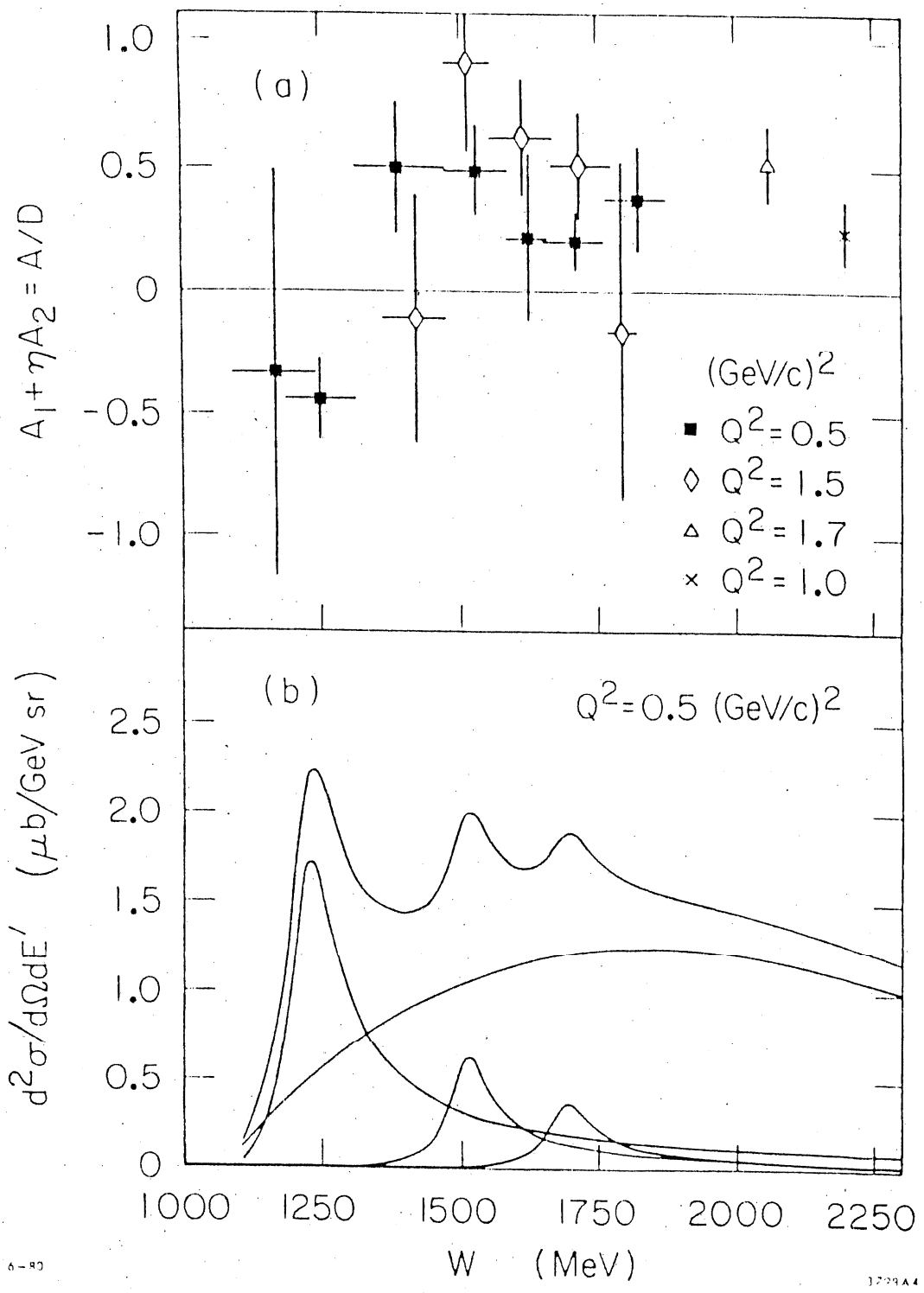
(a)
$A_1+\eta A_2 = A/D$
1.0
0.5
0
-0.5
-1.0
$(GeV/c)^2$
$Q^2=0.5$
$Q^2=1.5$
$Q^2=1.7$
$Q^2=1.0$
(b)
$Q^2=0.5$ $(GeV/c)^2$
$d^2\sigma/d\Omega dE'$ $(\mu b/GeV\ sr)$
2.5
2.0
1.5
1.0
0.5
0
1000
1250
1500
1750
2000
2250
W (MeV)

Fig. 1

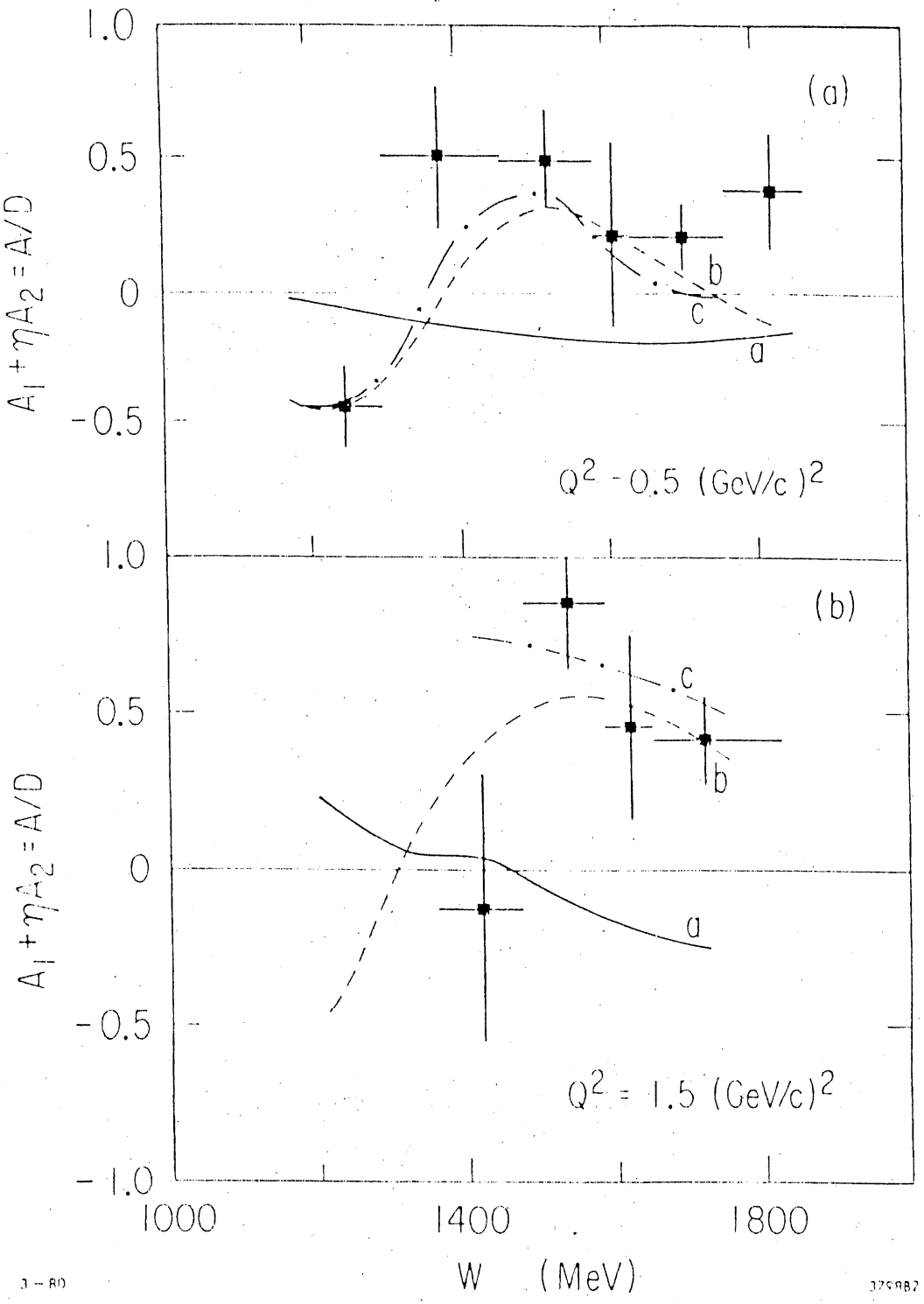
1.0
0.5
0
-0.5
(a)
b
c
a
$A_1 + \eta A_2 = A/D$
Q^2 - 0.5 (GeV/c)^2
1.0
0.5
0
-0.5
-1.0
(b)
c
b
a
$A_1 + \eta A_2 = A/D$
Q^2 = 1.5 (GeV/c)^2
1000
1400
1800
W (MeV)

Fig. 2

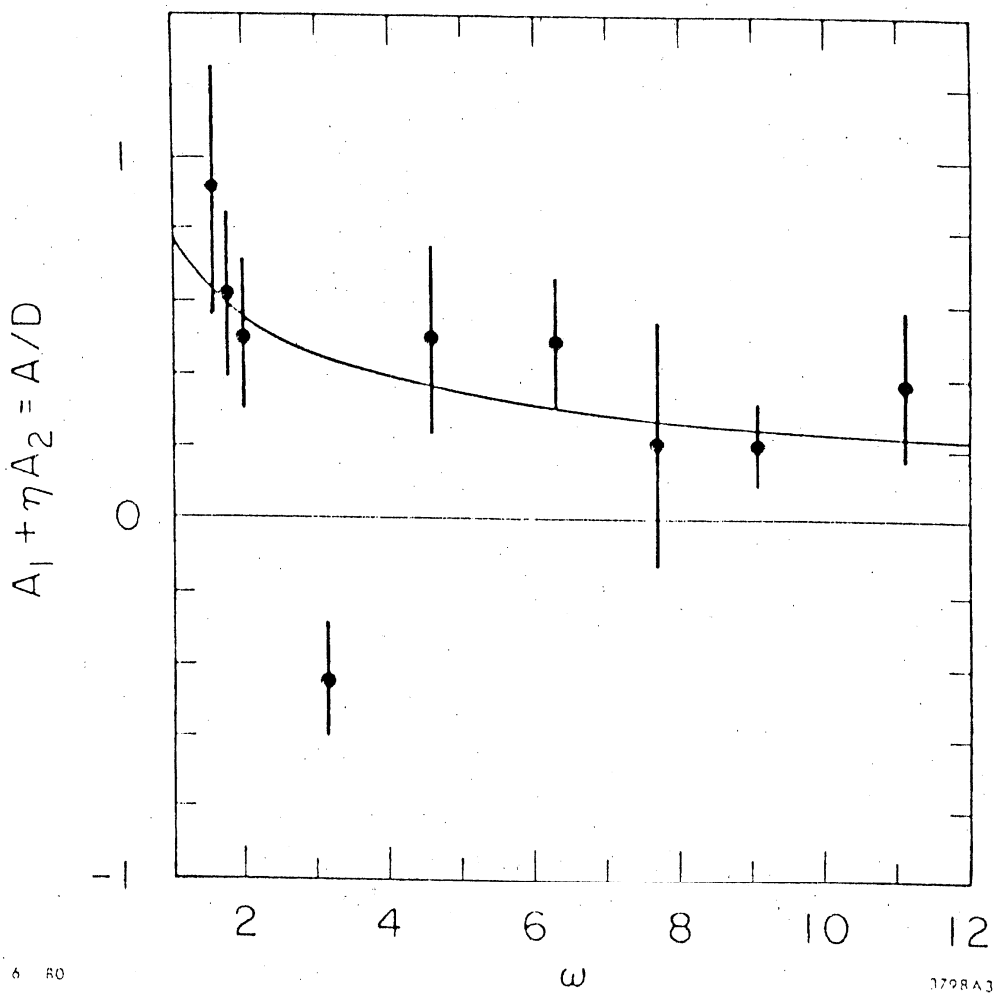

Fig. 3

Submitted to Fifth International Symposium on Polarization Phenomena in Nuclear Physics, Santa Fe, August 1980.

APPENDIX VI

DYNAMIC NUCLEAR POLARIZATION OF IRRADIATED TARGETS*

M.L. Seely, M.R. Bergstrom, S.K. Dhawan, R.A. Fong-Tom, V.W. Hughes, R.F. Oppenheim, K.P. Schiller, and P.A. Souder, Yale Univ.; K. Kondo, S. Miyashita, I. Nakano, Univ. Tsukuba; S.J. St. Lorant, SLAC; Y.-N. Guo, Inst. H.E.P., Peking; A. Winnacker, Univ. Heidelberg

Polarized proton targets used in high energy physics experiments employ the method of dynamic nuclear polarization (DNP) to polarize the protons in an alcohol.[1] DNP requires the presence of paramagnetic centers, which are customarily provided by a chemical dopant. These targets suffer from loss of polarization as the target is irradiated, and also the hydrogen fraction for the alcohols is relatively low, e.g., 0.13 for butanol. If the paramagnetic centers formed when the target is irradiated could be used in the DNP process, the resulting targets might be more radiation-resistant. Also it might be possible to use materials which have high hydrogen fractions, but are not easily doped, such as NH_3 or HD.

The Yale-SLAC polarized proton target system[2] utilizes a ^4He cryostat to maintain 25 cm^3 of target material at 1 K, a superconducting magnet with a 50 kG field, a microwave system at 140 GHz, and an NMR system at 200 MHz. The target material, usually in the form of beads ~1 mm. in diameter, is contained in a mylar cup. The targets were irradiated at SLAC with an electron beam delivered at 10 pulses per second with currents ranging from 2×10^9 to 4×10^{10} e^- per 1.5 μs pulse and with energies of 6 or 22 GeV.

Several targets containing butanol (C_4H_9OH) with 5% H_2O were given total doses ranging from 5×10^{12} to 8×10^{14} e^-/cm^2. The proton polarizations, P, and the time constants for polarization, T_p, and for proton spin relaxation, T_1, were measured as a function of dose. Typical results are shown in Figs. 1, 2 and 3. The polarization reached a value of about 10% with a dose of (2 to 3)$\times10^{14}$ e^-/cm^2 and then decreased as the dose was increased further. Annealing the target at 100 K and 150 K caused the polarization to double approximately. Annealing at 100 K caused T_1 to increase but did not alter T_p. Both T_p and T_1 became very long as a result of annealing the target at 150 K. Although the values of P for irradiated butanol are small, the data on P, T_p, and T_1 may be useful for understanding the effect of irradiation on a butanol target.

High polarizations (up to 90%) have been observed at CERN[3] in ammonia targets that were irradiated in liquid nitrogen with protons and then transferred to a polarized target system. Typical results for the NMR signal for an NH_3 target irradiated at SLAC are shown in Fig. 4. We believe that high polarizations were observed in our targets; however, reliable quantitative measurements of the polarization were not possible. Ammonia escaping from the target cup settled on the NMR coil causing erratic behavior of the NMR signal. It appears that the NH_3 beads break up into a fine powder as they are irradiated at low temperatures. The powdered NH_3 then migrates out of the mylar target cup, possibly due to electrostatic repulsion between the particles.

The proton polarization in borane ammonia, (BH_3NH_3) (Fig. 5) leveled off at a value of ~10% with a dose of 4×10^{14} e^-/cm^2. The target was then annealed at a temperature of 150 K, causing the polarization to increase to ~25%. This large polarization attained as a result of the anneal decreased as the target was further irradiated. No significant polarization was observed in irradiated water.

In attempting to study $LiBH_4$ and ethane (C_2H_6) we again encountered the problem of target material migrating out of the target cup. The $LiBH_4$ was available only in powdered form. Ethane was prepared in the form of beads, but, as for ammonia, they seemed to disintegrate when irradiated. In both cases we believe that the observed polarizations were small (~10%).

Ammonia seems to be a promising material; however, the problem of migration of the ammonia out of the target cup must be solved before it could be useful in a target system such as ours. We plan to continue work at SLAC on ammonia and selected compounds, and to examine other materials including HD.[4]

REFERENCES

*Research supported in part by the U.S. Department of Energy under contracts No. DE-AC02-76ERO 3075 and No. DE-AC03-76SF00515.

1. High Energy Physics with Polarized Beams and Polarized Targets, ed. G.H. Thomas, AIP Conf. no. 51, Argonne, 1978.
2. M.J. Alguard et al., Phys. Rev. Lett. 41, 70 (1978).
3. T.O. Niinikoski et al., Phys. Lett. 72A, 141 (1979).
4. J.C. Solem, Nucl. Instr. and Meth. 117, 477 (1974).

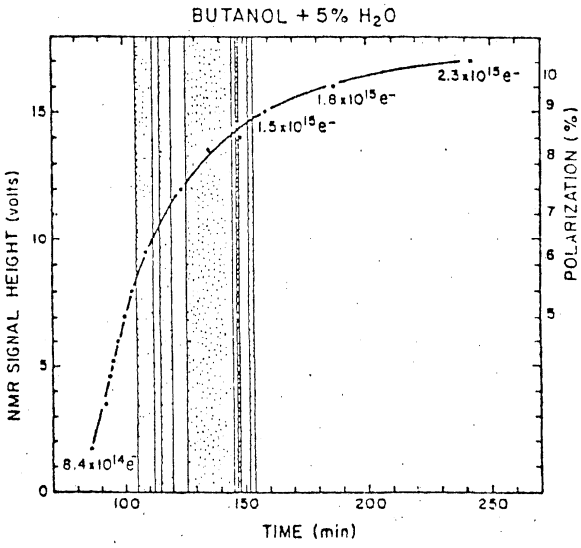

Fig. 1: Enhanced proton NMR signal (left vertical axis) versus time for butanol. Corresponding proton polarization (right vertical axis) is also shown. Shaded areas indicate periods with beam off. The e^- numbers give the total e^- dose on the target area of about 6.4 cm^2.

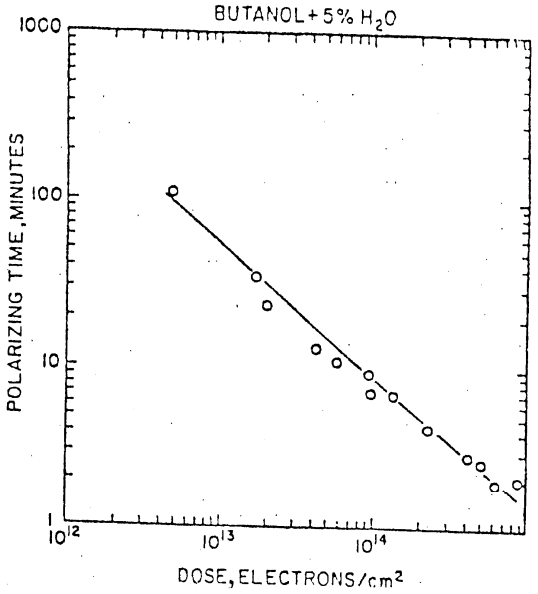

Fig. 2: Polarizing time, T_p, vs dose for butanol.

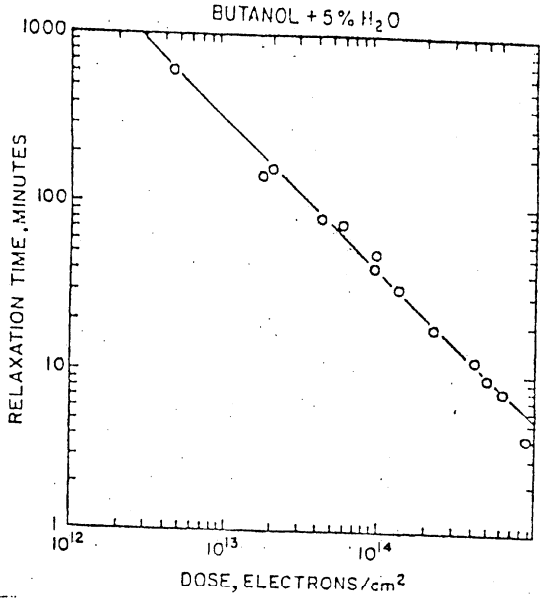

Fig. 3: Relaxation time, T_1, vs dose for butanol.

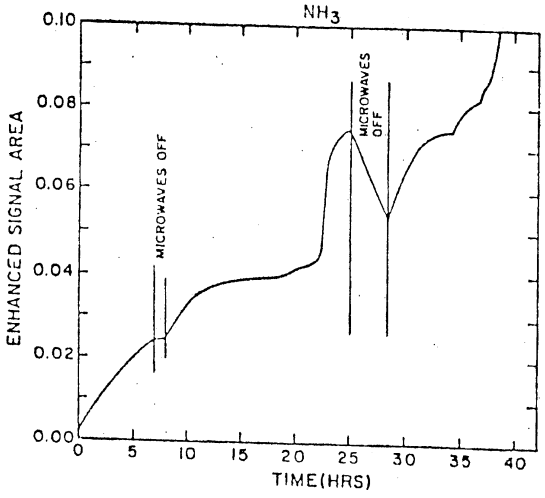

Fig. 4: Enhanced signal area vs irradiation time for an NH_3 target, illustrating the large values but rather erratic behaviour of the signal.

Fig. 5: Proton polarization vs time for BH_3NH_3 irradiated target.